THE UNIVERSITY OF SYDNEY

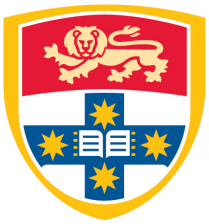

THE UNIVERSITY OF
SYDNEY

WIRELESS-POWERED COOPERATIVE COMMUNICATIONS: PROTOCOL DESIGN, PERFORMANCE ANALYSIS AND RESOURCE ALLOCATION

By

He (Henry) CHEN

A THESIS SUBMITTED IN FULFILLMENT OF THE
REQUIREMENTS FOR THE DEGREE OF
DOCTOR OF PHILOSOPHY
AT
SCHOOL OF ELECTRICAL AND INFORMATION ENGINEERING
FACULTY OF ENGINEERING AND INFORMATION TECHNOLOGIES
THE UNIVERSITY OF SYDNEY

APRIL 2015

To my loving wife Yanyan

and

my beloved parents Hongjiang Chen and Yueying Teng

Acknowledgements

My Ph.D. study at The University of Sydney has been one of the most memorable periods of my life. I felt very honored and lucky to have learned from and worked with so many remarkable people here.

First of all, I would like to express my sincere gratitude to my advisor Prof. Yonghui Li for his constructive guidance and continuous support over the past three years. Without his inspiration for my ideas and the efforts he personally put in, the smooth completion of my Ph.D. could not have been possible. Yonghui not only advises me on how to be a great researcher, but also shows me how to be a good person. I believe that what I learned from Yonghui will deeply affect and benefit me throughout my whole career and life.

I am also very grateful to Prof. Branka Vucetic for serving as my associate advisor. Her valuable suggestions and insightful comments have significantly improved the quality of my papers. I would also like to thank Dr. Raymond Louie for his patient guidance and enormous help during the first two years of my Ph.D. study. In addition, I am also thankful to my other co-authors Mr. Zheng Dong (McMaster University), Dr. Xiangyun Zhou (Australian National University), Prof. Zhu Han (University of Houston), Dr. João Luiz Rebelatto (Federal University of Technology-Parana), Prof. Bartolomeu F. Uchôa-Filhoand (Federal University of Santa Catarina), Mr. Yunxiang Jiang (Hong Kong Polytechnic University), Dr. Peng Wang, Dr. Jun Li and Mr. Yuanye Ma, for their helpful discussions and constructive suggestions.

Many thanks to current and past members of the Telecommunication Lab at The University of Sydney, including but not limited to Wibowo, Siavash, Shuang, Qimin, Shahriar, Neda, Mahyar, Jing, Kolyan, Rana, Yuehua, Rana, Loris, Di Zhai, Even, Youjia, Matt, Aishah, Yuanyuan and Mingjin, for creating a friendly and pleasant working environment. I am also indebted to all my friends at Sydney, especially Ying

and Jiyang, for making the past years so enjoyable.

I would like to thank my various sources of financial support. Firstly, I would like to acknowledge the Australian Research Council (ARC) for providing the IPRS and APA Scholarships, and the school of Electrical and Information Engineering at the University of Sydney for the Norman I Prize scholarship. Moreover, I would like to thank Prof. Yonghui Li and the University of Sydney's PRSS scheme for their financial support, which allowed me to attend several conferences.

At last, but at most, I wish to express my deepest gratitude to my wife and my parents for their unconditional love, support and encouragement. Their selfless dedication provided the solid foundation of this thesis and I would like to devote all my research achievements to them.

He (Henry) Chen
Sydney, Australia, January 2015

Statement of Originality

The work presented in this thesis is the result of original research carried out by myself, in collaboration with my supervisors, while enrolled in the School of Electrical and Information Engineering at the University of Sydney as a candidate for the Doctor of Philosophy.

These studies were conducted under the supervision of Prof. Yonghui Li and Prof. Branka Vucetic. It has not been submitted for any other degree or award in any other university or educational institution.

He (Henry) CHEN
School of Electrical and Information Engineering
The University of Sydney
January 2015

Abstract

Energy supply to mobile devices has always been a crucial issue faced by the development of wireless communication technologies. Recently, the radio frequency (RF) energy transfer technique, which is capable of supplying continuous and stable energy to wireless terminals over the air, has attracted much attention and has been regarded as a key enabling technique for wireless-powered communications. In such a wireless-powered communication network (WPCN), wireless devices have no embedded energy supply and only use the harvested RF energy to perform information processing/transmission. However, the high attenuation of RF energy transfer over distance has greatly limited the performance and applications of WPCNs in practical scenarios. To overcome this essential hurdle, in this thesis we propose to combat the propagation attenuation by incorporating cooperative communication techniques in WPCNs. This opens a new paradigm named *wireless-powered cooperative communication* and raises many new research opportunities with promising applications. In this thesis, we focus on the novel protocol design, performance analysis and resource allocation of wireless-powered cooperative communication networks (WPCCNs).

Although cooperative communication protocols have been extensively studied in the open literature, they were designed for conventional wireless communication networks. When applying cooperative communication techniques to WPCCNs, both energy transfer and information transmission need to be jointly designed and optimized to achieve the best network performance. As a result, the existing cooperative protocols handling the information transmission only may not be optimal in WPCCNs and new protocols should be developed. To this end, in this thesis we start with a simple WPCCN consisting of one hybrid access-point (AP), one wireless-powered source, and one wireless-powered relay. We propose a harvest-then-cooperate (HTC) protocol for WPCCNs. In HTC, the source and relay harvest energy from the AP in the downlink (DL) and work cooperatively in the uplink (UL) for transmitting

source information. The average throughput of the proposed HTC protocol is then analyzed. This analysis is further extended to the multi-relay scenario, where the average throughput performance of the HTC protocol with two single relay selection schemes is also derived. Numerical results show that the proposed HTC protocol significantly outperforms the existing harvest-then-transmit protocol.

We then consider another setup of WPCCNs, where a wireless-powered source harvests energy from a hybrid AP in the DL and transmits its information to the AP in the UL, under the help of a hybrid relay with a constant power supply. Besides cooperating with the source for UL information transmission, the hybrid relay also transmits RF energy concurrently with the AP during the DL energy transfer phase. This renders a new cooperation scenario, referred to as *energy cooperation*. According to different operations of the hybrid relay, we propose two novel cooperative protocols for the aforementioned WPCCN. We then jointly optimize the time and power allocation for DL energy transfer and UL information transmission to maximize the system throughput of both proposed protocols.

In practice, there could be wireless energy transmitters, referred to as power beacons (PBs), deployed to provide wireless charging services to wireless-powered users via RF energy transfer and these PBs may be installed by other operators. In this context, incentives (e.g., monetary payments) are required to motivate them to provide RF energy to their users. This results in *energy trading* between PBs and their users. In this thesis, we study this practical energy trading problem for a PB-assisted WPCCN consisting of one hybrid AP, one wireless-powered source, and multiple PBs. All PBs are assumed to be installed by different operators. To improve the system performance, the AP hires some PBs to boost the amount of energy harvested at the source by providing them with monetary payments. In this thesis, we take the strategic behaviors of the AP and PBs into consideration and formulate the energy trading process between them as a Stackelberg game. We derive the Stackelberg equilibrium (SE) for the formulated game. As a comparison, we also formulate and resolve the corresponding social welfare optimization problem. Numerical results showed that the social welfare optimization scheme always outperforms the game-theoretical scheme. Moreover, the performance gap between them is enlarged as either the numbers of the PBs or the value of the gain per unit throughput increase, and as the distance between the source and PBs decreases.

RF signals are able to carry not only the energy but also the information and we can

thus explore both to achieve *simultaneous wireless information and power transfer* (SWIPT). In this thesis, we study a large-scale WPCCN with SWIPT, where multiple source-destination pairs communicate through their dedicated wireless-powered relays. Each relay needs to split its received signal from sources into two parts: one for information forwarding and the other for energy harvesting. We develop a distributed power splitting framework using non-cooperative game theory. Specifically, non-cooperative games are respectively formulated for pure amplify-and-forward (AF) and decode-and-forward (DF) networks, in which each link is modeled as a strategic player who aims to maximize its own achievable rate. The existence and uniqueness for Nash equilibriums (NEs) of the formulated games are analyzed and a distributed algorithm with provable convergence to achieve the NEs is also developed. The developed framework is then extended to the more general network setting with mixed AF and DF relays. Simulation results show that the proposed game-theoretical approach can achieve a near-optimal network-wide performance on average, especially for the scenarios with relatively low and moderate interference.

Contents

List of Figures

List of Acronyms

AF	amplify-and-forward
AP	access-point
AWGN	additive white Gaussian noise
BS	base station
CSI	channel state information
D-C	dual cooperation
DF	decode-and-forward
DL	downlink
DSM	demand side management
E-C	energy cooperation
HTC	harvest-then-cooperate
INR	interference-to-noise ratio
MIMO	multiple-input multiple-output
MRC	maximum ratio combining
NE	Nash equilibrium
OR	opportunistic relaying
PB	power beacon
PRS	partial relay selection
RF	radio frequency
RFID	radio-frequency identification
SE	Stackelberg equilibrium
SINR	signal-to-interference-plus-noise ratio

SNR	signal-to-noise ratio
SWIPT	simultaneous wireless information and power transfer
UL	uplink
WET	wireless energy transfer
WIT	wireless information transmission
WPCN	wireless-powered communication network
WPCCN	wireless-powered cooperative communication network

List of Symbols and Notations

η	the RF-to-DC energy conversion efficiency
τ	the time duration for energy transfer
T	the time duration of each transmission block
R	the information transmission rate
$K_n(\cdot)$	the modified Bessel function of the second kind with order n
P_X	the transmit power of node X
d_{XY}	the distance between nodes X and Y
$P_X^{\max}$	the peak power of the node X
P_X^{avg}	the average power of the node X
$\mathbb{E}\{\cdot\}$	the expectation operation
h_{XY}	the channel power gain from node X to node Y
g_{AB}	the channel power gain from node A to node B
$\Pr(A)$	the probability of the event A
$\Pr(A, B)$	the probability of the events A and B happen simultaneously
$I_n(\cdot)$	the modified Bessel function of the first kind with order n
$\min(A, B)$	the minimum between A and B
$\lvert\cdot\rvert$	the absolute value operation

List of Publications

The following is a list of publications in refereed journals and conference proceedings produced during my Ph.D. candidature. In some cases, the journal papers contain material overlapping with the conference publications.

Journal Papers

[J1] H. Chen, Y. Li, Z. Han, Y. Ma, and B. Vucetic, "Energy Trading in Power Beacon-Assisted Wireless-Powered Communication using Stackelberg Game", submitted to *IEEE Transaction on Signal Processing*, Jan. 2015.

[J2] Y. Ma, H. Chen, Z. Lin, Y. Li and B. Vucetic, "Distributed Power Control in Interference Channel with SWIPT: A Game-Theoretic Approach", submitted to *IEEE Transactions on Vehicular Technology*, Feb. 2015.

[J3] Y. Jiang, H. Chen, F. Lau, P. Wang and Y. Li, "Full-Duplex OFDMA Multi-user Cellular Systems: Resource allocation and User Pairing", *IEEE Transactions on Vehicular Technology*, resubmitted after major revisions, Feb. 2015.

[J4] Y. Ma, H. Chen, Z. Lin, Y. Li and B. Vucetic, "Distributed and Optimal Resource Allocation for Power Beacon-Assisted Wireless-Powered Communications", *IEEE Transaction on Communications*, resubmitted after major revisions, Feb. 2015.

[J5] H. Chen, Y. Li, J. L. Rebelatto, B. F. Uchoa-Filho, and B. Vucetic, "Harvest-Then-Cooperate: Wireless-Powered Cooperative Communications", *IEEE Transaction on Signal Processing*, vol. 63, no. 7, April 2015.

[J6] H. Chen, Y. Li, Y. Jiang, Y. Ma, and B. Vucetic, "Distributed Power Splitting

for SWIPT in Relay Interference Channels using Game Theory", *IEEE Transaction on Wireless Communications*, vol. 14, no. 1, pp. 410-420, Jan. 2015.

[J7] H. Chen, Y. Li, R. H. Y. Louie, and B. Vucetic, "Autonomous demand side management based on energy consumption scheduling and instantaneous load billing: an aggregative game approach", *IEEE Transaction on Smart Grid*, vol. 5, no. 4, pp. 1744-1754, July 2014.

[J8] H. Chen, J. Liu, K. K. Wong, Y. Liu, and Z. Dong, "On the performance of selection cooperation with equal gain combining", *IET Signal Processing*, vol. 6, no. 3, pp. 264-272, May 2012.

[J9] H. Chen, J. Liu, Z. Dong, Y. Zhou, and W. Guo, "Exact capacity analysis of partial relay selection under outdated CSI over Rayleigh fading channels", *IEEE Transactions on Vehicular Technology*, vol. 60, no. 8. pp. 4014-4018, Oct. 2011.

[J10] W. Huang, H. Chen, Y. Li and B. Vucetic, "On the Performance of Multi-Antenna Wireless-Powered Communications with Energy Beamforming", accepted to appear in *IEEE Transactions on Vehicular Technology*, Mar. 2015.

[J11] J. Ma, H. Chen, L. Song and Y. Li, "Residential Load Scheduling in Smart Grid: A Cost Efficiency Perspective", accepted to appear in *IEEE Transaction on Smart Grid*, Mar. 2015.

[J12] D. Zheng, J. Liu, K. K. Wong, H. Chen, L. Chen, "Robust peer-to-peer collaborative-relay beamforming with ellipsoidal CSI uncertainties", *IEEE Communications Letters*, vol. 16, no. 4, pp. 442-445, April 2012.

Conference Papers

[C1] H. Chen, Y. Li, Z. Han, and B. Vucetic, "A Stackelberg Game-Based Energy Trading Scheme for Power Beacon-Assisted Wireless-Powered Communication", accepted to appear in Proc. of 2015 IEEE International Conference on Acoustics, Speech and Signal Processing (ICASSP), Brisbane, Australia, April 19-24, 2015.

[C2] H. Chen, Y. Li, J. Li, J. L. Rebelatto, B. F. Uchoa-Filho and B. Vucetic,

"A Harvest-Then-Cooperate Protocol for Wireless Powered Cooperative Communications", in Proc. of 2014 IEEE Global Communications Conference (Globecom), Austin, TX USA, 8-12 December, 2014.

[C3] H. Chen, X. Zhou, Y. Li, P. Wang and B. Vucetic, "Wireless-Powered Cooperative Communications via a Hybrid Relay", in Proc. of 2014 IEEE Information Theory Workshop (ITW), Tasmania, Australia, 2-5 November, 2014.

[C4] H. Chen, Y. Jiang, Y. Li, Y. Ma and B. Vucetic, "A Game-Theoretical Model for Wireless Information and Power Transfer in Relay Interference Channels", in Proc. of 2014 IEEE International Symposium on Information Theory (ISIT), Honolulu, USA, July 2014, pp. 1161-1165.

[C5] H. Chen, R. H. Y. Louie, Y. Li, P. Wang and B. Vucetic, "A Variational Inequality Approach to Instantaneous Load Pricing Based Demand Side Management for Future Smart Grid", in Proc. of 2013 IEEE International Conference on Communications (ICC), Budapest, Hungary, 9-13 June, 2013.

[C6] Y. Gu, H. Chen, Y. Li, and B. Vucetic, "An Adaptive Transmission Protocol for Wireless-Powered Cooperative Communications", accepted to appear in Proc. of 2015 IEEE International Conference on Communications (ICC), London, UK, 8-12 June, 2015.

[C7] Y. Ma, H. Chen, Z. Lin, Y. Li, and B. Vucetic, "Distributed Resource Allocation for Power Beacon-Assisted Wireless-Powered Communications", accepted to appear in Proc. of 2015 IEEE International Conference on Communications (ICC), London, UK, 8-12 June, 2015.

[C8] M. Gao, H. Chen, Y. Li, M. Shirvanimoghaddam and J. Shi, "Full-Duplex Wireless-Powered Communication with Antenna Pair Selection", in Proc. of 2015 IEEE International Conference on Wireless Communications and Networking (WCNC), New Orleans, LA USA, 9-13 March, 2015.

[C9] J. Ma, H. Chen, L. Song and Y. Li, "Cost-Efficient Residential Load Scheduling in Smart Grid", 2014 IEEE International Conference on Communication Systems (ICCS), Macau, China, 19-21 November, 2014.

[C10] Y. Chen, J. Li, H. Chen, Z. Lin, G. Mao and J. Cai, "A Belief Propagation Approach for Distributed User Association in Heterogeneous Networks", in Proc. of 2014 IEEE 25th International Symposium on Personal, Indoor and Mobile Radio Communications (PIMRC), Washington DC, USA, 2-5 September, 2014.

[C11] Y. Ma, Z. Lin, H. Chen and B. Vucetic, "Multiple Interpretations for Multi-source Multi-destination Wireless Relay Network Coded Systems", in Proc. of 2012 IEEE 23th International Symposium on Personal, Indoor and Mobile Radio Communications (PIMRC), Sydney, Australia, 9-12 Sept. 2012.

[C12] D. Zheng, J. Liu, H. Chen and H. Xu, "Optimization for Outage Probability Constrained Robust Downlink Collaborative Beamforming", in Proc. of 2012 IEEE 75th Vehicular Technology Conference (VTC), Yokohama, Japan, 6-9 May 2012.

Chapter 1

Introduction

In this chapter, we first introduce the background and motivation of our research. The principle research problems and the main contributions of this thesis are then summarized.

1.1 Background and Motivation

1.1.1 RF Energy Transfer

In energy-constrained wireless networks, devices are typically powered by batteries with limited operation duration, which significantly confines the network performance. The network lifetime can be extended by frequent battery recharging/repalcement, which, however, is often inconvenient in applications with massive devices (e.g., wireless sensor networks), dangerous for the devices located in toxic environments, or even infeasible in many applications (e.g., implanted medical devices). As a more sustainable approach to prolonging the network's lifetime, the energy harvesting technique has recently drawn significant interest since it allows terminals to replenish their batteries from external energy sources in the surrounding environment.

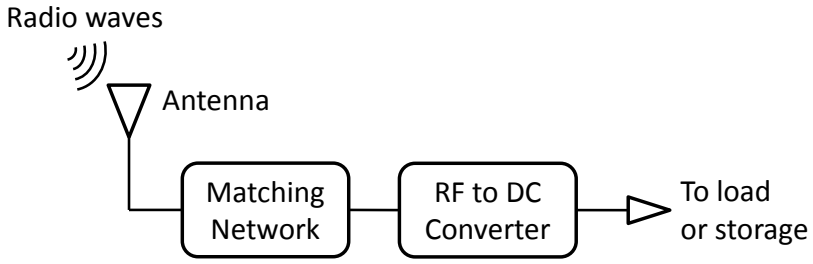

Figure 1.1: Block diagram of a typical RF energy receiver.

Initial efforts on integrating energy harvesting devices into wireless communication systems have mainly focused on renewable energy sources, such as solar, wind, thermal, vibration (see [1–5] and references therein). However, these natural energy sources are usually climate and/or location dependent. For example, in solar and wind energy harvesting communication systems, the amount of energy is highly affected by the duration and strength of solar radiation or wind. The intermittent and unpredictable nature of these renewable energy sources could make the energy harvesting technique inapplicable for many practical applications with minimum quality-of-service requirements.

An alternative energy harvesting technology that can overcome the above limitations is radio frequency (RF) energy transfer. It refers to a wireless energy transfer (WET) process of delivering energy from an energy transmitter wirelessly to charge devices by leveraging the far-field radiative properties of electromagnetic waves [6]. RF energy transfer is characterized by low-power and long-distance energy transfer, and thus is suitable for powering a large number of terminals with low energy consumption, distributed in a relatively wide area [7]. To enable RF energy transfer, a new energy scavenging module, namely an RF energy receiver, should be added to devices. As depicted in Fig. 1.1, an RF energy receiver typically consists of the

following components: a receiver antenna (or antenna array), a matching network, an RF-to-direct current (DC) converter/rectifier [8]. The antenna can be designed to work on either single frequency or multiple frequency bands. The matching network is a resonator circuit operating at the designed frequency to maximize the power transfer between the antenna and the RF-to-DC converter. At last, the converter uses a rectifying circuit to convert RF signals (alternating current signals in nature) into DC voltage, which can either power the load directly or charge an energy storage. The conversion efficiency of the RF energy receiver depends on the accuracy of the impedance matching between the antenna and the converter, and the power efficiency of the converter that rectifies the received RF signals to DC voltage. In RF energy transfer, the amount of harvested energy, E_H, can be calculated based on the Friis equation [9] as follows:

$$E_H = P_T \times G_T \times P_L \times G_R \times \eta \times \tau, \tag{1.1.1}$$

where P_T is the transmit power, G_T is the transmit antenna gain, P_L is the path loss, G_R is the receive antenna gain, η is the RF-to-DC energy conversion efficiency and τ is the energy transfer duration.

Although WET attracted an upsurge of research interest in recent years, it is actually a technology that has been developed for more than 100 years. It can be dated back to the end of 19th century, when Nikola Tesla first carried out a WET experiment and planned to use a power station, called Wardenclyffe Tower, to transmit wireless electricity [10, 11]. Unfortunately, Tesla's experiment was unsuccessful due to its large electric fields that dramatically reduce the power transfer efficiency. But, it shed light on later developments of WET technologies. The readers can refer to [12] for more details of the development history of WET.

It is worth mentioning that in addition to RF energy transfer, there are two other types of WET technologies, namely inductive coupling and magnetic resonant coupling [12, 13]. Inductive coupling [14] is based on magnetic coupling that transfers energy between two coils tuned to the same frequency, which is currently well-standard with many practical applications such as charging mobile phone and medical implanted devices. However, due to the significant drop of magnetic induction effect over distance, inductive coupling typically operates within only a several centimetres range [15]. Magnetic resonant coupling [16] exploits evanescent-wave coupling to generate and transfer energy between two resonators, its operating range can be as large as meters. However, magnetic resonant coupling WET requires the strict alignment of resonators at transmitters and receivers to guarantee high efficiency. Both of these two approaches are near-field WET techniques that exploit the non-radiative electromagnetic properties featured with high power density and conversion efficiency. Therefore, compared with RF energy transfer, they are not good choices for the replenishment/charging of devices in wireless networks.

Compared to energy harvesting from other renewable sources, RF energy transfer technique has appealing characteristics. More specifically, the energy source in RF energy transfer is stable and fully controllable in its transmit power, waveforms and occupied time/frequency resource. This enables RF energy transfer to provide predictable and relatively stable energy to distant devices with energy receivers, which is not subject to weather or location constraints as in energy harvesting techniques based on renewable energy sources. Therefore, the RF energy transfer technique has recently been regarded as a promising solution to power energy-constrained wireless networks [6, 7, 15, 17–19].

1.1.2 Wireless-Powered Communication

RF signals have been primarily used as medium to carry information in wireless communications. Recently, Varshney proposed the concept of making the dual usage of RF signals to not only deliver energy but also transport information in the same network [20]. This has opened a new research paradigm, named wireless-powered communication, where wireless terminals can harvest energy from RF signals radiated by dedicated energy transmitter(s) and use the harvested energy for processing or transmission [15, 19]. In wireless-powered communication networks, wireless devices would not be interrupted by the depletion of their batteries. Thus, wireless-powered communication can be regarded as a potential technology to realize truly perpetual communications. Moreover, it is expected to achieve higher network performance than its battery-powered counterpart with lower maintenance costs and enhanced deployment flexibility.

A conceptual network model of wireless-powered communication is presented in Fig. 1.2 to illustrate two basic operation modes of wireless-powered communication. The first mode is demonstrated by Terminal 1, where a hybrid[1] AP with a constant power supply transmits energy to Terminal 1 in the downlink (DL), and then Terminal 1 transmits information to the hybrid AP in the uplink (UL) using the energy harvested in the DL. Alternatively, the hybrid AP can also transmit information and energy jointly using the same RF signals, as depicted by Terminal 2 in Fig. 1.2. This operating mode is referred to as simultaneous wireless information and power transfer (SWIPT), which is shown to be more efficient in spectrum usage than transmitting information and energy in orthogonal time or channels. In SWIPT, the receivers

[1]We use "hybrid" here because that the AP can not only receive information but also transfer RF energy.

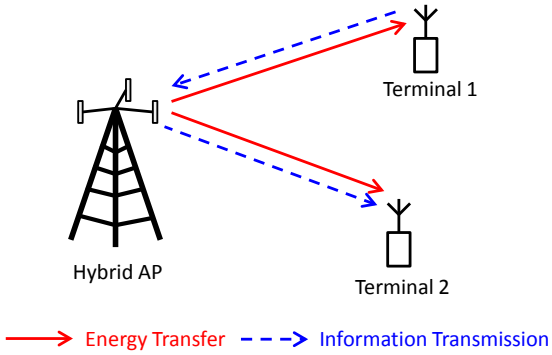

Figure 1.2: A conceptual network model for wireless-powered communication.

need to perform both information decoding and energy harvesting in the DL with the same received signals. An ideal SWIPT receiver is assumed to be able to harvest energy and decode information from the same signal [20]. However, this could not be achieved by practical circuits currently. To realize SWIPT practically, the received signal should be split in two distinct streams, one for energy harvesting and the other for information decoding. Some practical receiver structures for SWIPT, such as time switching [21], power splitting [21], antenna switching [21, 22], spatial switching [18] and integrated receiver [23], have been proposed in the literature. Besides, the design of SWIPT schemes for different wireless networks has attracted significant attention recently. SWIPT schemes for multiple-input-multiple-output (MIMO) broadcasting channels and multiple-input-single-output (MISO) interference channels were designed and evaluated in [21] and [24], respectively. The resource allocation algorithms for SWIPT in broadband wireless systems were investigated in [25], while an energy-efficient resource allocation algorithm was developed in [26] for SWIPT in orthogonal-frequency-division-multiple-access (OFDMA) systems.

Wireless-powered communication has already had many applications in practice

[27]. The most widely applied application of this technique could be wireless sensor networks, in which sensor nodes are equipped with an RF energy harvester to supply their energy. This kind of application has been successfully demonstrated by a prototype developed by Powercast Corp. [28], in which an energy transmitter continuously sends RF signals at 915MHz and the energy harvester on the sensor board converts the RF signals to DC voltage to power the information communication from the sensor board to a AP at 2.4GHz using 802.15.4-compliant radios. Another application of wireless-powered communication that has attracted intensive research is radio-frequency identification (RFID), which has been widely used for communication, identification, tracking and inventory management [29]. With recent development in wireless-powered communication, conventional RFID techniques have evolved from simple passive tags to smart tags with newly introduced functions such as sensing, on-tag data processing and intelligent power management. A good example of this kind of application is the wireless identification and sensing platform [27]. The wireless-powered communication technique also has attractive healthcare and medical applications, e.g., wireless body network [30].

Due to the high attenuation of RF energy over distance, wireless-powered communication is currently applied in wireless networks with low-power devices, such as sensors and RFID tags. However, with recent advances in wireless communication, such as small cells [31] and millimeter wave [32], the size of cellular networks will be significantly reduced and communication distances between the nodes will be decreased as well. For such short distance transmissions in future cellular networks, the propagation loss would not be very severe and the harvesting efficiency of RF energy transfer can be significantly increased by exploiting the sharp beamforming [19] in

massive MIMO systems [33]. Moreover, the operating power of wireless devices is continuously decreasing. Therefore, it can be deduced that wireless-powered communication technology will be an indispensable and irreplaceable building block of many commercial and industrial systems in the near future, including the upcoming internet of things (IoT) and wireless sensor networks [15].

1.1.3 Cooperative Communication

Another important technology which can effectively combat the propagation loss of wireless information or energy transmission is cooperative communication. It has attracted an upsurge of interest during the past decade due to its various advantages (see [34–41] and references therein). The key feature of cooperative communication is to enable single-antenna devices to share their antennas and transmit cooperatively such that a virtual MIMO can be constructed to achieve transmit diversity. As a result, the overall quality of the wireless transmission, such as reception reliability, energy efficiency, and network capacity, can be enhanced significantly [40]. Note that the concept of cooperative communication can actually be traced back to the early work of Cover and Gamal on the achievable capacity of a relay network [42], which analyzed the capacity of a three-node network consisting of a source, a destination, and a relay. Cooperative communication has demonstrated its great potential applications in cellular and wireless sensor networks. For example, it has recently been integrated into one of state-of-the-art features of 3GPP LTE-Advanced (LTE-A) [41].

Fig. 1.3 illustrates a classic three-node cooperative communication system that has been widely used in the existing literature. In this system, a source (S) transmits its information to a destination (D) with the help of a relay (R). This cooperative

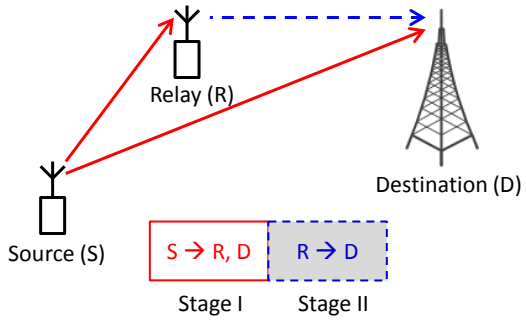

Figure 1.3: A classic three-node cooperative communication system.

communication includes two different transmission links. Besides a direct transmission channel from the source to the destination, there is an indirect channel from the source through the relay to the destination. A typical cooperative transmission can be divided into two stages. During the first stage (Stage I), the source broadcasts its information where both relay and destination nodes are listening. During the second stage (Stage II), the relay forwards the received signal to the destination. Therefore, the destination node receives two copies of the same packets transmitted through different wireless channels. This generates spatial diversity because the fading paths from the source and relay are statistically independent in general.

Design of efficient cooperative protocols has been an important issue in implementing cooperative communication in wireless networks. There are many existing strategies that can be applied on the relay node to process the signals received from the source node. The two most widely-used protocols are amplify-and-forward (AF) and decode-and-forward (DF). AF is one of the simplest relay protocols, where the relay node just simply forwards to the destination a scaled version of the received signals, including both information and noise. In contrast, in DF protocol, the relay decodes the received signals and re-encodes them before forwarding to the destination

to eliminate the noise effect.

In practice, there may be multiple relay nodes between the source and destination nodes. For such a multi-relay topology, a critical issue is how to use the relay nodes efficiently, including how many relay nodes are needed for data forwarding and how the selected relay nodes are configured. The system performance can be significantly improved by jointly optimizing the number of selected relays and performing the optimal resource allocation between them. However, such joint design is very complex and may not be suitable for some practical scenarios. Motivated by this, some simple and effective relay transmission strategies have been proposed. Among them, the single relay selection scheme that selects the "best" relay is attractive, since it minimizes the overhead due to orthogonal channels and also reduces the complexity of the selection process [43]. Several representative single relay selection schemes, such as opportunistic relaying (OR) [44], partial relay selection (PRS) [45], and selection cooperation [46], have been proposed and investigated for different cooperative communication scenarios.

1.1.4 Wireless-Powered Cooperative Communications

As we mentioned, the performance and applications of wireless-powered communications are still limited due to the high attenuation of RF energy over distance. On the other side, the cooperative communication technique has been developed and adopted to combat the propagation attenuation in conventional communication networks by achieving transmit diversity. Now, a natural question, which arises when the wireless-powered communication and cooperative communication techniques are put together, is "*how to efficiently implement the cooperative communication technique*

in wireless-powered communication network (WPCNs) to improve their performance and expand their applications?". This open and interesting question actually motivates this thesis. Although cooperative schemes for conventional networks have been well-studied, they were designed mainly for the purpose of information transmission and may no longer be suitable for WPCNs, in which wireless signals are used to not only carry information and but also deliver energy. Considering this inherent energy transfer feature in WPCNs, new cooperative protocols should be proposed for WPCNs, the network performance should be re-analyzed and the network resource allocation should be re-designed.

Besides the cooperation for information transmission as in conventional cooperative networks, the new usage of RF signals for the delivery of energy in WPCNs can render a new manner of cooperation. In particular, several wireless power transmitters can cooperatively transfer RF energy to charge the same terminal in WPCCNs, which is referred to as *energy cooperation* in this thesis. In the context of a cellular WPCN, [47] proposed the concept of installing wireless energy transmitters, named power beacons, to provide energy for mobile users to transmit data to their base stations (BSs). By assuming that power beacons (PBs) are deployed by the cellular network operator and resorting to the stochastic geometry theory, the functional relationships between the densities of BSs and PBs as well as their transmit power to achieve a prescribed communication outage probability were also derived. However, wireless energy transmitters may belong to different operators in practice. Thus, incentives (e.g., monetary payments) are needed for them to provide RF energy (i.e., a wireless charging service), which leads to *energy trading* between them and their users. A new framework should be developed to model and evaluate this practical

energy trading process in WPCNs.

The new paradigm SWIPT also opens up another new cooperation pattern for WPCNs. That is, a wireless-powered[2] relay can be deployed between a source-destination pair to first harvest energy and receive the message dedicated to the destination from the source, and then use the harvested energy to forward the received signal to the destination. This cooperation concept was first proposed in [48], where the performance of a typical three-node network was comprehensively studied. However, many source-relay-destination links may coexist and interfere mutually in practice, e.g., multi-cell networks. In this case, an efficient resource allocation approach that jointly considers the information transmission and energy transfer should be designed to achieve a good network-wide performance.

It is worth mentioning that the work in [48] has been extended in different aspects recently, such as MIMO relay system [49, 50], full-duplex relaying system [51], multiple source-destination pairs system [52], and multiple relay system with relay selection [53]. This thesis first studies the setup of relay interference channel with SWIPT. More potential future works along this direction has been identified in [54]. Note that these works considered that wireless energy transfer and wireless information transmission are in the same direction and focused on the characterization of the fundamental tradeoffs between energy transfer and information transmission. This is essentially different with other studied setups in this thesis, where the nodes need to first harvest RF energy in DL before transmitting information in the UL.

[2]In this thesis, a device without an embedded power supply and only powered by RF energy transfer is referred to as a wireless-powered device.

1.2 Research Problems and Contributions

In this thesis, a WPCN with cooperative techniques is referred to as a wireless-powered cooperative communication network (WPCCN). The focus of this thesis is on the protocol design, performance analysis and resource allocation of WPCCNs. The outcomes of this thesis will lead to new fundamental engineering design insights. The principle research problems and the corresponding contributions are elaborated as follows.

The *first* research problem we tackle in this thesis (Chapter 2) is how to develop a novel cooperative protocol for a time-switching WPCCN with DL WET and UL wireless information transmission (WIT). The considered network consists of a hybrid AP, a (information) source, and a relay that has no traffic and is willing to assist the information transmission of the source. The hybrid AP is connected to a constant power supply, while the source and relay are assumed to have no embedded energy sources. But they are equipped with a rechargeable battery and thus can harvest and store the RF energy broadcast by the hybrid AP. The main contributions regarding this research problem include:

- Based on the three-node reference model, we propose a harvest-then-cooperate (HTC) protocol for the considered WPCCN, *where the source and relay harvest energy from the AP during the DL phase and cooperate for the source's information transmission during the UL phase*. The AF relaying scheme [55] and the selection combining technique [56] are assumed to be implemented at the relay and the AP, respectively. Considering the delay-limited transmission mode [48], we derive the approximate closed-form expression of the average throughput for the proposed HTC protocol over Rayleigh fading channels.

- We subsequently extend the analysis to the multi-relay scenario, where the single relay selection technique is implemented. In particular, we consider that only one of relays will be selected out according to a certain criterion in each transmission block, and the selected relay will use the energy harvested in this block to forward the received signal from the source. Two popular relay selection schemes, i.e., opportunistic relaying and partial relay selection, are considered and the corresponding throughput performances are also analyzed.

- All theoretical results are validated by numerical simulations. The impacts of various system parameters, such as time allocation, relay number, and relay position, on the throughput performance of the considered schemes are extensively investigated. Numerical results show that the proposed scheme outperforms the existing *non-cooperative* harvest-then-transmit protocol [57] in all simulated cases.

The *second* research problem in this thesis (Chapter 3) is the development of new cooperative protocols for another practical setup of WPCCNs, where *a wireless-powered source harvests energy from a hybrid AP in the DL and transmits its information to the AP in the UL, under the help of a hybrid*[3] *relay with a constant power supply*. In this model, the hybrid relay can not only cooperate with the source for UL information transmission but also concurrently transmit RF energy to the source with the AP during the DL phase. The main contributions along this research problem include:

- We develop two new cooperative protocols, namely energy cooperation (E-C)

[3]Similar to the hybrid AP, we use "hybrid relay" here as the relay is not only an information forwarder but also an RF energy transmitter.

and dual cooperation (D-C), with different relay operations for the considered WPCCN. In the E-C protocol, the relay simply cooperates with the AP for DL energy transfer. In the D-C protocol, the relay first cooperates with the AP for energy transfer in the DL and then cooperates with the source for information transmission in the UL.

- We also formulate optimization problems to maximize the system throughput by jointly designing the time allocation and power allocation for the two proposed protocols, respectively. The optimal solutions are subsequently derived and compared by simulations.

- Numerical results show that the two proposed protocols can outperform each other in different network scenarios, which provides useful insights into the design of the hybrid relay in WPCCNs.

The *third* research problem in this thesis (Chapter 4) is on the development of an energy trading framework for a PB-assisted WPCCN consisting of one hybrid AP, one wireless-powered source, and multiple PBs that can potentially help the AP charge the source. The AP needs to collect the information from a source with no embedded power supply. Thus, the AP has to first transfer energy to the source in the DL before the source transmits information in the UL. Besides, there are multiple PBs nearby the source, which are assumed to be deployed by different operators. They provide wireless charging services such that they can assist the AP to charge the source in the DL.

To improve the system performance, the AP can rent some PBs to boost the amount of energy harvested at the source. However, since the PBs are installed

by different operators, they may be rational and self-interested such that monetary payments are needed to motivate them to get involved during the DL energy transfer phase. In this case, the AP would value its achievable throughput over its total payment to the PBs. On the other hand, the PBs consider not only the payments received from the AP but also their energy cost to provide the charging service. To embrace the strategic behaviors of the AP and PBs, we apply game theory [58, 59] to model this energy trading process. The main contributions regarding this research problem are summarized as follows:

- We develop an energy trading framework for this PB-assisted WPCCN using game theory. Specifically, we take the strategic behaviors of the AP and PBs into consideration and formulate the energy trading process between them as a Stackelberg game [60, 61]. In the formulated game, the AP acts as a leader who buys energy from the PBs to charge the source by offering an energy price on per unit of harvested energy from the RF signals radiated by the PBs. The AP optimizes its energy price and DL energy transfer time to maximize its utility function defined as the difference between the benefits obtained from the achievable throughput and its total payment to the PBs. On the other hand, the PBs are the followers of the formulated game, and determine their optimal transmit powers based on the released energy price from the AP to maximize their own profits. The profit of each PB is defined as the payment received from the AP minus its energy cost.

- We derive the Stackelberg equilibrium (SE) for the formulated game. Note that the number of involved PBs with positive transmit powers is actually a variable in the formulated game and largely affected by the energy price released by the

AP. This means that the specific expression of the AP's utility function should depend on the value of the released energy price. On the other hand, different forms of the AP's utility function can lead to different optimal values of the energy price and DL energy transfer time. This special property inherent in the formulated game makes it hard to derive closed-form expressions for the SE. Motivated by this, we solve the formulated game in two steps: we first derive a closed-form expression for the optimal energy price with a given DL energy transfer time. The optimal value of the DL energy transfer time is subsequently achieved in the second step via a one-dimensional search.

- To characterize the performance loss due to the self-interested behaviors of the PBs, we also formulate and resolve the corresponding social welfare optimization problem, in which the PBs are cooperative such that they can be fully controlled by the AP to maximize the social welfare, defined as the difference between the utility obtained from the achievable throughput at the AP and the total cost of the PBs. Numerical results showed that the social welfare optimization scheme always outperforms the game-theoretical scheme. Moreover, the performance gap between them is enlarged as either the numbers of the PBs or the value of the gain per unit throughput increase, and as the distance between the source and PBs decreases.

The *fourth* research problem in this thesis (Chapter 5) is on the design of a distributed power splitting framework for a large-scale WPCCN with SWIPT, where multiple source-destination pairs communicate via their dedicated wireless-powered relays. Each relay adopts the power splitting technique [21] and splits the signal received from all source nodes into two parts according to a power splitting ratio: one

part is sent to the information processing unit, and the rest is used to harvest energy for forwarding the received information in the second time slot. We consider that each link's performance is characterized by its achievable rate and thus regard the sum-rate of all links as a network-wide performance metric. The first natural question that arises from this system is "*how should the relays split their received signals for information receiving and energy harvesting in order to achieve a good network-wide performance?*". This is actually a very complex question to answer. The reason is that the power splitting ratio of each link not only affects the performance of this link, but also affects the performance of other links due to mutual interference between different links. This means that the optimization of each ratio depends on all other ratios and they are tangled together. Moreover, the maximization of the sum-rate of all links is shown to be a non-convex optimization problem. The global optimal power splitting ratios cannot be efficiently achieved even in a centralized fashion, and there is a heavy signaling overhead required by the centralized method.

To tackle the aforementioned problem, we apply the non-cooperative game theory to develop a distributed power splitting framework for the considered WPCCN with SWIPT. We consider both pure and hybrid networks. In a pure network, all relays adopt the same relaying protocol. We further classify a pure network into a pure AF network and a pure DF network. On the other hand, in a hybrid network, a mixture of AF and DF relaying protocols are implemented at the relays. The main contributions regarding this research problem are summarized as follows:

- We develop a distributed power splitting framework for a large-scale WPCCN with SWIPT consisting of multiple source-relay-destination links. In particular, each source-relay-destination link in the relay interference channels is modeled

as a strategic player who chooses its dedicated relay's power splitting ratio to maximize its individual rate.

- We analyze the existence and uniqueness of the Nash equilibrium (NE) for the formulated game in the pure network, where all relays employ either AF or DF relaying protocol. In addition, a distributed algorithm is proposed with provable convergence to achieve the NEs of pure networks. The theoretical analysis for pure networks is then extended to a more general hybrid network with mixed AF and DF relays coexisting.

- All analytical results are validated by extensive numerical simulations, which show that the proposed game-theoretical approach can achieve a near-optimal network-wide performance on average.

1.3 Additional Related Contributions

During this Ph.D. study, several other related contributions were made, which are not included in this thesis in order to maintain focus. But, the respective details can be found in my publications listed in the preface section. The additional contributions include:

- We apply game theory to study a practical demand side management (DSM) scenario in a smart grid, where the selfish consumers compete to minimize their individual energy cost through scheduling their future energy consumption profiles. We adopt an instantaneous load billing scheme to effectively convince the consumers to shift their peak-time consumption and to fairly charge the consumers for their energy consumption (see our publication [J7]).

  - For the considered DSM scenario, an aggregative game is first formulated to model the strategic behaviors of the selfish consumers. By resorting to the variational inequality theory, we analyze the conditions for the existence and uniqueness of the NE of the formulated game.
  - For the scenario where there is a central unit calculating and sending the real-time aggregated load to all consumers, we develop a one timescale distributed iterative proximal-point algorithm with provable convergence to achieve the NE of the formulated game.
  - Considering the alternative situation where the central unit does not exist, but the consumers are connected and they would like to share their estimated information with others, we present a distributed synchronous agreement-based algorithm and a distributed asynchronous gossip-based algorithm, by which the consumers can achieve the NE of the formulated game through exchanging information with their immediate neighbors.

- Other collaborative contributions, for which I was mainly a secondary contributor, include:
  - We develops a new distributed power control scheme for a power splitting-based interference channel (IFC) with SWIPT, which consists of multiple source-destination pairs. Each pair adjusts its transmit power and power splitting ratio to meet both the signal-to-interference-plus-noise ratio (SINR) and energy harvesting (EH) constraints at its corresponding destination. We apply non-cooperative game theory to characterize rational

behaviors of source-destination pairs. Specifically, we formulate a non-cooperative game for the considered system, where each pair is modeled as a strategic player who aims to minimize its own transmit power under both SINR and EH constraints at the destination. A sufficient condition for the existence and uniqueness of the NE is provided and the best response strategy of each player is derived to achieve the NE iteratively (see our publication [J2]).

– We investigate optimal resource allocation for a PB-assisted WPCCN, which consists of a set of hybrid AP-source pairs and a power beacon. Each source, which has no embedded power supply, first harvests energy from its associated AP and/or the PB in the DL and then uses the harvested energy to transmit information to its AP in the UL. We design distributed algorithms for both cooperative and non-cooperative scenarios based on whether the PB is cooperative with the APs or not (see our publication [J4]).

– We analyze the average throughput performance of energy beamforming in a multi-antenna WPCN. The considered network consists of one hybrid AP with multiple antennas and a wireless-powered user with a single antenna. Closed-form expressions for the average throughput and their asymptotic expressions at high signal-to-noise ratio (SNR) are derived for both delay-limited and delay-tolerant transmission modes. The optimal DL energy harvesting time, which maximizes the system throughput, is then obtained for high SNR (see our publication [J10]).

– We first introduce a novel concept of a cost efficiency-based residential load

scheduling framework in a smart grid to improve the economical efficiency of residential electricity consumption. The cost efficiency is defined as the ratio of a consumer's total consumption benefit to its total electricity payment during a certain period. We develop a cost-efficient load scheduling algorithm for the demand-side's day-ahead bidding process and real-time pricing mechanism by using a fractional programming approach (see our publication [J11]).

Chapter 2

A Harvest-Then-Cooperate Protocol for Wireless-Powered Cooperative Communications

In this chapter, we consider a WPCCN consisting of one hybrid AP, one source, and one relay. The source and relay in the considered network have no embedded energy supply, and need to rely on the energy harvested from the signals broadcasted by the AP for their cooperative information transmission. Based on this three-node reference model, we propose a HTC protocol, in which the source and relay harvest energy from the AP in the downlink and work cooperatively in the uplink for the source's information transmission. Considering a delay-limited transmission mode, the approximate closed-form expression for the average throughput of the proposed protocol is derived over Rayleigh fading channels. Subsequently, this analysis is extended to the multi-relay scenario, where the approximate throughput of the HTC protocol with two representative single relay selection schemes is derived. The asymptotic analysis for the throughput performance of the considered schemes at high SNR are also provided.

2.1 Introduction

As a sustainable solution to prolonging the lifetime of energy constrained wireless networks, the energy harvesting technique has recently drawn significant attention, e.g. see [2] and references therein. It enables wireless nodes to collect energy from the surrounding environment. Apart from the conventional renewable energy sources such as solar and wind, RF signals radiated by dedicated/ambient transmitters can be treated as a viable new source for energy harvesting. Thus, RF signals can be used to deliver information as well as energy. In recent years, some significant advances in wireless power technologies have highly increased the feasibility of RF energy transfer in practical wireless applications [12]. As an example, the successful communication between two terminals solely powered by ambient radio signals, such as the existing TV and cellular signals, has been realized and reported in [62]. Besides ambient radio signals, dedicated energy transmitters are deployed to implement RF energy transfer in some applications, e.g., passive RFID networks [27]. Moreover, with further advances in antenna technology and energy harvesting circuit designs, RF energy transfer is believed to be more efficient such that it will be implemented widely in the near future.

In this context, a new type of wireless network, termed wireless-powered communication network, has become a promising research topic and attracted more and more attention. In WPCNs, the wireless terminals are powered only by RF energy transfer and transmit their information using the harvested energy. The WPCNs under different setups have been studied in open literature. Specifically, [47] proposed a new network architecture to enable wireless energy transfer in hybrid cellular networks, where an uplink cellular network overlays with randomly deployed power

beacons for powering mobiles by microwave radiation. In [47], the deployment of this hybrid network under an outage constraint on data links was designed using the stochastic-geometry theory. In [63], a medium access control (MAC) protocol was proposed for sensor networks powered by RF energy transfer. RF energy transfer was considered for cognitive radio networks in [64], where secondary transmitters harvest ambient RF energy from transmissions by nearby active primary transmitters.

The throughput and energy-efficiency maximization of one-user WPCNs were considered in [65, 66], where a multi-antenna AP wirelessly charges a single-antenna user in the DL and receives the signal from the user in the UL. A classic multi-user WPCN was first investigated in [57]. In this work, a "harvest-then-transmit" protocol was developed, where the users first collect energy from the signals broadcasted by a single-antenna hybrid AP in the DL and then use their harvested energy to send *independent* information to the hybrid AP in the UL based on the time-division-multiple-access (TDMA). A similar network setup with a multi-antenna AP was investigated in [67], where multiple users can simultaneously transmit information to the AP in the UL through the space-division-multiple-access technique after they harvest energy in the DL. The minimum throughput of all users was maximized by jointly optimizing the time allocation, the DL energy beams, the UL transmit power allocation, and the receive beamforming vectors. Very recently, the full-duplex technique was adopted to further improve the performance of a multi-user WPCN in [68, 69], where the hybrid AP implements full-duplex using two antennas: one for broadcasting wireless energy to users in the DL and the other for receiving independent information from users via TDMA in the UL at the same time. Moreover, the throughput of a massive MIMO WPCN was optimized in [70], in which the hybrid AP is assumed to be equipped

with a large number of antennas.

On the other hand, cooperative diversity technique has rekindled enormous interests from the wireless communication community over the past decade. The key idea of this technique is that single-antenna nodes in wireless networks share their antennas and transmit cooperatively as a virtual MIMO system, thus spatial diversity can be achieved without the need of multiple antennas at each node [55, 71]. The advantages of this technique, such as increasing system capacity, coverage and energy efficiency, have been demonstrated by numerous papers in open literature. Very recently, the concept of user cooperation was applied to a WPCN in [72], where a (hybrid) destination node first charges two cooperative source nodes with wireless energy transfer and then collects information from them. A time-switching network-coded cooperative protocol was proposed, by which two source nodes can cooperatively transmit their information in two consecutive transmission blocks. The outage performance of the considered system was analyzed and optimized with respect to the time allocation parameter [72]. In cooperative networks, another (asymmetric) model, in which the relay nodes are deployed for information forwarding only, also has many applications in practice. However, to the best of our knowledge, there is no work that considered the design of the aforementioned model for WCPNs in open literature. This gap actually motivates our work in this chapter.

In this chapter, we study a time-switching cooperative communication network with DL WET and UL WIT. As shown in Fig. 2.1, the considered network consists of one hybrid AP, one (information) source (S), and one relay (R) that has no traffic and is willing to assist the information transmission of the source. The hybrid AP is connected to a constant power supply, while the source and relay are assumed to

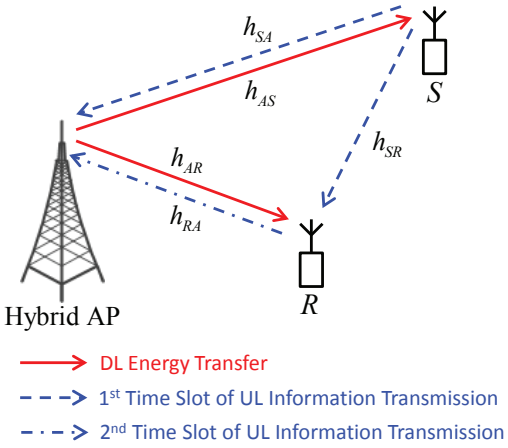

Figure 2.1: A reference model for a three-node WPCCN with energy transfer in the DL and cooperative information transmission in the UL.

have no other energy sources. But they are equipped with a rechargeable battery and thus can harvest and store the wireless energy broadcasted by the hybrid AP. Unlike prior work on the design of SWIPT in relay networks (e.g., [48, 52]) that focused on the WET and WIT in the same direction, we consider the scenario with WET in the DL and WIT in the UL[1]. Particularly, the hybrid AP broadcasts only wireless energy to the source and relay in the DL, while the source and relay cooperatively transmit the source's information using their individual harvested energy to the hybrid AP in the UL.

Based on the three-node reference model depicted in Fig. 2.1, in this chapter we propose a HTC protocol for the WPCCN, where the source and relay harvest energy from the AP during the DL phase and cooperate for the source's information transmission during the UL phase. The AF relaying scheme [55] and the selection combining technique [56] are assumed to be implemented at the relay and the AP,

[1]A more general setup is that with both WET and WIT in the DL and WIT in the UL. For the purpose of exposition, we ignore the DL WIT in this chapter.

respectively. Considering the delay-limited transmission mode [48], we derive the approximate closed-form expression of the average throughput for the proposed HTC protocol over Rayleigh fading channels. We subsequently extend the analysis to the multi-relay scenario, where the single relay selection technique is implemented. In particular, we consider that only one of the relays will be selected according to a certain criterion in each transmission block, and the selected relay will use the energy harvested in this block to forward the received signal from the source. Two popular relay selection schemes, i.e., opportunistic relaying and partial relay selection, are considered and the corresponding throughput performances are also analyzed. All theoretical results are validated by numerical simulations. The impacts of the system parameters, such as time allocation, relay number, and relay position, on the throughput performance of the considered schemes are extensively investigated. Numerical results show that the proposed scheme outperforms the *non-cooperative* harvest-then-transmit protocol [57] in all simulated cases.

It is worth emphasizing that the analytical approach adopted in this chapter is technically different from the existing ones for conventional cooperative networks. One difference is that the SNR of each link in the considered WPCCN is proportional to the product of two exponential random variables instead of one variable as in conventional cooperative networks. However, this is not the principal technical difference: due to the inherent energy transfer process in the considered WPCCN, the source's transmit power in the uplink is a random variable instead of a constant as in conventional cooperative networks. This makes the SNRs of the source-AP link and all source-relay-AP links mutually correlated, which is essentially different from the conventional cooperative networks with independent link SNRs. As a result, the

analytical tools for conventional cooperative networks cannot be directly used here.

The rest of this chapter is organized as follows. The system model and the proposed HTC protocol are described in Section 2.2. Section 2.3 derives the approximate closed-form expression for the average throughput of the proposed protocol in the three-node reference model. The extension to the multi-relay scenario is discussed and analyzed in Section 2.4. The simulation results are presented in Section 2.5 to validate the theoretical analyses and demonstrate the impacts of the system parameters.

Notations: Throughout this chapter, $\mathbb{E}\{\cdot\}$ and $|\cdot|$ denote the expectation and the absolute value operations, respectively. $X \sim \mathcal{CN}(\mu, \sigma^2)$ stands for a circularly symmetric complex Gaussian random variable X with mean μ and variance σ^2, while $X \sim \text{EXP}(\lambda)$ represents an exponentially distributed random variable X with mean λ. $\Pr(A)$ and $\Pr(A, B)$ denote the probability that the event A happens and the probability that the events A and B happen simultaneously, respectively.

2.2 System Model and Description of Protocol

As shown in Fig. 2.1, this chapter considers a WPCCN with energy transfer in the DL and cooperative information transmission in the UL. It is assumed that all nodes are equipped with one single antenna and work in the half-duplex mode. In addition, the source and relay are assumed to have no other embedded energy supply and thus need to first harvest energy from the signal broadcasted by the AP in the DL, which can be stored in a rechargeable battery and then used for the information transmission to the AP in the UL.

In the sequel, we use subscript-A for AP, subscript-S for source, and subscript-R

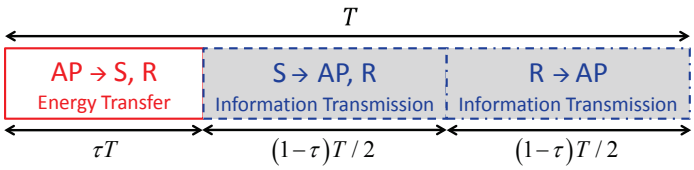

Figure 2.2: Diagram of the harvest-then-cooperate protocol.

for relay. We use $\tilde{h}_{XY} \sim \mathcal{CN}(0, \sigma_{XY}^2)$ to denote the channel coefficient from X to Y with $X, Y \in \{A, S, R\}$. The channel power gain $h_{XY} = \left|\tilde{h}_{XY}\right|^2$ from X to Y thus follows the exponential distribution with the mean σ_{XY}^2, i.e., $h_{XY} \sim \text{EXP}(\sigma_{XY}^2)$ [56]. In addition, it is assumed that all channels in both DL and UL experience independent slow and frequency flat fading, where the channel gains remain constant during each transmission block (denoted by T) but change independently from one block to another.

The proposed HTC protocol for the considered network is shown in Fig. 2.2. Specifically, in each transmission block of time duration T, the first τT amount of time with $0 < \tau < 1$ is assigned to the DL energy transfer from the AP to the source and relay. The remaining fraction $1 - \tau$ of the block is further divided into two time slots with the equal length of $(1 - \tau) T/2$ for cooperative information transmission in the UL. During the first time slot of the UL, the source uses the harvested energy to transmit data information to the AP, which can also be overheard by the relay due to the broadcasting feature of wireless communication. In the second time slot of the UL, the relay will use the energy harvested during the DL phase to help forwarding the source information through employing the AF relaying protocol due to its lower complexity[2] [55]. To reduce the complexity of the receiver structure, we assume

[2]In this chapter, the possibility of the source harvesting energy during the relay's transmission is not taken into account. Such amount of energy is neglected since, as commented in [72, 73], the energy transfer efficiency is maximized for narrowband links that operate at low frequencies.

that the selection combining (SC) technique[3] [56, 74] is implemented for information processing at the AP. Moreover, the SC technique enables the tractable closed-form analysis of the considered system. Specifically, the information receiver of the AP will select one of the received signals from the source and relay during the UL phase, which has larger SNR, to decode the source's information at the end of each block.

Let P_A denote the transmission power of the AP during the DL phase. Also, we assume that P_A is sufficiently large such that the energy harvested from the noise is negligible. Thus, the amount of energy harvested by the source and relay can be expressed as [57]

$$E_S = \eta\tau T P_A h_{AS}, \text{ and } E_R = \eta\tau T P_A h_{AR}, \tag{2.2.1}$$

where $0 < \eta < 1$ is the RF-to-DC energy conversion efficiency. The state-of-the-art rectenna technology can achieve close-to-one (e.g., 80%) efficiency [75]. For convenience but without loss of generality, we consider a normalized unit block time (i.e., $T = 1$) hereafter.

After the terminals replenish their energy during the DL phase, they work cooperatively for the information transmission in the subsequent UL phase. For the purpose of exploration, we follow [48, 57] and assume that both terminals exhaust the harvested energy for uplink information transmission. Note that instead of exhausting their harvested energy, the source and relay can also choose to perform power control (allocation) across different transmission blocks to further improve the network performance, which, however, is out the scope of this chapter. On the other hand, the

(*continued the footnote of the previous page*) However, the relay's data transmission needs a high data rate with even larger bandwidth and consequently leads to a lower energy harvesting efficiency.

[3]Note that besides SC, other signal combination schemes (e.g., maximal ratio combining (MRC)) can also be applied in the considered system. However, it is very complicated to derive the closed-form expression on MRC performance. This has been considered as the future work.

network throughput performance derived in this chapter can actually be treated as the lower bound of the aforementioned power control scenario.

The transmit power of the source and relay during the UL phase are thus given by

$$P_S = E_S/\left[(1-\tau)/2\right] = 2\eta\tau P_A h_{AS}/\left(1-\tau\right), \tag{2.2.2}$$

$$P_R = E_R/\left[(1-\tau)/2\right] = 2\eta\tau P_A h_{AR}/\left(1-\tau\right). \tag{2.2.3}$$

Thus, the received SNR at the AP after the source's transmission can be written as

$$\gamma_{SA} = P_S h_{SA}/N_0 = \mu h_{AS} h_{SA}, \tag{2.2.4}$$

where N_0 is the power of the noise suffered by all receivers and

$$\mu = 2\eta\left(P_A/N_0\right)\tau/(1-\tau). \tag{2.2.5}$$

At the same time, the signal sent by the source can also be overheard by the relay. In the second time slot of the UL phase, the relay will amplify and forward the received signal to the AP using the power P_R given in (2.2.3) and the amplification factor $\beta = 1/\sqrt{P_S h_{SR} + N_0}$ [76]. After some algebraic manipulations, we can express the received SNR at the AP from the link *S-R-A* as

$$\gamma_{SRA} = \frac{\mu h_{AS} h_{SR} \mu h_{AR} h_{RA}}{\mu h_{AS} h_{SR} + \mu h_{AR} h_{RA} + 1}. \tag{2.2.6}$$

Since the SC technique is adopted at the AP receiver, the output SNR of the HTC protocol is given by

$$\gamma_A = \max\left(\gamma_{SA}, \gamma_{SRA}\right). \tag{2.2.7}$$

In the following section, we will analyze the average throughput performance of the proposed HTC protocol in the three-node reference model depicted in Fig. 4.1.

2.3 Throughput Analysis of the HTC Protocol

In this chapter, we consider the delay-limited transmission mode, where the average throughput can be obtained by evaluating the outage probability of the system with a fixed transmission rate [48]. Specifically, the throughput of a given system with transmission rate R, outage probability P_{out} and transmission duration t is given by $R(1-P_{\text{out}})t$.

To facilitate the readers' understanding and highlight the differences between performance analysis of the considered WPCCN and that of the conventional cooperative networks, we first analyze the throughput of the HTC protocol in the three-node reference model, which will be extended to the general multi-relay scenario in the subsequent section. To this end, we first characterize the outage probability of the proposed protocol and have the following proposition:

Proposition 2.3.1. *The outage probability of the HTC protocol can be approximately*[4] *expressed as*

$$\begin{aligned} P_{\text{out}}^{\text{HTC}} \approx & 1-\mathcal{S}\left(\frac{4\nu}{\mu\sigma_{AS}^2\sigma_{SA}^2}\right)-\mathcal{S}\left(\frac{4\nu}{\mu\sigma_{AR}^2\sigma_{RA}^2}\right)\times \\ & \left[\mathcal{S}\left(\frac{4\nu}{\mu\sigma_{AS}^2\sigma_{SR}^2}\right)-\mathcal{S}\left(\frac{4\nu}{\mu\sigma_{AS}^2\sigma_{SR}^2}+\frac{4\nu}{\mu\sigma_{AS}^2\sigma_{SA}^2}\right)\right], \end{aligned} \tag{2.3.1}$$

where

$$\mathcal{S}(x)=\sqrt{x}K_1\left(\sqrt{x}\right) \tag{2.3.2}$$

is defined for notation simplification with $K_1(\cdot)$ denoting the modified Bessel function of the second kind with first order [77], and

$$\nu=2^{2R}-1 \tag{2.3.3}$$

[4] *Due to the complex structure of the resulting SNR given in (2.2.6), it is difficult to achieve a closed-form expression for the exact outage probability. Motivated by this, we perform an approximation to the resulting SNR and derive an approximate expression for the outage.*

with R denoting the (fixed) transmission rate of the source.

Proof. See Appendix A.1. □

Given the fixed transmission rate R at the source and the outage probability $P_{\text{out}}^{\text{HTC}}$, the effective transmission rate can be written as $R\left(1-P_{\text{out}}^{\text{HTC}}\right)$. Then, the throughput of the considered system can be obtained by calculating the product of the effective transmission rate and the time of UL information transmission. Based on the approximate expression of the outage probability $P_{\text{out}}^{\text{HTC}}$ in (2.3.1), we can have the following corollary on the average throughput of the proposed protocol in the reference model:

Corollary 2.3.1. *An approximate closed-form expression for the average throughput of the HTC protocol in the three-node reference model can be expressed as*

$$\mathcal{T}_{\text{HTC}} \approx R\left(1-P_{\text{out}}^{\text{HTC}}\right)(1-\tau). \tag{2.3.4}$$

Similarly, we can derive the average throughput of the harvest-then-transmit protocol proposed in [57], where the source transmits its information in the UL without the assistance of the relay. This can be summarized in the following corollary:

Corollary 2.3.2. *The average throughput of the harvest-then-transmit protocol can be expressed as*

$$\mathcal{T}_{\text{HTT}} = R\left(1-P_{\text{out}}^{\text{HTT}}\right)(1-\tau), \tag{2.3.5}$$

where $P_{\text{out}}^{\text{HTT}} = 1-\mathcal{S}\left(\frac{4\nu'}{\mu'\sigma_{AS}^2\sigma_{SA}^2}\right)$ *with* $\nu' = 2^R-1$ *and* $\mu' = \eta\left(P_A/N_0\right)\tau/(1-\tau)$.

Remark 2.3.1. It can be observed from (A.1.2) that the outage probability and the parameter μ defined in (2.2.5) are in inverse proportion since both γ_{SA} and γ_{SRA} are directly proportional to μ. Moreover, the value of μ is proportional to that of the

time allocation parameter τ. Thus, the larger the value of τ, the lower the outage probability. This observation is understandable since the larger value of τ means the more harvested energy at the source and relay, which can result in lower outage probability. However, when it comes to the throughput, indefinitely increasing the value of τ (to 1) may not always be beneficial. Although the larger value of τ can lead to a higher probability of successful delivery of the source's packet, the effective time that the source can transmit its information (i.e., $1-\tau$) is reduced. *Therefore, there should exist an optimal value of τ between 0 and 1 such that the throughput of the considered system is highest.* This hypothesis will be validated by numerical results in Section 2.5.

Compared to the harvest-then-transmit protocol, the proposed HTC protocol can potentially improve the network performance, especially for the case where the source-AP link suffers from deep fading and the relay can help deliver the source information to the AP. But, when the AP-source link is poor and the amount of energy harvested at the source is very small, both the source-AP and source-relay links may suffer from outage. However, since the relay is relatively nearer to the source than the AP, the average outage probability of the source-relay link will be lower than that of the source-AP link. The outage probability of the source-relay link can be further reduced by deploying the relay relatively nearer to the source. In this case, the probability of a good channel condition between the source and relay will be high. Then, the transmission from the source to the relay can still be successful with relatively high probability even when the source only has a limited amount of energy. Thus, we can deduce that the relay should be deployed nearer to the source side to relieve the performance loss due to the cases when the AP-source link is poor. This analysis will

also be validated by simulation results in Section 2.5. □

2.4 Extension to Multi-Relay Scenario

In practice, there may exist more than one relay that are located between the source and AP and would like to assist the communication between them. In this section, we extend our previous analysis to the multi-relay scenario. In conventional multi-relay cooperative networks, the (single) relay selection technique has attracted a lot of interest since it can improve the network performance while avoiding the reduction in spectral efficiency. Opportunistic relaying[5] (OR) [44] and partial relay selection (PRS) [45] are two representative relay selection schemes that were proposed for the AF relaying. In the OR scheme, only the relay that can provide the best end-to-end path between source and destination would be selected from all the available candidates. In contrast, the relay selection procedure of the PRS scheme is performed based on only the channel state information (CSI) of one of the two hops, thereby resulting in lower complexity. Although it has been shown in the literature that the PRS scheme is inferior to the OR scheme, it is still interesting to analyze its performance and compare it with the OR scheme since it has relatively lower complexity [45]. The throughput performance of the considered WPCCN with these two relay selection protocols will both be analyzed in this section.

We assume that there are N relays located between the source and AP, denoted by R_i, $i \in \mathcal{N} = \{1, \ldots, N\}$. We use $h_{AR_i} \sim \text{EXP}\left(\sigma^2_{AR_i}\right)$, $h_{SR_i} \sim \text{EXP}\left(\sigma^2_{SR_i}\right)$ and $h_{R_iA} \sim \text{EXP}\left(\sigma^2_{R_iA}\right)$ to denote the channel power gains from the AP to the relay

[5]Note that the OR scheme can achieve the same diversity-multiplexing tradeoff as the space-time coded cooperative diversity scheme, no matter whether the relays implement AF or DF protocols [44].

R_i, that from the source to the relay R_i, and that from the relay R_i to the AP, respectively. Then, for the relay R_i, the instantaneous SNR for the first hop and second hop of the UL information transmission are respectively given by

$$\gamma_{SR_i} = \mu h_{AS} h_{SR_i}, \text{ and } \gamma_{R_iA} = \mu h_{AR_i} h_{R_iA}. \tag{2.4.1}$$

For convenience, we assume that the relays are clustered relatively close together (i.e., location-based clustering). This assumption is commonly used in the context of cooperative diversity systems (e.g., [45, 78] and references therein) and results in the equivalent average channel power gains of the links A-R_i, S-R_i and R_i-A, respectively. For convenience, we define $\sigma^2_{AR_i} = \sigma^2_{AR}$, $\sigma^2_{SR_i} = \sigma^2_{SR}$, and $\sigma^2_{R_iA} = \sigma^2_{RA}$ for any $i \in \mathcal{N}$.

To proceed, we first formally describe the selection criteria of the OR and PRS protocols in the following:

- In the OR protocol, the relay selection decision is determined by jointly considering the hops $\{S \to R_i\}$ and $\{R_i \to A\}$. Particularly, the relay with the highest $\min(\gamma_{SR_i}, \gamma_{R_iA})$ will be selected [44]. We use R_b to denote the selected relay hereafter. Then, the index of the selected relay in the OR protocol is given by

$$b_{\text{OR}} = \arg\max_{i \in \mathcal{N}} \{\min(\gamma_{SR_i}, \gamma_{R_iA})\}. \tag{2.4.2}$$

- In the PRS scheme, it is assumed that only the CSI of either the hop $\{S \to R_i\}$ or the hop $\{R_i \to A\}$ is available. The relay selection procedure is modified accordingly such that only one of the two hops is taken into account. Specifically, when only the links in the first hop $\{S \to R_i\}$ are considered, the index of the selected relay is determined by [45]

$$b_{\text{PRS-I}} = \arg\max_{i \in \mathcal{N}} \{\gamma_{SR_i}\}. \tag{2.4.3}$$

Similarly, for the case that only the second hop[6] $\{R_i \to A\}$ is taken into consideration, a single relay is selected according to

$$b_{\text{PRS}-\text{II}} = \arg\max_{i\in\mathcal{N}} \{\gamma_{R_iA}\}. \tag{2.4.4}$$

For the purpose of exposition, we consider that the selected relay will only exhaust the energy harvested during the current transmission block to forward the signal received from the source. In the following two subsections, we will derive the closed-form expressions of the approximate throughput and asymptotic throughput at high SNR for the considered network with OR and PRS protocols, respectively.

2.4.1 OR Protocol

Similar to the analysis in Section 2.3, we first derive the outage probability of the HTC protocol with OR and obtain the following result:

Proposition 2.4.1. *The approximate outage probability of the OR protocol in the considered WPCCN is given by*

$$\begin{aligned} P_{\text{out}}^{\text{HTC,OR}} \approx & 1 - \mathcal{S}\left(\frac{4\nu}{\mu\sigma_{AS}^2\sigma_{SA}^2}\right) + \sum_{n=1}^{N}\binom{N}{n}(-1)^n\left[\mathcal{S}\left(\frac{4\nu}{\mu\sigma_{AR}^2\sigma_{RA}^2}\right)\right]^n \times \\ & \left[\mathcal{S}\left(\frac{4n\nu}{\mu\sigma_{AS}^2\sigma_{SR}^2}\right) - \mathcal{S}\left(\frac{4n\nu}{\mu\sigma_{AS}^2\sigma_{SR}^2} + \frac{4\nu}{\mu\sigma_{AS}^2\sigma_{SA}^2}\right)\right]. \end{aligned} \tag{2.4.5}$$

Proof. See Appendix A.2. □

It can observed that (2.4.5) is simplified to (2.3.1) when N is set to one, which validates our derivation. Based on (2.4.5), we can have the following corollary regarding the throughput of the considered WPCCN with OR:

[6] In the PRS scheme proposed in [45], only the CSI of the first hop (i.e., $\{S \to R_i\}$) is used. Here we also consider the scheme based on the CSI of the second hop because unlike the conventional relay systems, the relays harvest energy from the AP in the considered WPCCN. Also, this can achieve a comparative analysis of all possible schemes.

Corollary 2.4.1. *The throughput of the proposed HTC protocol with OR scheme can be approximated as*

$$\mathcal{T}_{\mathrm{HTC}}^{\mathrm{OR}} \approx R\left(1 - P_{\mathrm{out}}^{\mathrm{HTC,OR}}\right)(1-\tau). \tag{2.4.6}$$

In many practical applications, the system performance at high SNR is of great importance and use. Thus, we investigate the asymptotic throughput of the considered network with OR implemented and have the following proposition:

Proposition 2.4.2. *When P_A/N_0 is sufficiently large, the throughput in (2.4.6) can be asymptotically expressed as*

$$\mathcal{T}_{\mathrm{HTC}}^{\mathrm{OR},asymp} = R\left(1 - P_{\mathrm{out}}^{\mathrm{OR},asymp}\right)(1-\tau), \tag{2.4.7}$$

where

$$\begin{aligned} P_{\mathrm{out}}^{\mathrm{OR},asymp} = &- \mathcal{W}\left(\frac{4\nu}{\mu\sigma_{AS}^2\sigma_{SA}^2}\right) + \sum_{n=1}^{N}\binom{N}{n}(-1)^n\left[1 + \mathcal{W}\left(\frac{4\nu}{\mu\sigma_{AR}^2\sigma_{RA}^2}\right)\right]^n \times \\ &\left[\mathcal{W}\left(\frac{4n\nu}{\mu\sigma_{AS}^2\sigma_{SR}^2}\right) - \mathcal{W}\left(\frac{4n\nu}{\mu\sigma_{AS}^2\sigma_{SR}^2} + \frac{4\nu}{\mu\sigma_{AS}^2\sigma_{SA}^2}\right)\right] \end{aligned} \tag{2.4.8}$$

with

$$\mathcal{W}(x) = \frac{x}{2}\ln\frac{\sqrt{x}}{2}.$$

Proof. See Appendix A.3. □

Note that the asymptotic throughput of the three-node reference model can be obtained by substituting $N = 1$ into (2.4.7).

2.4.2 PRS protocol

To obtain the analytical expression for the throughput of the HTC protocol with PRS schemes, we first investigate the outage probability of these two schemes and have the following proposition:

Proposition 2.4.3. *The approximate expressions for the outage probability of the PRS protocols with the selection criteria in (2.4.3) and (2.4.4) are respectively given by*

$$P_{\text{out}}^{\text{HTC,PRS}-\text{I}} \approx 1 - \mathcal{S}\left(\frac{4\nu}{\mu\sigma_{AS}^2\sigma_{SA}^2}\right) - \mathcal{S}\left(\frac{4\nu}{\mu\sigma_{AR}^2\sigma_{RA}^2}\right) N \sum_{n=0}^{N-1} \binom{N-1}{n} \frac{(-1)^n}{n+1} \times \left[\mathcal{S}\left(\frac{4\left(n+1\right)\nu}{\mu\sigma_{AS}^2\sigma_{SR}^2}\right) - \mathcal{S}\left(\frac{4\left(n+1\right)\nu}{\mu\sigma_{AS}^2\sigma_{SR}^2} + \frac{4\nu}{\mu\sigma_{AS}^2\sigma_{SA}^2}\right)\right], \tag{2.4.9}$$

$$P_{\text{out}}^{\text{HTC,PRS}-\text{II}} \approx 1 - \mathcal{S}\left(\frac{4\nu}{\mu\sigma_{AS}^2\sigma_{SA}^2}\right) - \left\{\sum_{n=1}^{N} \binom{N}{n} (-1)^{n+1} \left[\mathcal{S}\left(\frac{4\nu}{\mu\sigma_{AR}^2\sigma_{RA}^2}\right)\right]^n\right\} \times \left[\mathcal{S}\left(\frac{4\nu}{\mu\sigma_{AS}^2\sigma_{SR}^2}\right) - \mathcal{S}\left(\frac{4\nu}{\mu\sigma_{AS}^2\sigma_{SR}^2} + \frac{4\nu}{\mu\sigma_{AS}^2\sigma_{SA}^2}\right)\right]. \tag{2.4.10}$$

Proof. See Appendix A.4. □

Subsequently, we can have the following corollary regarding the approximate throughput of the PRS schemes and the corresponding asymptotic performance:

Corollary 2.4.2. *The approximate throughput of the considered system with PRS is given by*

$$\mathcal{T}_{\text{HTC}}^{\text{PRS}-\text{X}} \approx R\left(1 - P_{\text{out}}^{\text{HTC,PRS}-\text{X}}\right)(1-\tau), \tag{2.4.11}$$

where $\text{X} \in \{\text{I}, \text{II}\}$ *corresponds to the two different PRS schemes in (2.4.3) and (2.4.4). Moreover, the throughput in (2.4.11) can be asymptotically expressed as*

$$\mathcal{T}_{\text{HTC}}^{\text{PRS}-\text{X},asymp} = R\left(1 - P_{\text{out}}^{\text{PRS}-\text{X},asymp}\right)(1-\tau), \tag{2.4.12}$$

where

$$P_{\text{out}}^{\text{PRS}-\text{I},asymp} = -\mathcal{W}\left(\frac{4\nu}{\mu\sigma_{AS}^2\sigma_{SA}^2}\right) - \left[1 + \mathcal{W}\left(\frac{4\nu}{\mu\sigma_{AR}^2\sigma_{RA}^2}\right)\right] N \sum_{n=0}^{N-1} \binom{N-1}{n} \frac{(-1)^n}{n+1} \times \left[\mathcal{W}\left(\frac{4\left(n+1\right)\nu}{\mu\sigma_{AS}^2\sigma_{SR}^2}\right) - \mathcal{W}\left(\frac{4\left(n+1\right)\nu}{\mu\sigma_{AS}^2\sigma_{SR}^2} + \frac{4\nu}{\mu\sigma_{AS}^2\sigma_{SA}^2}\right)\right], \tag{2.4.13}$$

$$P_{\text{out}}^{\text{PRS-II},asymp} = -\mathcal{W}\left(\frac{4\nu}{\mu\sigma_{AS}^2\sigma_{SA}^2}\right) - \left\{\sum_{n=1}^{N}\binom{N}{n}(-1)^{n+1}\left[1+\mathcal{W}\left(\frac{4\nu}{\mu\sigma_{AR}^2\sigma_{RA}^2}\right)\right]^n\right\}\times \left[\mathcal{W}\left(\frac{4\nu}{\mu\sigma_{AS}^2\sigma_{SR}^2}\right) - \mathcal{W}\left(\frac{4\nu}{\mu\sigma_{AS}^2\sigma_{SR}^2}+\frac{4\nu}{\mu\sigma_{AS}^2\sigma_{SA}^2}\right)\right]. \tag{2.4.14}$$

Remark 2.4.1. In the considered relay selection schemes, only one relay out of the cluster is chosen to assist the source's information transmission in each block. If a relay is not chosen in a certain block, it can store the harvested energy for its own future transmission. Since the channel gains for all relays are assumed to be i.i.d, each relay is selected to help the source with the probability $\frac{1}{N}$. Thus, the average energy harvested by each relay is $\left(1-\frac{1}{N}\right)\eta\tau P_A\sigma_{AR}^2$. *This amount of energy can actually be regarded as the motivation of the relays to keep active for voluntary cooperation instead of sleeping. On the other hand, the performance of the considered system can be further improved when the energy accumulation at the relays is considered, i.e., the selected relay can use the accumulated energy harvested during the previous non-selected block. In this case, a more sophisticated relay scheduling scheme needs to be designed, which is out of the scope of this chapter and can actually be lower bounded by the schemes investigated in this chapter.* □

2.5 Numerical Results

In this section, we present some numerical results to illustrate and validate the above theoretical analysis. In the context of wireless energy transfer, distances between nodes are particularly important since they determine not only the reception reliability but also energy attenuation of the received signals. In this chapter, even

though we do not consider the spatial randomness of node locations [79, 80], we follow some recent works in the literature (e.g. [48, 52]) and adopt a practical path loss model that captures the effect of node distance on the system performance. This allows us to obtain meaningful insights into the network performance. It is noteworthy that considering the spatial node distributions [79, 80] would lead to a more practical framework. However, this will require a new analytical framework, which is out of the scope of this chapter.

To capture the effect of node distance on the network performance, we use the channel model that $\sigma_{AS}^2 = \sigma_{SA}^2 = 10^{-3}\left(d_{AS}\right)^{-\chi}$, $\sigma_{AR}^2 = \sigma_{RA}^2 = 10^{-3}\left(d_{AR}\right)^{-\chi}$, and $\sigma_{SR}^2 = \sigma_{RS}^2 = 10^{-3}\left(d_{SR}\right)^{-\chi}$, where d_{XY} denotes the distance between nodes X and Y and $\chi \in [2, 5]$ is the path loss factor [81]. Note that a 30dB average signal power attenuation is assumed at a reference distance of 1 meter (m) in the above channel model [57]. A linear topology that the relay(s) is (are) located on a straight line between the source and hybrid AP is considered, i.e, $d_{AR} = d_{AS} - d_{SR}$. In all simulations, we set the distance between the AP and source $d_{AS} = 10$m, the path loss factor $\chi = 2$, the noise power $N_0 = -80$dBm, the energy harvesting efficiency $\eta = 0.5$, and the fixed transmission rate of the source $R = 1$ bit per channel use (bpcu).

First, we compare the approximate and asymptotic expressions for the average throughput of the considered network derived in the sections above with the corresponding simulation results. Fig. 2.3 illustrates the throughput performance of the proposed HTC protocol in the three-node reference model and that of the harvest-then-transmit protocol [57] versus P_A for given values of d_{SR}, τ and R. We can see from Fig. 2.3 that the derived approximate expression for the throughput of the proposed protocol becomes very tight in medium and high SNR conditions. Moreover,

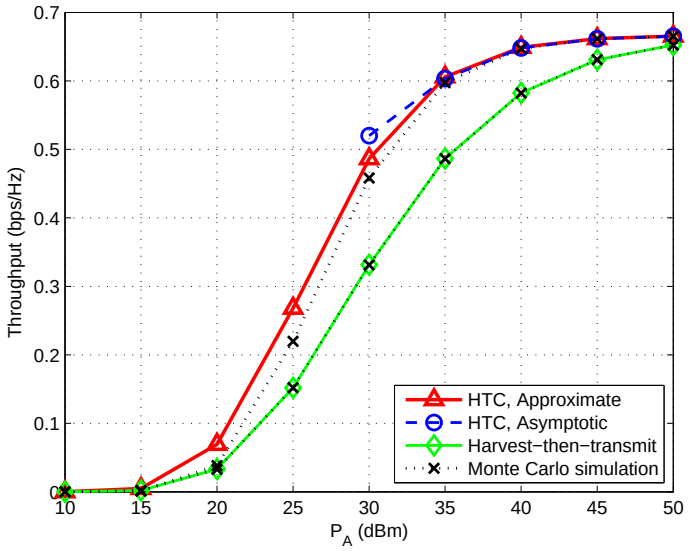

Figure 2.3: Average throughput of the proposed protocol in the three-node reference model (i.e., $N = 1$) and that of harvest-then-transmit protocol versus P_A, where $d_{SR} = 3$m, and $\tau = 1/3$.

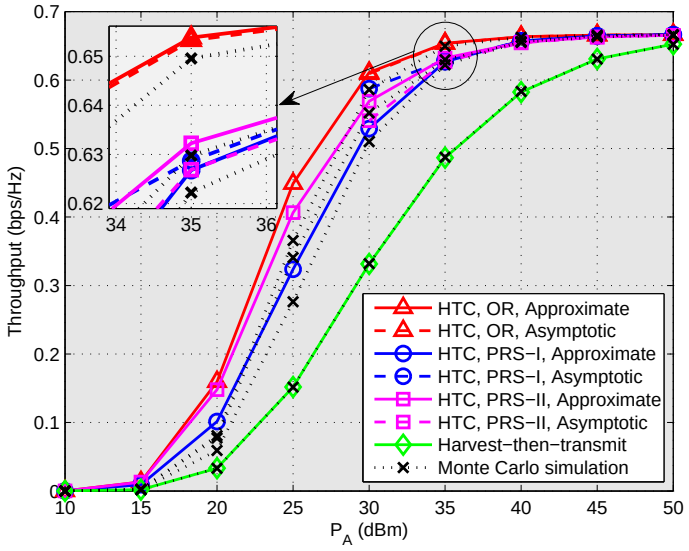

Figure 2.4: Average throughput of the proposed protocol with different relay selection schemes versus P_A, where $N = 3$, $d_{SR} = 3$m, and $\tau = 1/3$.

the asymptotic result[7] tends to coincide with the simulated one at high SNR. Similar phenomenon can also be observed from Fig. 2.4, in which the throughput curves of the HTC protocol with three different relay selection schemes are plotted for a 3-relay network with the same set of parameters as in Fig. 2.3. These observations validate our theoretical analyses. It can also be observed from Figs. 2.3-2.4 that even when there is only one relay node, the proposed HTC protocol can introduce obvious performance gain compared with the harvest-then-transmit protocol. Moreover, this performance gain can be further enlarged in the multi-relay scenario by employing relay selection techniques. From Figs. 2.3-2.4, we can also observe that the throughput of the HTC protocol tends to be saturated when the SNR is high enough. This observation is understandable since for a given value of τ, the throughput of the system will approach to its maximal value $R\,(1-\tau)$ as the outage probability goes to 0 when the SNR is high enough.

Next, we will investigate the impact of the system parameters on the throughput performance in medium and high SNR conditions. Since the theoretical analyses agree well with the simulations in this SNR range, we will only plot the analytical results in the remaining figures. In Fig. 2.5, we plot the throughput curves of the HTC protocol and harvest-then-transmit protocol versus the time allocation parameter τ for a two-relay network with $P_A = 35$dBm and $d_{SR} = 3$m. It can be seen from Fig. 2.5 that there exists a optimal value of τ for all schemes. This phenomenon actually coincides with our hypothesis in Remark 1. Moreover, we can observe from Fig. 2.5 that the optimal values of τ for the HTC protocol are smaller than that for the harvest-then-transmit protocol. This means that the latter needs to consume more

[7]The asymptotic results in Figs. 2.3-2.4 were plotted only when the values of P_A exceed certain values to avoid abnormal curves.

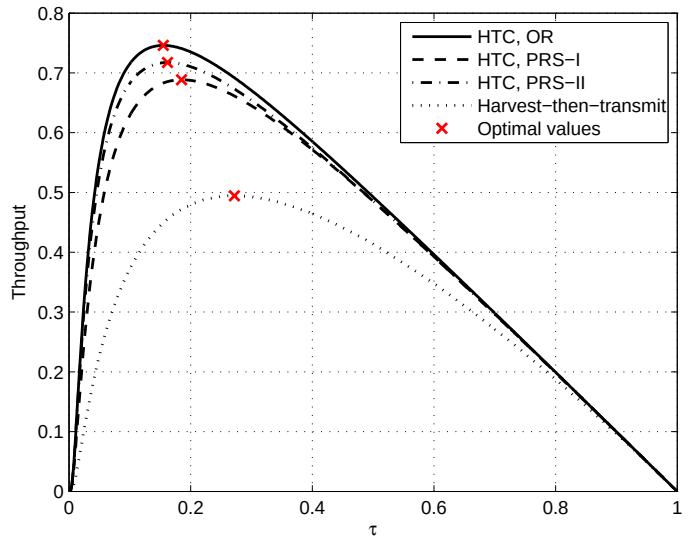

Figure 2.5: Average throughput versus τ with $P_A = 35$dBm, $N = 2$, $d_{SR} = 3$m.

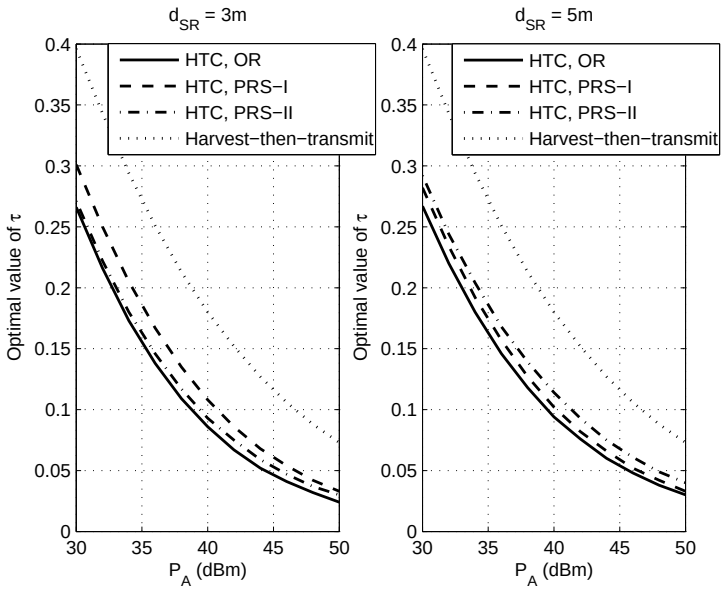

Figure 2.6: Optimal value of τ versus P_A with different relay positions, where $N = 2$.

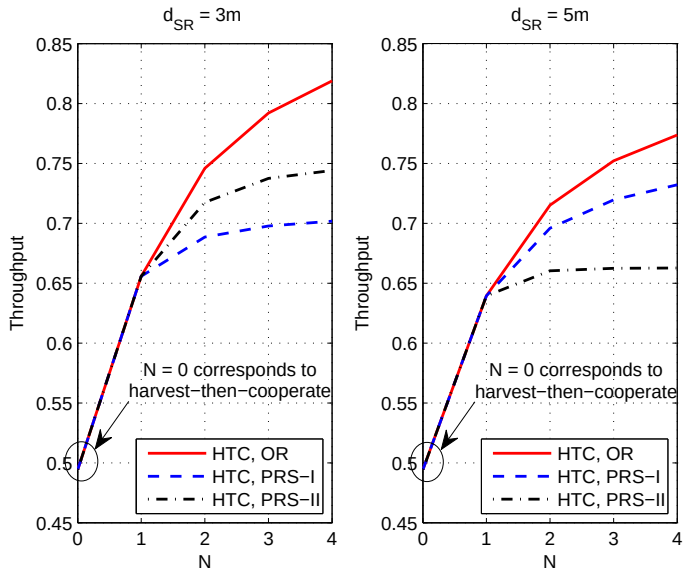

Figure 2.7: The impact of relay number on the average throughput with optimal τ's and different relay positions, where $P_A = 35$dBm.

energy at the AP than the former to achieve its maximal throughput. In Fig. 2.6, we evaluate the optimal value of τ versus the value of P_A for different schemes. Note that the optimal value of τ can easily be obtained by a one-dimensional exhaustive search. It can be observed from Fig. 2.6 that the optimal values of τ for all schemes monotonically decrease as P_A increases. This indicates that the higher the SNR, the smaller the optimal value of τ. This observation makes sense since the source can harvest the same amount of energy with shorter time when the AP transmit power increases, and more time could be allocated to the information transmission to improve the throughput. In the considered SNR range, the OR scheme achieves the smallest value of optimal τ, while that of the harvest-then-transmit protocol is the largest one. The optimal τ's of two PRS schemes lie in the middle, which can be larger than each other depending on the relay position.

In Fig. 2.7, we demonstrate the influence of the relay number on the throughput

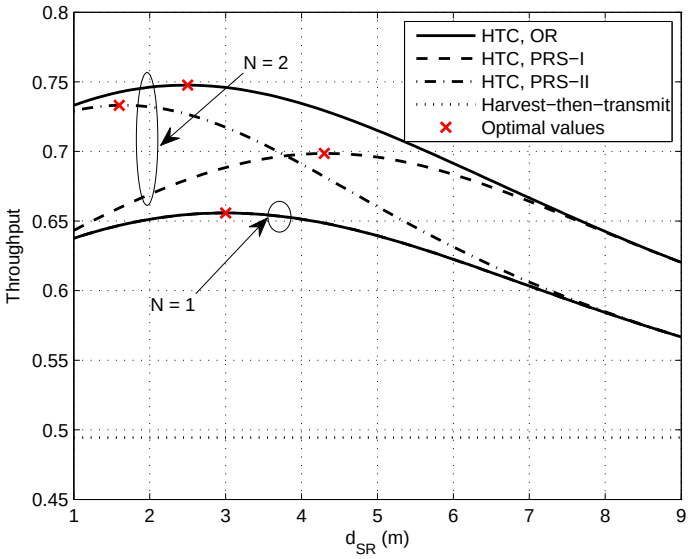

Figure 2.8: The impact of relay position on the average throughput with optimal τ's, where $P_A = 35$dBm and $N = 1,\ 2$.

performance of three different relay selection schemes with the optimal τ's and different relay positions. As a comparison, the performance of the harvest-then-transmit protocol is also included in Fig. 2.7 as a special case of the HTC protocol for the case that the relay number is zero. We can see from this figure that the curves of the three relay selection schemes coincide when $N = 1$. The understanding of this result is straightforward and verifies the correctness of our derivations once again. It can also be observed from Fig. 2.7 that the throughput performance of all three schemes is improved when the relay number increases. However, the slope of the performance improvement is decreasing, especially for the PRS schemes. Moreover, it is shown in both subfigures of Fig. 2.7 that the OR scheme always achieves the best performance, while the two PRS schemes (i.e., PRS-I and PRS-II) can outperform each other determined by the position of relays. In particular, when the relays are closed to the

source (i.e., the case $d_{SR} = 3$m), the PRS-II scheme can achieve better throughput than the PRS-I scheme. However, this phenomenon is reversed when the distance between the source and relays is far enough (e.g., $d_{SR} = 5$m). This observation reveals that in the PRS schemes, the single relay should be selected based on the CSIs of the second hop if the relays are very close to the source, otherwise this procedure should be performed based on the first hop. The reason behind this conclusion is that the performance of the S-R_i-A paths is actually determined by the weaker hop.

Fig. 2.8 depicts the effect of relay location on the throughput performance of the proposed HTC protocol with different relay selection schemes, in which the throughput curves are plotted versus d_{SR} with the optimal values of τ's and different relay numbers. As a comparison, we also plot the corresponding throughput of the harvest-then-transmit protocol, which are straight lines since the throughput of the harvest-then-transmit protocol is independent of the relay position. Similar to the observation from Fig. 2.7, we can see from Fig. 2.8 that the three HTC schemes coincide when there is only one relay. It is worth mentioning that the optimal value of d_{SR} is around 3m when $N = 1$. This indicates that the single relay should be deployed relatively nearer to the source side, which is in line with our discussions in Remark 1 regarding the relay position. For the case $N = 2$, the OR scheme always possesses the best performance, and the performance of two PRS schemes (i.e., PRS-I (2.4.3) and PRS-II (2.4.4)) depends on the position of the relays. It can also be seen from Fig. 2.8 that there exists a throughput-optimal value of d_{SR} for a given relay number. In addition, the optimal value of d_{SR} for the PRS-I scheme is larger than that for the PRS-II scheme. Moreover, with the optimal values of d_{SR}, the OR scheme performs the best and the PRS-II scheme performs better than the PRS-I scheme.

This observation can be regarded as the tradeoff between the performance and the complexity since these three relay selection schemes require different amounts of CSI. Specifically, the OR scheme needs to collect the most amount of CSI[8] (i.e., $\{h_{AR_i}\}$, $\{h_{SR_i}\}$, and $\{h_{R_iA}\}$). The PRS-II scheme requires a less amount of CSI (i.e., $\{h_{AR_i}\}$ and $\{h_{R_iA}\}$), while the PRS-I scheme need the least amount of CSI (i.e., $\{h_{SR_i}\}$). Finally, jointly considering Figs. 2.3-2.8, it is worth claiming that the proposed HTC protocol is superior to the harvest-then-transmit protocol in all considered cases.

[8]It is worth mentioning that the acquisition of these CSI requires signalling overhead/feedback in practice, which could consume some portion of the harvested energy at the source and relays. Here, for simplicity, we ignore this portion of energy since it is normally negligible compared to the energy used for information transmission.

Chapter 3

Wireless-Powered Cooperative Communications via a Hybrid Relay

In this chapter, we consider an alternative practical setup of WPCCN, which consists of a hybrid AP, a hybrid relay, and an information source. The source is assumed to have no embedded energy supply. Thus, it first needs to harvest energy from the signals broadcast by the AP and/or relay, which have a constant power supply, in the DL before transmitting the information to the AP in the UL. The hybrid relay can not only help to forward information in the UL but also charge the source by means of RF energy transfer in the DL. Considering different possible operations of the hybrid relay, we propose two cooperative protocols for the considered WPCCN. We jointly optimize the time and power allocation for DL energy transfer and UL information transmission to maximize the system throughput of the proposed protocols. Numerical results are presented to compare the performance of the proposed protocols and illustrate the impacts of system parameters.

3.1 Introduction

Due to the various advantages of the cooperative communication technique mentioned in the previous chapter, supportive relay nodes have already been deployed to improve the performance of cellular networks, WLANs and wireless sensor networks in practice [71]. When these existing cooperative networks are upgraded to wireless-powered ones, an unavoidable and important question that arises is "*how to utilize the (deployed) relays that are normally constantly powered in the upgraded networks?*". This question actually identifies another practical setup of WPCCNs.

To study this new type of WPCCN, in this chapter we consider a network setup consisting of a hybrid AP, a hybrid relay (R), and an information source (S) that wants to transmit its information to the AP, as depicted in Fig. 3.1. The AP and relay are connected to a constant power supply, while the source is assumed to have no embedded energy source. But it is equipped with a rechargeable battery and thus can harvest and store the wireless energy broadcasted by the AP and/or relay. Besides the information forwarding function like the conventional relay, the hybrid relay in the considered network can also help the AP to charge the source via RF energy transfer. This is in contrast to the scenarios considered in Chapter 2 and other existing works that studied RF energy transfer in cooperative networks (e.g., [48, 82]), where the relay was assumed to have no embedded power supply and need to harvest energy from other nodes.

In this chapter, we develop two cooperative protocols with different relay operations for the considered WPCCN. Furthermore, we formulate optimization problems to maximize the system throughput by jointly designing the time allocation and power allocation for the two proposed protocols, respectively. The optimal solutions are

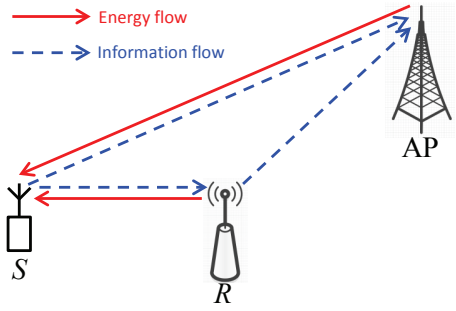

Figure 3.1: System model for wireless-powered cooperative communications via a hybrid relay.

subsequently derived and compared by simulations. Numerical results show that the two proposed protocols can outperform each other in different network scenarios, which provides useful insights into the design of the hybrid relay in WPCCNs.

The rest of this chapter is organized as follows. The system model and the proposed protocols are described in Section 3.2. Section 3.3 derives the jointly optimal time and power allocation of the AP and relay to maximize the achievable throughput of the two protocols, respectively. Numerical results are presented in Section 3.4 to illustrate and compare the performance of the proposed protocols.

3.2 System Model and Description of Protocols

As shown in Fig. 3.1, this chapter considers a wireless-powered cooperative communication network. It is assumed that all the nodes are equipped with a single antenna and work in the half-duplex mode. The source is assumed to have no embedded energy supply and thus needs to first harvest energy from the signal broadcasted by the hybrid AP and/or the relay in the DL, which can be stored in a rechargeable battery and then used for the UL information transmission.

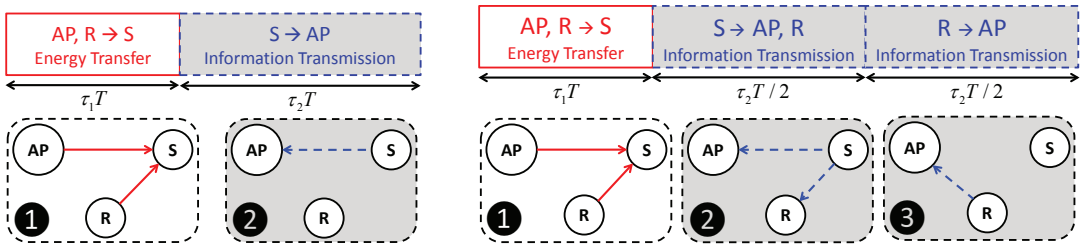

(a) E-C Protocol (b) D-C Protocol

Figure 3.2: Block diagrams for the two proposed cooperative protocols.

In the sequel, we use subscript A for AP, S for source, and R for relay. We use f_{XY} to denote the channel coefficient from X to Y with $X, Y \in \{A, S, R\}$. The channel power gain is thus given by $h_{XY} = |f_{XY}|^2$. In addition, it is assumed that all channels in both DL and UL experience independent slow and frequency flat fading, where the channel gains remain constant during each transmission block (denoted by T) but change independently from one block to another.

In this chapter, we develop two cooperative protocols for the considered WPCC-N, referred to as *energy cooperation (E-C)*[1] and *dual cooperation (D-C)*, which are different in relay operations during each transmission block, as shown in Fig. 3.2. In the E-C protocol, the relay simply cooperates with the AP for DL energy transfer. In the D-C protocol, the relay first cooperates with the AP for energy transfer in the DL and then cooperates with the source for information transmission in the UL. Thus, we name this protocol as D-C (i.e., both energy and information cooperation) protocol. In the subsequent subsections, we describe the proposed protocols and analyze their

[1]It is worth mentioning that the term "energy cooperation" was first used in [83], where energy cooperation is used to term the following protocol: all nodes harvest a certain amount of energy from nature, and the source node sends some energy to the relay, which in return forwards the source's data via user cooperation to the destination.

end-to-end SNRs. Note that the operation of E-C protocol is simpler than that of D-C protocol. Moreover, compared to D-C protocol, the E-C protocol has higher spectrum-usage efficiency during the information transmission phase and thus may achieve better performance when the UL channel from source to AP is good enough.

3.2.1 E-C Protocol

In the E-C protocol shown in Fig. 3.2 (a), the first $\tau_1 T$ amount of time with $0 \leq \tau_1 \leq 1$ is assigned to the DL energy transfer, during which the AP and the relay transmit concurrently to charge the source with WET. In the following τ_2 fraction of the block, the source will use the harvested energy to send its information to the AP, while the relay remains idle.

Let P_A and P_R denote the transmit power of the AP and relay, respectively. Here, we consider that the AP and relay have both peak and average power constraints. Mathematically, we have

$$P_A \leq P_A^{\max},\ \tau_1 P_A \leq P_A^{\text{avg}}, \tag{3.2.1}$$

$$P_R \leq P_R^{\max},\ \tau_1 P_R \leq P_R^{\text{avg}}, \tag{3.2.2}$$

where $P_X^{\max}$ and P_X^{avg} are the peak power and average power of the node X, $X \in \{A, R\}$. For simplicity, we consider

$$\frac{P_A^{\text{avg}}}{P_A^{\max}} = \frac{P_R^{\text{avg}}}{P_R^{\max}} = \mu. \tag{3.2.3}$$

In general, the average power should be no larger than the peak power. Hence, we have $\mu \leq 1$. Note that the analytical method proposed in this chapter can be readily extended to the case

$$\frac{P_A^{\text{avg}}}{P_A^{\max}} \neq \frac{P_R^{\text{avg}}}{P_R^{\max}}.$$

Besides, x_A^E and x_R^E are used to denote the randomly generated energy signals with unit average energy (i.e., $\mathbb{E}\left\{\left|x_A^E\right|^2\right\} = \mathbb{E}\left\{\left|x_R^E\right|^2\right\} = 1$) transmitted by the AP and the relay. Then, the received signal at the source during the DL phase, denoted by y_S, can be expressed as

$$y_S = \sqrt{P_A} f_{AS} x_A^E + \sqrt{P_R} f_{RS} x_R^E + n_S, \tag{3.2.4}$$

where n_S is the AWGN at the source. Moreover, we consider that the noise power is too small and below the sensitivity of the energy harvesting device. Thus, the amount of energy harvested by the source in the E-C protocol is given by

$$E_S = \eta \tau_1 T \left(P_A h_{AS} + P_R h_{RS}\right), \tag{3.2.5}$$

where $0 < \eta < 1$ is the energy harvesting efficiency. It is worth emphasizing that phase synchronization between the AP and relay is not required for the WET in the DL since they transmit independent energy signals. For convenience but without loss of generality, we consider a normalized unit block time (i.e., $T = 1$) hereafter.

After the source replenishes its energy during the DL phase, it transmits its information to the AP by itself in the subsequent UL phase. It is assumed that the source exhausts the harvested energy for the information transmission. The transmission power of the source during the UL phase in this protocol is thus given by

$$P_S^{E-C} = \frac{E_S^{E-C}}{\tau_2}. \tag{3.2.6}$$

Therefore, the end-to-end SNR at the hybrid AP in the E-C protocol can be expressed as

$$\gamma_{E-C} = \frac{P_S^{E-C} h_{SA}}{N_0} = \frac{\eta \tau_1 \left(P_A h_{AS} + P_R h_{RS}\right) h_{SA}}{\tau_2 N_0}, \tag{3.2.7}$$

where N_0 denotes the power of the noise suffered by all receivers.

3.2.2 D-C Protocol

The D-C protocol is shown in Fig. 3.2 (b). Analogous to the E-C protocol, the first $\tau_1 T$ amount of each transmission block is allocated for the DL energy transfer from the AP and relay to the source. The subsequent τ_2 fraction of the block is further divided into two time slots with equal length of $\tau_2 T/2$ for cooperative information transmission in the UL. During the first time slot of the UL phase, the source uses the harvested energy to transmit data information to the AP, which can also be overheard by the relay due to the broadcasting feature of wireless communication. In the second time slot of the UL phase, the relay will help forward the source's information using the AF relaying protocol due to its lower complexity[2] [55]. At the end of each block, the AP combines the signals received in the first and second time slots using the maximum ratio combining[3] (MRC) technique and performs coherent detection.

Let P_R^D and P_R^U denote the transmit power of the relay during the DL and UL phases, respectively. Then, the peak and average power constraints for the relay in (3.2.2) can be re-written as

$$P_R^D \leq P_R^{\max},\ P_R^U \leq P_R^{\max}, \tag{3.2.8a}$$

$$\tau_1 P_R^D + \frac{\tau_2}{2} P_R^U \leq P_R^{\text{avg}}. \tag{3.2.8b}$$

Following the similar analysis for the E-C protocol, we can readily obtain that the received SNR at the AP from the source in this protocol can be expressed as

$$\gamma_{SA} = \frac{2\eta\tau_1 \left(P_A h_{AS} + P_R^D h_{RS}\right) h_{SA}}{\tau_2 N_0}. \tag{3.2.9}$$

The received SNR at the hybrid AP from the link *S*-*R*-*A* can thus be written

[2]For the purpose of exposition, the possibility of the source harvesting energy during the relay's transmission is not taken into account in this chapter.

[3]To characterize the best performance of the considered system, we use MRC instead of SC in this chapter.

as [76]

$$\gamma_{SRA} = \frac{\gamma_{SR}\gamma_{RA}}{\gamma_{SR} + \gamma_{RA} + 1}, \tag{3.2.10}$$

where

$$\gamma_{SR} = \frac{2\eta\tau_1 \left(P_A h_{AS} + P_R^D h_{RS}\right) h_{SR}}{\tau_2 N_0}, \tag{3.2.11}$$

$$\gamma_{RA} = \frac{P_R^U h_{RA}}{N_0}. \tag{3.2.12}$$

Since the MRC technique is adopted at the AP receiver, the end-to-end SNR of the D-C protocol is given by

$$\gamma_{D-C} = \gamma_{SA} + \gamma_{SRA}. \tag{3.2.13}$$

It is worth mentioning that there exists another possible scheduling of the hybrid relay. That is, the relay keeps silent during the DL phase and only cooperates with the source for UL information transmission. However, this protocol can be regarded as a special case of the D-C protocol by setting $P_R^D = 0$, which is thus omitted.

3.3 Throughput Maximization for the Proposed Protocols

In this section, we design the joint time and power allocation for the two proposed protocols to maximize their corresponding throughput. For the purpose of exposition, full CSI[4] is assumed to be known at the AP.

[4]Note that the CSI acquisition also consumes energy in practice. Here, we ignore this portion of energy to focus on the energy consumed for energy transfer and information transmission.

3.3.1 Throughput Maximization for the E-C Protocol

The throughput (bps/Hz) of the E-C protocol can be expressed as

$$\mathcal{T}_{E-C} = \tau_2 \log_2 \left(1 + \gamma_{E-C}\right), \tag{3.3.1}$$

where γ_{E-C} is given in (3.2.7).

To maximize the throughput of this protocol, we formulate the following optimization problem:

$$\begin{aligned} (\text{P3.1}): \quad & \max_{P_A, P_R, \tau_1, \tau_2} \mathcal{T}_{E-C} \\ & \text{s.t. (3.2.1), (3.2.2), } \tau_1 + \tau_2 \leq 1, \\ & P_A, P_R, \tau_1, \tau_2 \geq 0. \end{aligned} \tag{3.3.2}$$

Unfortunately, it is easy to verify that the Problem (P3.1) is not convex. To tackle this non-convexity, we introduce two new variables $E_A = \tau_1 P_A$ and $E_R = \tau_1 P_R$. Based on this variable substitution, the throughput of the E-C protocol can be rewritten as

$$\mathcal{T}'_{E-C} = \tau_2 \log_2 \left(1 + \frac{\eta \left(E_A h_{AS} + E_R h_{RS}\right) h_{SA}}{\tau_2 N_0}\right). \tag{3.3.3}$$

Accordingly, the Problem (P3.1) can be reformulated as

$$\begin{aligned} (\text{P3.2}): \quad & \max_{E_A, E_R, \tau_1, \tau_2} \mathcal{T}'_{E-C} \\ & \text{s.t. } E_A \leq \tau_1 P_A^{\max}, \ E_A \leq P_A^{\text{avg}}, \\ & \quad E_R \leq \tau_1 P_R^{\max}, \ E_R \leq P_R^{\text{avg}}, \\ & \quad \tau_1 + \ \tau_2 \leq 1, \\ & \quad E_A, E_R, \tau_1, \tau_2 \geq 0. \end{aligned} \tag{3.3.4}$$

To solve the Problem (P3.2), we first consider its simplified problem by removing the constraints

$$E_A \leq P_A^{\text{avg}}, \ E_R \leq P_R^{\text{avg}}. \tag{3.3.5}$$

In this case, we have the following problem:

$$\text{(P3.2.1)}: \begin{aligned} &\max_{E_A,E_R,\tau_1,\tau_2} \mathcal{T}'_{E-C} \\ &\text{s.t. } E_A \le \tau_1 P_A^{\max},\ E_R \le \tau_1 P_R^{\max}, \\ &\quad \tau_1 + \ \tau_2 \le 1, \\ &\quad E_A, E_R, \tau_1, \tau_2 \ge 0. \end{aligned} \tag{3.3.6}$$

It is straightforward to see that the throughput $\mathcal{T}'_{E-C}$ in (3.3.3) is monotonically increasing with E_A and E_R for the given values of τ_1 and τ_2. Then, we can deduce that the optimal E_A and E_R should satisfy

$$E_A = \tau_1 P_A^{\max},\ E_R = \tau_1 P_R^{\max}. \tag{3.3.7}$$

Accordingly, we can further simplify the Problem (P3.2.1) to the following one regarding time allocation only:

$$\text{(P3.2.2)}: \begin{aligned} &\max_{\tau_1,\tau_2} \mathcal{T}'_{E-C} \\ &\text{s.t. } \tau_1 + \ \tau_2 \le 1,\ \tau_1, \tau_2 \ge 0. \end{aligned} \tag{3.3.8}$$

The above Problem (P3.2.2) can be regarded as a special case of the one addressed in [57]. Following the analyses in [57], we can steadily obtain the optimal solution of the Problem (P3.2.1) given by

$$\tau_1^\bullet = \frac{z^\bullet - 1}{A + z^\bullet - 1},\ \tau_2^\bullet = 1 - \tau_1^\bullet, \tag{3.3.9a}$$

$$E_A^\bullet = \tau_1^\bullet P_A^{\max},\ E_R^\bullet = \tau_1^\bullet P_R^{\max}, \tag{3.3.9b}$$

where $z^\bullet$ is the unique solution of the equation

$$z \ln z - z + 1 = \frac{\eta \left(P_A^{\max} h_{AS} + P_R^{\max} h_{RS}\right) h_{SA}}{N_0}. \tag{3.3.10}$$

Based on the above analyses, we can obtain the following proposition in terms of the optimal solution to the original Problem (P3.2):

Proposition 3.3.1. *The optimal solution to the Problem (P3.2), denoted by*

$(E_A^*, E_R^*, \tau_1^*, \tau_2^*)$, is given by

$$E_X^* = \begin{cases} \tau_1^\bullet P_X^{\max}, \text{ if } \tau_1^\bullet \leq \mu, \\ P_X^{\text{avg}}, \qquad \text{if } \tau_1^\bullet > \mu, \end{cases} \quad X \in \{A, R\}, \tag{3.3.11}$$

$$\tau_1^* = \begin{cases} \tau_1^\bullet, \text{ if } \tau_1^\bullet \leq \mu, \\ \mu, \quad \text{if } \tau_1^\bullet > \mu, \end{cases}, \ \tau_2^* = 1 - \tau_1^*, \tag{3.3.12}$$

where μ is defined in (3.2.3).

Proof. Firstly, it is easy to verify that if $\tau_1^\bullet \leq \mu$, the optimal solution in (3.3.9) can also achieve the maximum of the Problem (P3.2) without violating the conditions in (3.3.5).

For the case when $\tau_1^\bullet > \mu$, however, the optimal solution in (3.3.9) violates the conditions in (3.3.5). In this case, the optimal E_A and E_R should satisfy that $E_X^* = P_X^{\text{avg}}$, $X \in A, R$ regardless of the value of τ_1. Moreover, it can be shown that the condition $\tau_1^* + \tau_2^* = 1$ should be met by the optimal τ_1^* as well as τ_2^*, and the objective function of Problem (P3.2) is monotonically increasing with τ_2. Thus, the value of τ_1 should be as small as possible. Thus, $\tau_1^* = \frac{E_X^*}{P_X^{\max}} = \mu$ and $\tau_1^* = 1 - \tau_2^*$. This completes the proof. □

Then, we can find the optimal values of P_A and R_R for the original Problem (P3.1) by performing $P_X^* = E_X^*/\tau_1^*$.

Remark 3.3.1. It is interesting to notice that the optimal $P_X^* = P_X^{\max}$ for any value of τ_1^*. In other words, the AP and relay in the E-C protocol should always transmit with the peak power regardless the value of the optimal time allocation.

3.3.2 Throughput Maximization for the D-C Protocol

In the D-C protocol, the relay power needs to be split into two fractions that are respectively used for DL energy transfer and UL information forwarding. Analogous to the previous subsection, we can formulate the following throughput maximization problem in terms of power allocation and time allocation for the D-C protocol:

$$\begin{aligned}(\text{P3.3}): \quad & \max_{P_A, P_R^D, P_R^U, \tau_1, \tau_2} \mathcal{T}_{D-C} \\ & \text{s.t. (3.2.1), (3.2.8), } \tau_1 + \tau_2 \leq 1, \\ & P_A, P_R^D, P_R^U, \tau_1, \tau_2 \geq 0.\end{aligned} \tag{3.3.13}$$

where $\mathcal{T}_{D-C}$ denotes the throughput of the D-C protocol given by

$$\mathcal{T}_{D-C} = \frac{\tau_2}{2}\log_2\left(1 + \gamma_{D-C}\right) \tag{3.3.14}$$

with γ_{D-C} defined in (3.2.13).

To proceed, we introduce three new variables defined as $E_A = \tau_1 P_A$, $E_R^D = \tau_1 P_R^D$ and $E_R^U = \frac{\tau_2}{2} P_R^U$. Furthermore, it can be shown that $\mathcal{T}_{D-C}$ increases with τ_1 for a fixed τ_2 and increases with τ_2 with a fixed τ_1. This means that the optimal values of τ_1 and τ_2 should satisfy $\tau_1 + \tau_2 = 1$. Then, we can remove one of the variables and reformulate the Problem (P3.3) as

$$\begin{aligned}(\text{P3.4}): \quad & \max_{E_A, E_R^D, E_R^U, \tau_1} \mathcal{T}'_{D-C} \\ & \text{s.t. } E_A \leq \tau_1 P_A^{\max}, \ E_A \leq P_A^{\text{avg}}, \\ & \quad E_R^D \leq \tau_1 P_R^{\max}, \ E_R^U \leq \tfrac{1-\tau_1}{2} P_R^{\max}, \\ & \quad E_R^D + E_R^U \leq P_R^{\text{avg}}, \\ & \quad E_A, E_R^D, E_R^U, \tau_1 \geq 0,\end{aligned} \tag{3.3.15}$$

where

$$\mathcal{T}'_{D-C} = \frac{1-\tau_1}{2}\log_2\left(1 + \gamma'_{D-C}\right) \tag{3.3.16}$$

with

$$\gamma'_{D-C} = \frac{2\eta\left(E_A h_{AS} + E_R^D h_{RS}\right) h_{SA}}{(1-\tau_1) N_0} + \frac{\frac{2\eta\left(E_A h_{AS}+E_R^D h_{RS}\right) h_{SR}}{(1-\tau_1)N_0} \frac{2E_R^U h_{RA}}{(1-\tau_1)N_0}}{\frac{2\eta\left(E_A h_{AS}+E_R^D h_{RS}\right) h_{SR}}{(1-\tau_1)N_0} + \frac{2E_R^U h_{RA}}{(1-\tau_1)N_0} + 1}. \quad (3.3.17)$$

However, the simplified Problem (P3.4) is still hard to address due to the complexity of the objective function. To resolve this, we adopt the following method: we first solve the Problem (P3.4) for a given value of τ_1 and then find the optimal τ_1 via numerical method (e.g., a one-dimensional exhaustive search). After careful observation of its structure, the Problem (P3.4) can be simplified to the following three problems based on the given value of τ_1:

(1) When $0 \leq \tau_1 \leq 2\mu - 1$: Note that this case happens only if $\mu \geq 0.5$. For any $\tau_1 \in [0, 2\mu - 1]$, it is evident that the average power constraints $E_A \leq P_A^{\text{avg}}$ and $E_R^D + E_R^U \leq P_R^{\text{avg}}$ can be removed. Moreover, $\mathcal{T}'_{D-C}$ is shown to be monotonically increasing with E_A, E_R^D and E_R^U, respectively. Thus, the optimal values for E_A, E_R^D and E_R^U are given by

$$E_A^\circ = \tau_1 P_A^{\max},\ E_R^{D,\circ} = \tau_1 P_R^{\max},\ E_R^{U,\circ} = \frac{1-\tau_1}{2} P_R^{\max}. \quad (3.3.18)$$

(2) When $2\mu - 1 < \tau_1 \leq \mu$: The constraint $E_A \leq P_A^{\text{avg}}$ can still be ignored and the optimal value of E_A is still given by $E_A^\circ = \tau_1 P_A^{\max}$. But, the constraint $E_R^D + E_R^U \leq P_R^{\text{avg}}$ should be considered and updated as $E_R^D + E_R^U = P_R^{\text{avg}}$. We define an auxiliary variable $t = E_R^U / E_R^D$ to facilitate the problem solving. Then, we can reformulate the Problem (P3.4) with a given τ_1 as

$$(\text{P3.4.1}): \quad \max_t \gamma''_{D-C} \quad \text{s.t. } t_L \leq t \leq t_U, \quad (3.3.19)$$

where

$$\gamma''_{D-C} = a + \frac{b}{t+1} + \frac{\left(c + \frac{d}{t+1}\right)\frac{et}{t+1}}{c + \frac{d}{t+1} + \frac{et}{t+1} + 1}, \quad (3.3.20)$$

$$t_L = (\mu - \tau_1)/\tau_1, \quad (3.3.21)$$

$$t_U = \begin{cases} (1-\tau_1)\,/\,(2\mu-1+\tau_1)\,, \text{ if } \tau_1 > 1-2\mu, \\ \infty, \text{ otherwise,} \end{cases} \tag{3.3.22}$$

with $a = \frac{2\eta E_A^{\circ} h_{AS} h_{SA}}{(1-\tau_1)N_0}$, $b = \frac{2\eta P_R^{\text{avg}} h_{RS} h_{SA}}{(1-\tau_1)N_0}$, $c = \frac{2\eta E_A^{\circ} h_{AS} h_{SR}}{(1-\tau_1)N_0}$, $d = \frac{2\eta P_R^{\text{avg}} h_{RS} h_{SR}}{(1-\tau_1)N_0}$, and $e = \frac{2P_R^{\text{avg}} h_{RA}}{(1-\tau_1)N_0}$, which are defined for the notation's simplicity.

After some algebraic manipulations, we can obtain the following lemma regarding the optimal solution to the Problem (P3.4.1):

Lemma 3.3.1. *The optimal solution to the Problem (P3.4.1) can be expressed as*

$$t^* = \arg \max_{t \in \{t_L, t_1, t_2, t_U\}} \gamma''_{D-C}, \tag{3.3.23}$$

where

$$t_1 = \begin{cases} t'_1, \text{ if } \triangle \geq 0 \text{ and } t_L \leq t'_1 \leq t_U, \\ \emptyset, \text{ otherwise,} \end{cases} \tag{3.3.24a}$$

$$t_2 = \begin{cases} t'_2, \text{ if } \triangle \geq 0 \text{ and } t_L \leq t'_2 \leq t_U, \\ \emptyset, \text{ otherwise,} \end{cases}, \tag{3.3.24b}$$

in which, $\triangle = B^2 - 4AC$, $t'_1 = \frac{-b+\sqrt{\triangle}}{2A}$, $t'_2 = \frac{-b-\sqrt{\triangle}}{2A}$. *Here,* $A = ce - 2bc - 2be - b - de - bc^2 - be^2 + c^2e - de^2 - 2bce$, $B = 2ce - 4bc - 2bd - 2be - 2b - 2bc^2 + 2c^2e - 2bcd - 2bce - 2bde + 2cde$, $C = ce - 2bc - 2bd - b + de - bc^2 - bd^2 + c^2e + d^2e - 2bcd + 2cde$.

Proof. We calculate the first-order derivative of γ''_{D-C} with respect to t and obtain that

$$\partial \gamma''_{D-C} / \partial t \propto At^2 + Bt + C, \tag{3.3.25}$$

which means that γ''_{D-C} has up to two extreme points in terms of t without considering the constraint. Thus, the maximizer of Problem (P3.4.1) can be easily obtained through evaluating the values of γ''_{D-C} at feasible extreme points and two limits. Mathematically, we have (3.3.23), which completes the proof. □

Then, the optimal values for E_A, E_R^D and E_R^U are accordingly given by

$$E_A^\circ = \tau_1 P_A^{\max},\ E_R^{D,\circ} = \frac{P_R^{\text{avg}}}{t^*+1},\ E_R^{U,\circ} = \frac{t^* P_R^{\text{avg}}}{t^*+1}. \tag{3.3.26}$$

(3) When $\tau_1 > \mu$: In this scenario, the two average power constraints for the AP and relay are both active and updated as $E_A = P_A^{\text{avg}}$ and $E_R^D + E_R^U = P_R^{\text{avg}}$. However, the two constraints $E_A \leq \tau_1 P_A^{\max}$ and $E_R \leq \tau_1 P_R^{\max}$ can be ignored. Following the similar analysis as in the proof of Proposition 3.3.1, we can deduce that when the allocation parameter t of the relay is given, the maximum energy harvested by the source is fixed for any τ_1 that is no less than μ. In this case, the time allocated for energy transfer should be as small as possible. Intuitively, we have the following lemma:

Lemma 3.3.2. *For any $\tau_1 \in (\mu, 1]$, the corresponding maximal throughput is less than that of the case when $\tau_1 = \mu$.*

Note that the above lemma reveals that the interval $(\mu, 1]$ is not needed to consider when we calculate the optimal value of τ_1.

By combining the three cases analyzed above, we can obtain the optimal solution to the original Problem (P3.4) given in the following proposition:

Proposition 3.3.2. *The optimal value for τ_1 of the Problem (P3.4) can be expressed as*

$$\tau_1^* = \arg \max_{\tau_1 \in [0,\mu]} \mathcal{T}'_{D-C}\left(E_A^\circ, E_R^{D,\circ}, E_R^{U,\circ}\right), \tag{3.3.27}$$

where E_A°, $E_R^{D,\circ}$, and $E_R^{U,\circ}$ are given in (3.3.18) or (3.3.26) based on the value of τ_1. Accordingly, the optimal values for other parameters can be calculated via $P_A^* = \frac{E_A^\circ(\tau_1^*)}{\tau_1}$, $P_R^{D,*} = \frac{E_R^{D,\circ}(\tau_1^*)}{\tau_1}$, $\tau_2^* = 1 - \tau_1^*$, and $P_R^{U,*} = \frac{2E_R^{U,\circ}(\tau_1^*)}{\tau_2}$.

Remark 3.3.2. It is worth noting that although the closed-form optimal solution to the Problem (P3.4) with five variables is not given, this problem can be efficiently

solved via a one-dimensional exhaustive search regarding the parameter τ_1 with the proposed method. The one-dimensional search can be performed at the AP. Moreover, our analyses reduce the interval of the exhaustive search. Thus, the computational complexity should be very low.

3.4 Numerical Results

In this section, we present some numerical results to illustrate and compare the performance of the proposed protocols. To obtain meaningful results, we restrict our attention to a linear topology as it is the most commonly used topology in conventional cooperative networks to characterize to the effect of relay position on the system performance. Thus, the conclusions achieve in this section may not be valid for all topologies. But the comparisons of the two proposed protocols for other topologies can be readily achieved since the developed resource allocation framework is independent of network topology. Specifically, the relay is located on a straight line between the AP and source, i.e, $d_{AR} = d_{AS} - d_{SR}$ with d_{XY} denoting the distance between nodes X and Y. The channel short-term fading is assumed to be Rayleigh distributed. To capture the effect of path-loss on the network performance, we use the channel model that $\mathbb{E}\{h_{XY}\} = 10^{-3}(d_{XY})^{-\alpha}$, where $\alpha \in [2, 5]$ is the path loss factor [81]. Note that a 30dB average signal power attenuation is assumed at a reference distance of 1m in the above channel model [57]. In all following simulations, we set equal average transmit power for the AP and relay, the distance between the AP and source $d_{AS} = 10$m, the path-loss exponent $\alpha = 2$, the noise power $N_0 = -80$dBm, and the energy harvesting efficiency $\eta = 0.5$. Moreover, each curve for the average throughput is obtained by averaging over 5000 randomly generated channel realizations.

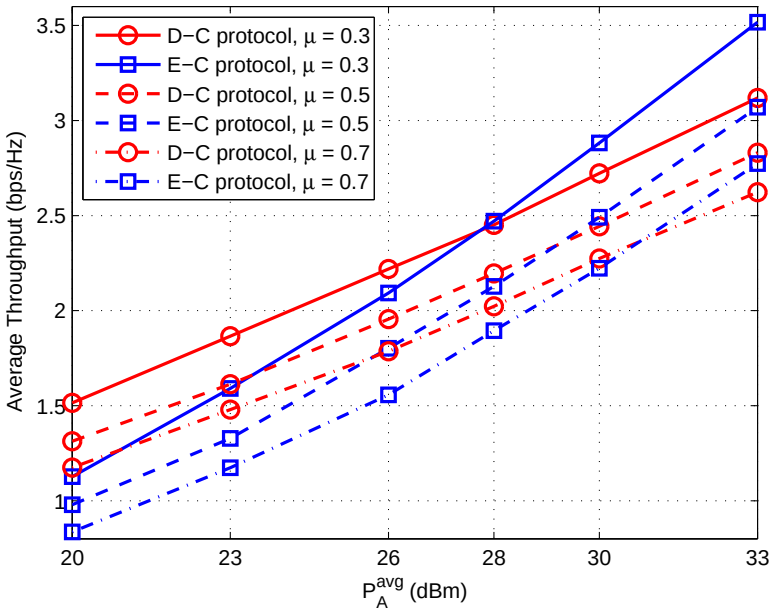

Figure 3.3: The average throughput of the proposed protocols versus the average transmit power of the AP (i.e., P_A^{avg}), where $d_{SR} = 5$m and $P_R^{\text{avg}} = P_A^{\text{avg}}$.

Fig. 3.3 plots the average throughput curves of the E-C and D-C protocols versus the average transmit power of the AP with different values of μ, where the relay is located in the middle of the AP and source. We can see that the performance of both protocols increases monotonically with the average transmit power of the AP for any value of μ. For both E-C and D-C protocols, we can observe that the average throughput decreases as the parameter μ increases. This is because that for a given average transmit power, the peak transmit power decreases when μ increases, which reduces the feasible sets of the transmit powers and thus degrades the throughput performance. It can also be observed from Fig. 3.3 that the D-C protocol is superior to the E-C protocol when the average transmit power is relatively small to medium. But this observation is reversed when the average transmit power is high enough.

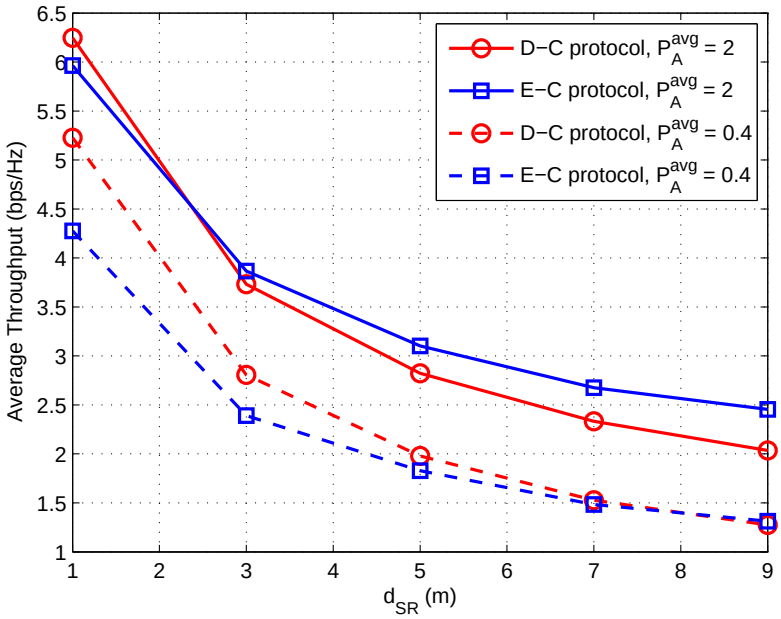

Figure 3.4: The average throughput of the proposed protocols versus d_{SR}, where $\mu = 0.5$ and $P_R^{\text{avg}} = P_A^{\text{avg}}$.

This is understandable since the throughput is highly affected by the information transmission time at high SNR and the time utilization of the E-C protocol is better than that of the D-C protocol. Furthermore, higher average transmit power is needed for the E-C protocol to outperform the D-C protocol when the value of μ grows.

Fig. 3.4 depicts the impact of the relay position on the average throughput of the proposed protocols, in which the throughput curves are plotted versus the distance between the source and relay (i.e., d_{SR}) with two different values of P_A^{avg}. From Fig. 3.4, we can observe that the average throughput of both protocols decreases smoothly with the increase of d_{SR}. This observation indicates that the hybrid relay should be deployed nearer to the source to obtain better throughput. Besides, it is observed from Fig. 3.4 that when the average transmit power is equal to 2Watt (i.e.,

at high SNR), the E-C protocol is superior to the D-C protocol unless the relay is very close to the source. In contrast, in a lower SNR regime (i.e., P_A^{avg} is 0.4Watt), the D-C protocol outperforms the E-C protocol until the relay is very far away from the source.

Chapter 4

Energy Trading in Power Beacon-Assisted WPCCNs using Stackelberg Game

This chapter studies a power beacon-assisted WPCCN consisting of one hybrid AP, one information source, and multiple PBs. The source has no embedded power supply, and thus, has to harvest RF energy from the AP in the DL before transmitting its information to the AP in the uplink. The PBs are deployed to help the AP charge the source in the DL. However, in practice, the AP and PBs may belong to different operators. Thus, incentives are needed for the PBs to assist the AP during the DL energy transfer phase, which is referred to as "energy trading". We formulate this energy trading process as a Stackelberg game, in which the AP is a leader and the PBs are the followers. We then derive the Stackelberg equilibrium of the formulated game. As a comparison, we also formulate and resolve the corresponding social welfare optimization problem. Simulation results show that both schemes can achieve better performance as either the numbers of the PBs or the value of the gain per unit throughput increase, and as the distance between the source and PBs decreases.

4.1 Introduction

Very recently, Huang *et al.* proposed a novel idea of deploying dedicated wireless energy transmitters, referred to as power beacons (PBs), that can provide wireless charging services to terminals via the RF energy transfer technique [19, 47]. The deployment of dedicated PBs in an existing cellular network was designed in [47] such that the updated network can provide both wireless access and wireless charging services. By considering quality-of-service constraints on data links, a tradeoff between the densities of the base stations and PBs was quantified in [47] by modeling the network using stochastic geometry theory. Note that it is assumed in [47] that the PBs are deployed by the *same operator* of the existing network. However, in general, PBs can be deployed by *different authorities*. In such situations, incentives (e.g., monetary payments) are needed for the PBs to provide wireless charging services to their users. Here, we call the subscription and provision of wireless charging services as *energy trading* between PBs and their users. To the best of our knowledge, there are no published references that modeled and investigated this hierarchical interaction between the PBs and their users for the WPCNs. This gap motivates the work in this chapter.

In this chapter, we consider a WPCCN consisting of one hybrid AP, one information source and multiple PBs that are deployed by different operators. The AP needs to collect the information from a source with no embedded power supply. Thus, the AP has to first transfer energy to the source in the DL before the source transmits information in the UL. Besides, there are multiple deployed PBs nearby the source. They provide wireless charging services such that they can perform energy cooperation with the AP to charge the source in the DL. To improve the system performance,

the AP can hire some PBs to boost the amount of energy harvested at the source. However, since the PBs are deployed by different operators, they may be rational and self-interested such that monetary payments are needed to motivate them to get involved during the DL energy transfer phase. In this case, the AP would value its achievable throughput from the source over its total payment to the PBs. On the other hand, the PBs consider not only the payments received from the AP but also their cost to provide the charging service. To embrace the strategic behaviors of the AP and PBs, we apply game theory to model this energy trading process [58, 59]. Here, it is worth mentioning that there are only several works in the open literature that adopt game theory to model the conflicting scenarios in wireless networks with RF energy transfer [52, 80, 84]. Moreover, none of them [52, 80, 84] investigated the energy trading interactions between the AP and PBs in WPCNs.

In this chapter, we develop an energy trading framework[1] for the considered PB-assisted WPCCN using game theory. Specifically, we take the strategic behaviors of the AP and PBs into consideration and formulate the energy trading process between them as a Stackelberg game [60, 61]. In the formulated game, the AP acts as a leader who buys energy from the PBs to charge the source by offering an energy price on per unit of harvested energy from the signals radiated by the PBs. The AP optimizes its energy price and DL energy transfer time to maximize its utility function defined as the difference between the benefits obtained from the achievable throughput and its total payment to the PBs. On the other hand, the PBs are the followers of the formulated game, and determine their optimal transmit powers based on the released energy price from the AP to maximize their own profits. The profit of each PB is

[1]Note that the developed framework can be non-trivially extended to the PB-assisted networks with multiple AP-source pairs.

defined as the payment received from the AP minus its energy cost. We then derive the SE for the formulated game. Note that the number of involved PBs with positive transmit powers is actually a variable in the formulated game and largely affected by the energy price released by the AP. This means that the specific expression of the AP's utility function should depend on the value of the released energy price. On the other hand, different forms of the AP's utility function can lead to different optimal values of the energy price and DL energy transfer time. This special property inherent in the formulated game makes it hard to derive closed-form expressions for the SE. Motivated by this, we solve the formulated game in two steps: we first derive a closed-form expression for the optimal energy price with a given DL energy transfer time. The optimal value of the DL energy transfer time is subsequently achieved in the second step via a one-dimensional search.

To characterize the performance loss due to the self-interested behaviors of the PBs, we also formulate and resolve the corresponding social welfare optimization problem, in which the PBs are cooperative such that they can be fully controlled by the AP to maximize the social welfare, defined as the difference between the utility obtained from the achievable throughput at the AP and the total cost of the PBs. Numerical simulations are performed to compare the proposed game-theoretical scheme and the social welfare optimization scheme, and investigate the impacts of various system parameters, such as the gain per unit throughput for the AP, the number of PBs, and the distance between the source and PBs, on the performance of both schemes.

The rest of this chapter is organized as follows. We describe the system model and formulate a Stackelberg game for the considered system in Section 4.2. Section

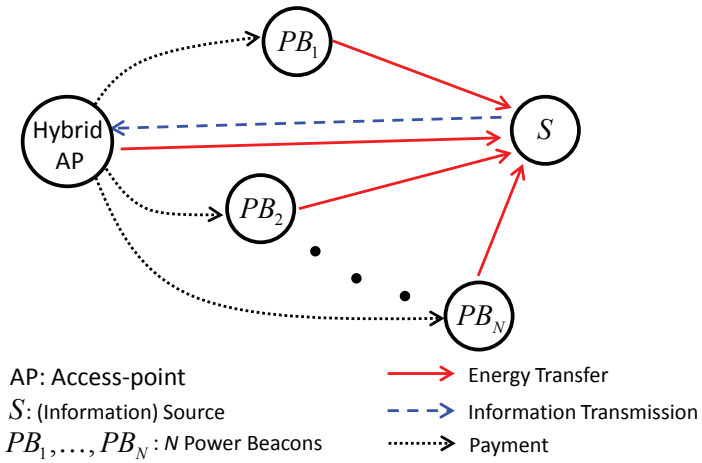

Figure 4.1: System model for the considered power beacon-assisted WPCCN.

4.3 derives the SE of the formulated game, formulates and resolves the corresponding social welfare optimization problem. Simulation results are presented in Section 4.4.

4.2 System Model and Game Formulation

In this section, we first describe the system model and derive the expression of the achievable system throughput with the help of the PBs. Then, we formulate the Stackelberg game to model the energy trading process between the AP and PBs.

4.2.1 System Model

As shown in Fig. 4.1, we consider a PB-assisted WPCN consisting of one hybrid AP, one information source, and N deployed PBs. We denote the set of these PBs as $\mathcal{N} = \{1, \ldots, N\}$. It is assumed that each node in the considered network is

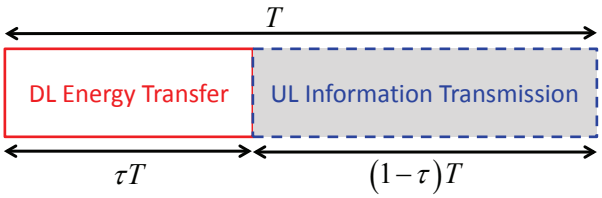

Figure 4.2: Diagram of the harvest-then-transmit protocol.

equipped with a single antenna[2] and works in a half-duplex mode. The AP collects the information from the source. In addition, we assume that the AP and PBs are connected to constant power supplies. In contrast, the source has no embedded energy supplies, and thus needs to replenish energy from the RF signal sent by the AP and PBs. The "harvest-then-transmit" protocol proposed in [57] is implemented in the considered network, as depicted in Fig. 4.2. In particular, during the first τT $(0 < \tau < 1)$ amount of time in each transmission block, the source harvests wireless energy broadcast by the AP and the PBs in the DL. In the remaining $(1-\tau)T$ amount of time, the source uses the harvested energy to transmit its information to the AP in the UL. For convenience, but without loss of generality, we assume $T = 1$ and refer to the value of τ as the DL energy transfer time in the rest of this chapter.

Let p_a and p_m denote the transmit powers of the AP and the mth PB during the DL energy transfer phase, respectively. It is assumed that the energy-carrying signals sent by the AP and PBs are independent and identically distributed (i.i.d.) random variables with a zero mean and unit variance[3]. In addition, we assume that all channels experience independent slow and frequency flat fading, where the channel

[2]The proposed framework can be readily extended to the scenario where the AP and PBs are equipped with multiple antennas. Assuming CSI is available at the transmitter side, the maximal (*continued*) ratio transmission (MRT) and MRC techniques should be adopted at the energy transmitters and information receiver, respectively [21].

[3]It is worth noting that phase synchronization between the AP and PBs is not required for the DL energy transfer since they transmit independent energy signals.

gains remain constant during each transmission block but change independently from one block to another. For simplicity, we consider a reciprocal channel model in this chapter. That is, the channel gains between two nodes for the DL and UL phases are the same in each transmission block. We use $G_{a,s}$ and $G_{m,s}$ to denote the channel power gains between the AP and source, and that between the mth PB and the source, respectively.

The amount of energy harvested by the source can be expressed as [23]

$$E_s = \eta\tau \left(p_a G_{a,s} + \sum_{m=1}^{N} p_m G_{m,s} \right), \tag{4.2.1}$$

where $0 < \eta < 1$ is the energy harvesting efficiency. Note that the receiver noise at the source is ignored in (4.2.1) since it is in practice negligible for the energy receiver.

After the source replenishes its energy during the DL phase, it will transmit its information to the AP in the subsequent UL phase. It is assumed that the harvested energy is exhausted by the source for information transmission. The transmission power of the source is thus given by

$$p_s = \frac{E_s}{1-\tau} = \frac{\eta\tau \left(p_a G_{a,s} + \sum\limits_{m=1}^{N} p_m G_{m,s} \right)}{1-\tau}. \tag{4.2.2}$$

Then, the SNR of the received signal at the hybrid AP during the UL phase can be expressed by

$$\gamma_a = \frac{p_s G_{a,s}}{N_0}, \tag{4.2.3}$$

where N_0 is the power of the AWGN at the hybrid AP. Hence, the achievable throughput (bps) at the AP can be written as

$$\begin{aligned} R_{sa} &= (1-\tau)\, W \log_2 (1+\gamma_a) \\ &= (1-\tau)\, W \log_2 \left(1 + \frac{\eta\tau G_{a,s}\left(p_a G_{a,s} + \sum_{m=1}^{N} p_m G_{m,s}\right)}{(1-\tau)\, N_0}\right), \end{aligned} \tag{4.2.4}$$

where W is the bandwidth. As can be observed from (4.2.4), the achievable throughput at the AP can be increased with the wireless charging services of the PBs, since R_{sa} is an increasing function of any p_m. In addition, the value of the DL energy transfer time τ can affect that of R_{sa} to a large extent. More specifically, the term inside the logarithm function of (4.2.4) increases as the value of τ approaches one. However, as τ increases, the value of the term in front of the logarithm function decreases at the same time. Therefore, we can deduce that there should exist an optimal τ.

4.2.2 Stackelberg Game Formulation

In general, the PBs in the considered WPCCN may belong to different authorities and act strategically. Incentives need to be provided by the AP to the PBs for their wireless charging services, i.e., assisting the energy replenishment of the source in the DL. Consequently, the AP needs to choose the most beneficial PBs. To efficiently exploit the PBs to achieve a good throughput, two fundamental questions need to be answered: (1) which PBs should be included and what are their optimal transmit powers (i.e., p_m's)? (2) what is the optimal value of the DL energy transfer time τ? To answer these questions, we model the strategic interactions between the AP and PBs as a Stackelberg game. A Stackelberg game is a strategic game that consists of a leader and several followers competing with each other for certain resources [60, 61]. The leader acts first and the followers respond to the actions of leader subsequently. In this chapter, we formulate the AP as the leader, and the PBs as the followers.

The AP (leader) imposes a price on per unit of energy harvested from the RF signals radiated by the PBs, referred as to the *energy price* in the following. Then, the PBs (followers) optimize their transmit powers based on the released energy price to maximize their individual profits.

Let λ denote the energy price released by the AP. Mathematically, the total payment of the AP to the PBs can be expressed as

$$\Gamma\left(\tau, \lambda, \boldsymbol{p}\right) = \sum_{m=1}^{N} \lambda\left(\tau p_m G_{m,s}\right), \tag{4.2.5}$$

where $\boldsymbol{p} = \left[p_1, \ldots, p_N\right]^T$ is the vector of the PBs' transmit powers, with $p_m \geq 0$ denoting the transmit power of the mth PB. Then, we define the utility function of the AP as

$$\mathcal{U}_a\left(\tau, \lambda, \boldsymbol{p}\right) = \mu R_{sa} - \Gamma\left(\tau, \lambda, \boldsymbol{p}\right), \tag{4.2.6}$$

where R_{sa} is defined in (4.2.4) and $\mu > 0$ is the gain per unit throughput for the AP. Therefore, the optimization problem for the AP or the *leader-level* game can be formulated as

$$\begin{aligned} &\max_{\tau,\lambda} \ \mathcal{U}_a\left(\tau, \lambda, \boldsymbol{p}\right) \\ (\text{P4.2.1}): \quad &\text{s.t. } \tau \in (0,1), \\ &\lambda \geq 0. \end{aligned} \tag{4.2.7}$$

Each PB in the considered network can be modelled as a follower that wants to maximize its individual earning, which is defined as follows:

$$\mathcal{U}_m\left(p_m, \lambda, \tau\right) = \lambda \tau p_m G_{m,s} - \tau \mathcal{C}_m\left(p_m\right), \tag{4.2.8}$$

where the function $\mathcal{C}_m\left(\cdot\right)$ is used to model the cost of the mth PB per unit time for wirelessly charging the source with the transmit power p_m. In this chapter, we consider the following quadratic model for the cost function of the PBs:

$$\mathcal{C}_m\left(x\right) = a_m x^2 + b_m x, \tag{4.2.9}$$

where $a_m > 0$ and $b_m \geq 0$ are pre-determined parameters that may be different for the PBs. Note that the quadratic function given in (4.2.9) has been widely adopted in the power market to model the energy cost [85].

Thus, the optimization problem for the mth PB or the *follower-level* game is given by

$$(\text{P4.2.2}): \quad \max_{p_m} \ \mathcal{U}_m\left(p_m, \lambda, \tau\right) \quad \text{s.t. } p_m \geq 0. \tag{4.2.10}$$

The Stackelberg game for the considered WPCCN has been formulated by combining Problems (P4.2.1) and (P4.2.2). In this game, the AP is the leader who aims to solve Problem (P4.2.1), while the PBs are the followers who aim to solve their individual Problem (P4.2.2). Once a game is formulated, the subsequent question is to find its equilibrium point(s). For the solution of the formulated game, the most well-known concept is the SE, which can be formally defined as follows:

Definition 4.2.1. We use (τ^*, λ^*) and p_m^* to denote the solutions of Problems (P4.2.1) and (P4.2.2), respectively. Then, the triple $(\tau^*, \lambda^*, \boldsymbol{p}^*)$ is a SE of the formulated game if the following conditions are satisfied

$$\mathcal{U}_a\left(\tau^*, \lambda^*, \boldsymbol{p}^*\right) \geq \mathcal{U}_a\left(\tau, \lambda, \boldsymbol{p}^*\right), \tag{4.2.11}$$

$$\mathcal{U}_m\left(p_m^*, \lambda^*, \tau^*\right) \geq \mathcal{U}_m\left(p_m, \lambda^*, \tau^*\right), \tag{4.2.12}$$

for all $0 < \tau < 1$, $\lambda \geq 0$ and $\boldsymbol{p} \geq \boldsymbol{0}$.

4.3 Analysis of the Proposed Game

In this section, we first derive the SE of the formulated game by analyzing the optimal strategies for the AP and PBs to maximize their own utility functions. Subsequently, the practical implementation of the proposed game-theoretical scheme is

briefly discussed. As a comparison, the corresponding social welfare optimization problem is finally formulated and resolved.

4.3.1 SE of the Formulated Game

It can be observed from (4.2.10) that for given values of τ and λ, the utility function of the mth PB is a quadratic function of its transmit power p_m and the constraint is affine, which indicates that the Problem (P4.2.2) is a convex optimization problem. Thus, it is straightforward to obtain its optimal solution given in the following lemma:

Lemma 4.3.1. *For given values of τ and λ, the optimal solution for Problem (P4.2.2) is given by*

$$p_m^* = \left(\frac{\lambda G_{m,s} - b_m}{2a_m} \right)^+, \tag{4.3.1}$$

where $(\,\cdot\,)^+ = \max(\cdot, 0)$.

Proof. The proof of this lemma follows by noting that the objective function of problem (P4.2.2) given in (4.2.8) is a concave function in terms of p_m. □

It can observed from Lemma 4.3.1 that the transmit power of the mth PB is larger than 0 only if the energy price λ provided by the AP exceeds a certain threshold. This observation can be explained since the strategic PBs will sell their energy only if their profits are positive. Based on this fact, the AP can easily perform the selection of PBs by appropriately setting the value of its energy price.

Subsequently, we need to solve Problem (P4.2.1) by replacing p_m with p_m^* given in (4.3.1). However, it is extremely hard to find the optimal expressions for λ and τ at the same time due to the complexity of the objective function of Problem (P4.2.1) after the substitution of (4.3.1). To tackle this, we solve this problem optimally by

two steps. *Specifically, we first find the closed-form expression for the optimal λ with a fixed value of τ. Then, the optimal value for τ is achieved in the second step via a one-dimensional exhaustive search.* After substituting (4.3.1) into (4.2.7), the optimization problem at the AP side *for a given value of τ* can be expressed as

$$\text{(P4.3.1)}: \begin{array}{c} \max\limits_{\boldsymbol{\kappa},\lambda} \ \mathcal{U}'_a(\tau, \boldsymbol{\kappa}, \lambda) \\ \text{s.t. } \kappa_m \in \{0,1\}, \forall m \in \mathcal{N}, \\ \lambda \geq 0, \end{array} \tag{4.3.2}$$

where $\boldsymbol{\kappa} = [\kappa_1, \ldots, \kappa_N]^T$ is the indicator vector with the mth indicator defined as

$$\kappa_m = \begin{cases} 1, & \text{if } \lambda > \frac{b_m}{G_{m,s}}, \\ 0, & \text{if } \lambda \leq \frac{b_m}{G_{m,s}}, \end{cases} \tag{4.3.3}$$

and

$$\begin{aligned} \mathcal{U}'_a(\tau, \boldsymbol{\kappa}, \lambda) =& W' \ln C - \sum_{m=1}^{N} \kappa_m \lambda \tau \frac{\lambda G_{m,s} - b_m}{2a_m} G_{m,s} + \\ & W' \ln \left(1 + \frac{D}{C} \sum_{m=1}^{N} \kappa_m \frac{\lambda G_{m,s} - b_m}{2a_m} G_{m,s}\right), \end{aligned} \tag{4.3.4}$$

in which, $W' = \mu(1-\tau)W/\ln 2$, $C = 1 + \frac{\eta\tau G_{a,s} p_a G_{a,s}}{(1-\tau)N_0}$, and $D = \frac{\eta\tau G_{a,s}}{(1-\tau)N_0}$ are defined for notation simplification.

Unfortunately, Problem (P4.3.1) is still not convex due to the indicator vector $\boldsymbol{\kappa}$, even if we regard the parameter τ as a constant. To address this issue, *we first consider a special case of Problem (P4.3.1) by assuming that the gain per unit throughput (i.e., the parameter μ) is sufficiently large such that all PBs are involved during the DL energy transfer phase.* Thus, each indicator $\kappa_m = 1$ for any $m \in \mathcal{N}$. That is, $\lambda > \frac{b_m}{G_{m,s}}$, $\forall m$ holds. In this case, Problem (P4.3.1) can be simplified to the following one:

$$\text{(P4.3.2)}: \begin{array}{c} \max\limits_{\lambda} \ \mathcal{U}''_a(\tau, \lambda) \\ \text{s.t. } \lambda \geq 0, \end{array} \tag{4.3.5}$$

where

$$\mathcal{U}_a''(\tau,\lambda) = W'\ln C - \lambda^2\tau X_N + 2\lambda\tau Y_N + W'\ln\left(1+\frac{D}{C}\left(\lambda X_N - 2Y_N\right)\right), \quad (4.3.6)$$

with $X_N = \sum_{n=1}^{N}\frac{G_{n,s}^2}{2a_n}$ and $Y_N = \sum_{n=1}^{N}\frac{b_n G_{n,s}}{4a_n}$.

We now solve Problem (P4.3.2) and have the following proposition:

Proposition 4.3.1. *The optimal solution to Problem (P4.3.2) is given by*

$$\lambda^\star = \frac{-\left(\frac{C}{D}-3Y_N\right)+\sqrt{\left(\frac{C}{D}-Y_N\right)^2+\frac{2X_N W'}{\tau}}}{2X_N}. \quad (4.3.7)$$

Proof. See Appendix B.1. □

We can see from Proposition 4.3.1 that there always exists a unique optimal energy price when all the PBs are involved.

Now, a natural question that arises is "*under what conditions, the optimal solution to the simplified problem in Proposition 4.3.1 is also that to the original problem (i.e., Problem (P4.3.1))?*" To answer this question, we formulate the following proposition,

Proposition 4.3.2. *The optimal energy price given in (4.3.7) is also the optimal solution to the Problem (P4.3.1)* if and only if *the following condition holds*

$$\mu > \frac{2\tau(\ln 2)\left(X_N\max_{m\in\mathcal{N}}Z_m - 2Y_N + \frac{C}{D}\right)\left(X_N\max_{m\in\mathcal{N}}Z_m - Y_N\right)}{X_N(1-\tau)W}, \quad (4.3.8)$$

where

$$Z_m = \frac{b_m}{G_{m,s}}. \quad (4.3.9)$$

Proof. See Appendix B.2. □

From Proposition 4.3.2, we can observe that all PBs will involve during the DL energy transfer phase only when the gain per unit throughput of the source exceeds a certain threshold.

Based on the above analysis, we are now ready to derive the optimal solution to Problem (P4.3.1) given in the following proposition,

Proposition 4.3.3. *Let us assume that all PBs are sorted in the order* $Z_1 < \ldots < Z_{N-1} < Z_N$. *Then the optimal solution to Problem (P4.3.1) is given by*

$$\lambda^* = \begin{cases} \tilde{\lambda}_N, & \text{if } \mu > Q_N, \\ \tilde{\lambda}_{N-1}, & \text{if } Q_{N-1} < \mu \leq Q_N, \\ \quad \vdots & \\ \tilde{\lambda}_1, & \text{if } Q_1 < \mu \leq Q_2, \end{cases} \tag{4.3.10}$$

where

$$\tilde{\lambda}_K = \frac{-\left(\frac{C}{D} - 3Y_K\right) + \sqrt{\left(\frac{C}{D} - Y_K\right)^2 + \frac{2X_K W'}{\tau}}}{2X_K}, \tag{4.3.11}$$

$$Q_K = \frac{2\tau \left(\ln 2\right) \left(X_K Z_K - 2Y_K + \frac{C}{D}\right) \left(X_K Z_K - Y_K\right)}{X_K \left(1 - \tau\right) W}, \tag{4.3.12}$$

with $X_K = \sum_{n=1}^{K} \frac{G_{n,s}^2}{2a_n}$ *and* $Y_K = \sum_{n=1}^{K} \frac{b_n G_{n,s}}{4a_n}$, $\forall K \in \mathcal{N}$.

Proof. The expression of the optimal energy prices for the cases $\mu > Q_N$ and $Q_{N-1} < \mu \leq Q_N$, i.e., $\lambda^\star$ and $\tilde{\lambda}^\star$ given in (4.3.7) and (B.2.8), have already been proved in Appendix B.2. The proofs for other cases are omitted here due to their similarity with these two cases. □

We have already obtained the optimal energy price of the AP for a fixed τ. Substituting the appropriate expression of λ^* given in (4.3.10) base on the value of μ into Problem (P4.3.1), we have the following optimization problem regarding parameter τ:

$$\text{(P4.3.3)}: \begin{array}{l} \max\limits_{\tau} \ \mathcal{U}_a'\left(\tau, \lambda^*\right) \\ \text{s.t. } 0 < \tau < 1. \end{array} \tag{4.3.13}$$

Note that Problem (P4.3.3) can be efficiently solved via a one-dimensional exhaustive search. We denote the optimal solution to Problem (P4.3.3) by

$$\tau^* = \arg \max_{\tau \in (0,1)} \mathcal{U}'_a(\tau, \lambda^*). \tag{4.3.14}$$

This has completed the derivation of the SE for the formulated Stackelberg game, which is summarized in the following corollary,

Corollary 4.3.1. *The triple* $(\tau^*, \lambda^*, \boldsymbol{p}^*)$ *is the SE of the formulated Stackelberg game, where* τ^**,* λ^**, and* $\boldsymbol{p}^*$ *are given in (4.3.14), (4.3.10), and (4.3.1), respectively.*

4.3.2 Implementation Discussion

In practice, based on the above analysis, the formulated game can be implemented in the following manner,

- *Firstly*, the AP transfers energy to the source for a short while. The source uses the harvested energy to broadcast a pilot signal, based on which the AP and PBs perform channel estimation. Due to the channel reciprocality, the AP and PBs can also know the channel information from themselves to the source. Note that we assume that this channel estimation duration is very short such that it is ignorable compared with the length of the whole transmission block.

- *Secondly*, the PBs reveal[4] the values of a_m's, b_m's and $G_{m,s}$'s to the AP through the backhaul links between them such that the AP can calculate the values of Z_m's and X_K's, Y_K's and Q_K's. The AP is now ready to calculate the values of the optimal DL energy transfer time τ and the corresponding optimal energy price λ. This can be achieved by performing a one-dimensional search with

[4]Here we assume that there is no cheating behavior during this information revealing procedure. And the corresponding mechanism design is out of the scope of this chapter.

respect to τ, since the AP can calculate the optimal value of λ for any given τ based on (4.3.10). Then, these optimal values are fed back to the PBs.

- *Finally*, the PBs decide their transmit power according to (4.3.1), once they receive the value of energy price from the AP.

Notice that in the above implementation, the PBs are required to release the values of a_m's and b_m's, which could be the *private* information of the PB operators. Thus, this revealing procedure may lead to privacy concerns of the PB operators. To overcome this issue, we exploit the special structures of Z_m's, X_K's and Y_K's to design an *advanced* information releasing scheme. Specifically, instead of revealing the values of a_m's, b_m's and $G_{m,s}$'s, the PBs tell the AP their values of $\frac{b_m}{G_{m,s}}$'s (i.e., Z_m's) and $\frac{G_{m,s}^2}{2a_m}$'s. In this case, the AP can first calculate the values of the terms $\frac{b_m G_{m,s}}{4a_m}$'s and then calculate the values of X_K's and Y_K's, which means that the AP can still calculate the optimal energy price for a given τ according to (4.3.10). However, this advanced scheme can protect the PBs' privacy since the AP has no knowledge of $G_{m,s}$'s and thus is not able to acquire the exact values of a_m's and b_m's based on those of $\frac{b_m}{G_{m,s}}$'s and $\frac{G_{m,s}^2}{2a_m}$'s.

4.3.3 Social Welfare Optimization Scheme

To demonstrate the performance loss of the AP due to the rationality of PBs in the proposed game-theoretical scheme, we investigate a social welfare optimization scheme in this subsection. Specifically, we consider that the AP and PBs cooperate to maximize the social welfare, defined as the difference between the benefits obtained from the achievable throughput at the AP and the total cost of the PBs. This is done by jointly optimizing the DL energy transfer time and the transmit powers of the

PBs. Mathematically, we have the following social welfare maximization problem:

$$(\text{P4.3.4}): \begin{array}{c} \max\limits_{\tau,\boldsymbol{p}} \ \mathcal{U}_{sw}(\tau,\boldsymbol{p}) \\ \text{s.t. } \tau \in (0,1), \\ \boldsymbol{p} \geq \mathbf{0}, \end{array} \tag{4.3.15}$$

where

$$\begin{aligned} \mathcal{U}_{sw}(\tau,\boldsymbol{p}) =& \mu R_{sa} - \sum_{m=1}^{N} \tau \mathcal{C}_m(p_m) \\ =& W' \ln C + W' \ln\left(1 + \frac{D}{C}\sum_{m=1}^{N} p_m G_{m,s}\right) - \tau \sum_{m=1}^{N} \left(a_m p_m^2 + b_m p_m\right) \end{aligned} \tag{4.3.16}$$

is the social welfare. Note that the above social welfare optimization scheme can correspond to an alternative scenario where the AP and PBs are deployed by the same operator, as the one considered in [47].

Problem (P4.3.4) is non-convex due to the coupled variables in the objective function. We solve this non-convex problem optimally by the following two steps: (1) we first fix the DL energy transfer time τ and derive the optimal transmit powers of the PBs, (2) the time allocation parameter is obtained via a one-dimensional search to maximize the social welfare given in (4.3.16). This enables numerical comparisons of the proposed game-theoretical scheme and its corresponding social welfare optimization scheme to be carried out in the next section.

For a fixed τ, Problem (P4.3.4) reduces to the following power control problem with individual constraints:

$$(\text{P4.3.5}): \begin{array}{c} \max\limits_{\boldsymbol{p}} \ \mathcal{U}'_{sw}(\boldsymbol{p}) \\ \text{s.t. } \boldsymbol{p} \geq \mathbf{0}, \end{array} \tag{4.3.17}$$

where

$$\mathcal{U}'_{sw}(\boldsymbol{p}) = W' \ln\left(1 + \frac{D}{C}\sum_{m=1}^{N} p_m G_{m,s}\right) - \tau \sum_{m=1}^{N} \left(a_m p_m^2 + b_m p_m\right). \tag{4.3.18}$$

It is easy to verify that Problem (P4.3.5) is convex. Utilizing the structure of

Problem (P4.3.5) and following a similar procedure to solve Problem (P4.3.1), we can divide it into several unconstrained optimization problems according to parameter μ. Solving these problems, we then get the following proposition regarding the optimal solution to Problem (P4.3.5),

Proposition 4.3.4. *Let us assume that all PBs are sorted in the order* $Z_1 < \ldots < Z_{N-1} < Z_N$. *Then the optimal solution to Problem (P4.3.5) can be expressed as*

$$\boldsymbol{p}^{\dagger} = \begin{cases} \left[\frac{\Lambda_N G_{1,s}-b_1}{2a_1}, \frac{\Lambda_N G_{2,s}-b_2}{2a_2}, \ldots, \frac{\Lambda_N G_{N,s}-b_N}{2a_N}\right]^T, & \text{if } \mu > \widetilde{Q}_N, \\ \left[\frac{\Lambda_{N-1} G_{1,s}-b_1}{2a_1}, \frac{\Lambda_{N-1} G_{2,s}-b_2}{2a_2}, \ldots, \frac{\Lambda_{N-1} G_{N-1,s}-b_{N-1}}{2a_{N-1}}, 0\right]^T, & \text{if } \widetilde{Q}_{N-1} < \mu \leq \widetilde{Q}_N, \\ \vdots & \vdots \\ \left[\frac{\Lambda_1 G_{1,s}-b_1}{2a_1}, 0 \ldots, 0\right]^T, & \text{if } \widetilde{Q}_1 < \mu \leq \widetilde{Q}_2, \end{cases} \tag{4.3.19}$$

where

$$\Lambda_K = \frac{-\left(\frac{C}{D} - 2Y_K\right) + \sqrt{\left(\frac{C}{D} - 2Y_K\right)^2 + \frac{4X_K W'}{\tau}}}{2X_K}, \ \forall\, K \in \mathcal{N}, \tag{4.3.20}$$

$$\widetilde{Q}_K = \frac{(\ln 2)\,\tau \left(X_K Z_K - 2Y_N + \frac{C}{D}\right) Z_K}{(1-\tau)\,W}, \ \forall\, K \in \mathcal{N}. \tag{4.3.21}$$

Proof. See Appendix B.3 □

Substituting the optimal solution of Problem (P4.3.5) according to the value of μ into Problem (P4.3.4), we get the following optimization problem in terms of the DL energy transfer time τ

$$(\text{P4.3.6}): \begin{array}{l} \max\limits_{\tau} \ \mathcal{U}_{sw}\left(\tau, \boldsymbol{p}^{\dagger}\right) \\ \text{s.t. } \tau \in (0,1), \end{array} \tag{4.3.22}$$

which can be efficiently solved by a one-dimensional search. We use $\tau^{\dagger}$ to denote the optimal solution to Problem (P4.3.6). Then, a complete solution to the social welfare maximization Problem (P4.3.4) is obtained by putting $\tau^{\dagger}$ and $\boldsymbol{p}^{\dagger}$ together.

In practice, this social welfare optimization scheme can be implemented in a similar manner as the proposed Stackelberg scheme presented in Section 4.3.2. However, the AP needs to calculate the optimal transmit powers of the PBs and feed them back to the PBs since there is no pricing mechanism in this scheme.

4.4 Numerical Results

In this section, we present some numerical results to demonstrate the performance of the proposed game-theoretical scheme and its comparison with the social welfare optimization scheme. We also illustrate the impact of various system parameters to provide further insights into the considered network. The channel short-term fading is assumed to be Rayleigh distributed. To capture the effect of path loss on the network performance, we use the channel model that $\mathbb{E}\left[G_{x,y}\right] = 10^{-3}\left(d_{x,y}\right)^{-\alpha}$, where $d_{x,y}$ is the distance between nodes x and y, and $\alpha \in [2, 5]$ is the path-loss factor [81]. Note that a 30dB average signal power attenuation is assumed at a reference distance of 1m in the above channel model [57]. In all following simulations, the gain per unit throughput (i.e, μ) is measured in per Mbps and the transmit powers of PBs (i.e., p_m's) are measured in milliWatt (mW). Accordingly, the units of the energy price λ released by the AP, and the cost parameters a_m's and b_m's of the PBs are per mW, per mW^2, and per mW. In addition, we set the AP transmit power $p_a = 1000$mW, the distance between the AP and source $d_{a,s} = 15$m, the path-loss exponent $\alpha = 2$, the noise power $N_0 = 10^{-8}$mW, the energy harvesting efficiency $\eta = 0.5$ and the bandwidth $W = 1$MHz. For simplicity, we choose the same values $a_m = 2 \times 10^{-6}$ and $b_m = 2 \times 10^{-3}$ for all PBs. To evaluate the impact of the number of PBs on the system performance, we assume that the distances from the PBs to the source are

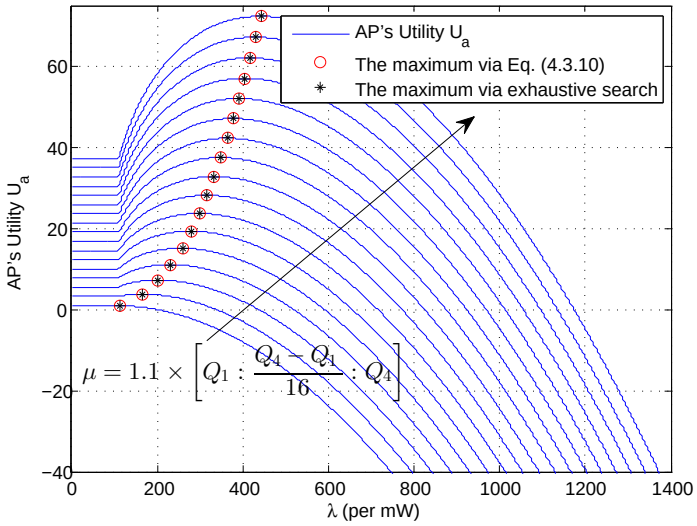

Figure 4.3: The AP's utility $\mathcal{U}_a$ versus the energy price λ in a four-PB network, in which the channel gains are given in (4.4.1) and $\tau = 0.5$.

the same, i.e., $d_{m,s} = d, \forall m$.

We first validate our theoretical analysis presented in Section 4.3. To this end, we consider a four-PB network with one randomly generated channel realization given by

$$G_{a,s} = 8.0846 \times 10^{-6}, \tag{4.4.1a}$$

$$[G_{m,s}]_{m=1,2,3,4} = [0.0470, 0.0787, 0.1798, 0.1824] \times 10^{-4}. \tag{4.4.1b}$$

Now, we can calculate the values of Q_1, Q_2, Q_3 and Q_4 based on (4.3.12). Then, for any given value of μ, we can obtain the optimal energy price λ^* according to (4.3.10) and (4.3.11), and then the maximum value of the AP's utility. To verify the correctness of these calculations, we draw the curves of the AP's utility $\mathcal{U}_a$ versus the value of λ for different values of μ in Fig. 4.3, in which the maximum values of the AP's utility corresponding to the optimal price λ^* are also calculated by an exhaustive search. We can see from Fig. 4.3 that the maximum values of the AP's

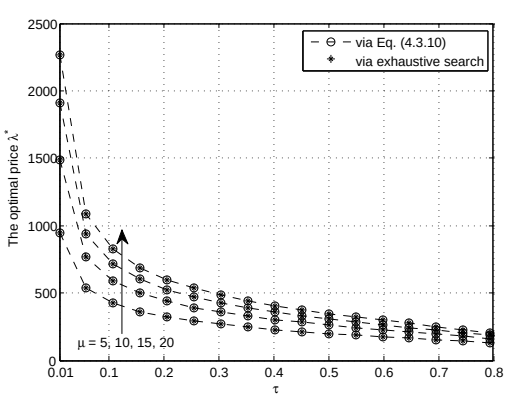

(a) The optimal energy price λ^*

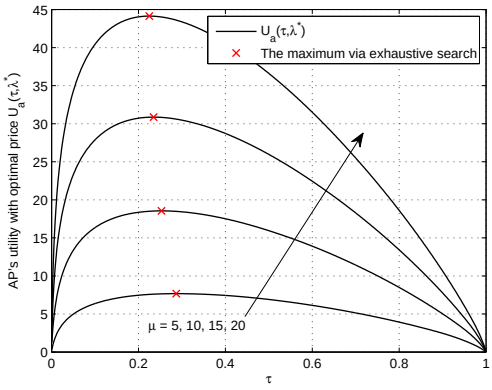

(b) The AP's utility with the optimal energy price

Figure 4.4: The impact of the DL energy transfer time τ on (a) the optimal energy price λ^* and (b) the AP's utility with the optimal energy price.

utility obtained via (4.3.10)-(4.3.12) and the exhaustive search coincide very well, which validates our procedure to solve Problems (P4.3.1) and (P4.3.5). We also can observe from Fig. 4.3 that the optimal price λ^* gradually increases as the value of μ rises. This is because the larger the parameter μ, the more benefits the AP can obtain from each unit of throughput. Thus, the AP will tend to buy more energy from the PBs through increasing its energy price λ.

With the same setup given in (4.4.1), Fig. 4.4 illustrates the impact of the DL energy transfer time τ on both the optimal energy price λ^* and the AP's utility with the optimal energy price. It can be observed from Fig. 4.4 (a) that the values of the optimal price obtained via (4.3.10) and exhaustive search coincide with each other for all simulated cases, which confirms our analysis once again. In addition, we can see from this subfigure that the optimal energy price decreases monotonically when the value of τ increases. The reason is that with a longer DL energy transfer time τ,

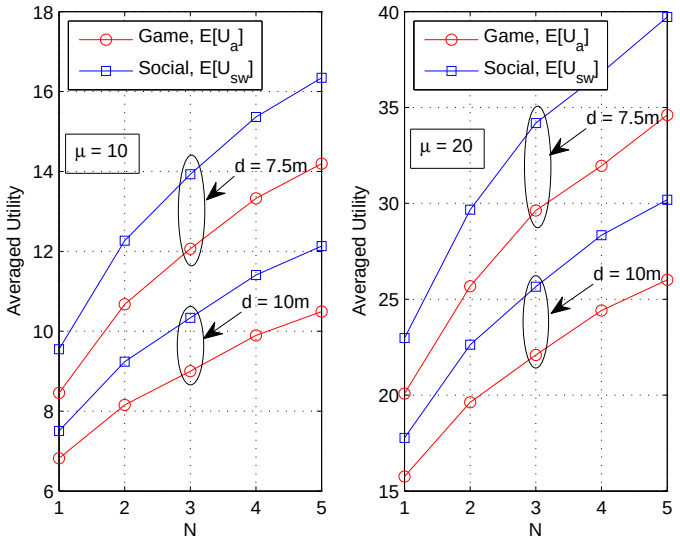

Figure 4.5: The averaged utility of the AP for two considered schemes versus the number of PBs with different values of μ.

the source can harvest more energy from its associated AP and less energy is required from the PBs, which renders the decrease of the optimal energy price. From Fig. 4.4 (b), we can see that there always exists a utility-optimal energy transfer time τ when the energy price is set to the optimal one. Furthermore, we can observe from this subfigure that the optimal value of τ slightly shifts to the left as the parameter μ increases. Note that due to space limitation, we only show results in Figs. 4.3-4.4 for one network setup with one random channel realization, although similar results can also be shown for other network setups and channel realizations.

Next, we investigate and compare the averaged performance of the proposed game-theoretical scheme and its corresponding social welfare optimization scheme in the remaining figures, in which each curve is obtained by averaging over 10000 randomly generated channel realizations. We use "game" and "social" in figure legends to refer to the proposed game-theoretical scheme and social welfare optimization scheme,

respectively. Fig. 4.5 compares the averaged utilities of the AP with the game-theoretical scheme and the social welfare optimization scheme, denoted by $\mathbb{E}[\mathcal{U}_a]$ and $\mathbb{E}[\mathcal{U}_{sw}]$, respectively. We can observe from Fig. 4.5 that the value of $\mathbb{E}[\mathcal{U}_{sw}]$ is always larger than that of $\mathbb{E}[\mathcal{U}_a]$ for all simulated cases, which indicates that the AP can achieve higher utilities in the social welfare optimization scheme. This is understandable since the PBs are cooperative and selfless in the social welfare optimization scheme, while they are rational and self-interested in the game-theoretical scheme. It can also be observed from this figure that both $\mathbb{E}[\mathcal{U}_a]$ and $\mathbb{E}[\mathcal{U}_{sw}]$ are improved with the increase of the number of PBs and the value of μ. But, they are reduced when the distance between the source and PBs is increased from 7.5m to 10m. This is because the nearer the PBs to the source, the higher the efficiency of DL energy transfer from the PBs to the source, which can reduce the AP's payments to the PBs for their wireless charging services. Finally, the performance gaps between the game-theoretical scheme and its corresponding social welfare optimization scheme are enlarged as the number of PBs and the parameter μ increases, but reduced as the distance between the source and PBs increases.

Fig. 4.6 demonstrates the impacts of the number of PBs, the distance between the source and PBs, and the value of μ on the averaged optimal energy transfer time of the two considered scheme, denoted by $\mathbb{E}[\tau^*]$ and $\mathbb{E}\left[\tau^\dagger\right]$, respectively. As we can observe from this figure, the values of $\mathbb{E}\left[\tau^\dagger\right]$ are lower than that of $\mathbb{E}[\tau^*]$ for all simulated cases, which reveals that the social welfare optimization scheme should allocate less time for DL energy transfer than the game-theoretical scheme. Both $\mathbb{E}[\tau^*]$ and $\mathbb{E}\left[\tau^\dagger\right]$ decrease monotonically as the number of PBs increases. Moreover, the increase of the parameter μ and the decrease of the distance d can also lead to smaller values

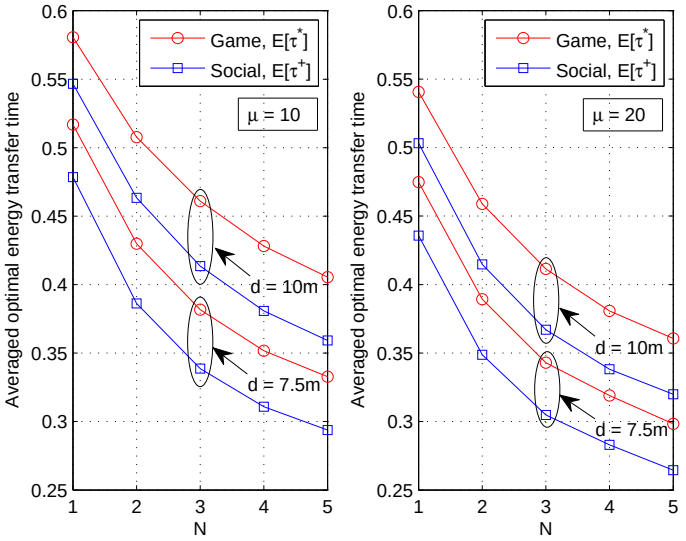

Figure 4.6: Averaged optimal energy harvesting time for both considered schemes versus the number of PBs with different values of μ.

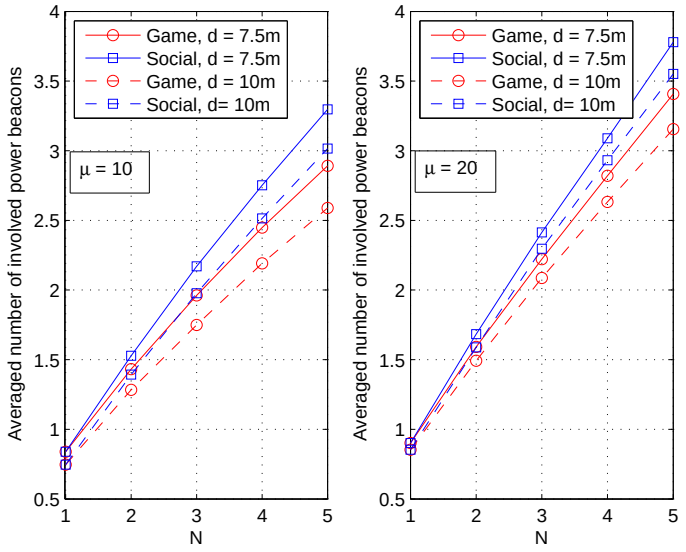

Figure 4.7: Averaged number of involved PBs for both considered schemes versus the number of PBs with different values of μ.

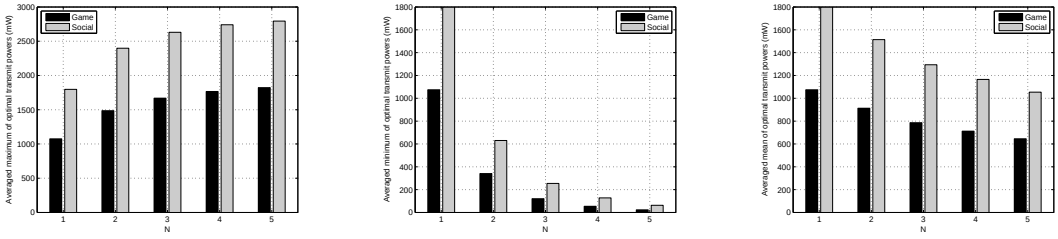

(a) Averaged maximum of PBs' optimal transmit powers

(b) Averaged minimum of PBs' optimal transmit powers

(c) Averaged mean of PBs' optimal transmit powers

Figure 4.8: The averaged maximum, minimum and mean of the optimal transmit powers of all PBs for both considered schemes with $d = 10$m and $\mu = 20$.

of $\mathbb{E}[\tau^*]$ and $\mathbb{E}\left[\tau^\dagger\right]$. In Fig. 4.7, we illustrate the influences of the aforementioned parameters on the averaged number of involved PBs for the two considered schemes. Here, we refer to the PBs with transmit powers larger than zero as "involved" PBs. It can be observed from Fig. 4.7 that the averaged number of involved PBs for both schemes increases when more PBs exists in the network. Also, more PBs will join the DL energy transfer when their distance to the source is shorter (i.e., d is smaller) or the value of the parameter μ is increased. In all simulated setups of Fig. 4.7, the two considered schemes involve almost the same averaged numbers of PBs when $N = 1$. But, the social welfare optimization scheme involves more PBs than the corresponding game-theoretical scheme for $N \geq 2$. Furthermore, the gap between them is gradually enlarged with the increase of N.

Fig. 4.8 depicts the averaged maximum, minimum and mean of the optimal transmit powers of all PBs for both the game-theoretical scheme and social welfare optimization scheme. That is, it shows $\mathbb{E}[\max(\boldsymbol{p}^*)]$, $\mathbb{E}[\min(\boldsymbol{p}^*)]$ and $\mathbb{E}\left[\left(\sum_m p_m^*\right)/N\right]$ for the game-theoretical scheme, and $\mathbb{E}\left[\max\left(\boldsymbol{p}^\dagger\right)\right]$, $\mathbb{E}\left[\min\left(\boldsymbol{p}^\dagger\right)\right]$ and $\mathbb{E}\left[\left(\sum_m p_m^\dagger\right)/N\right]$

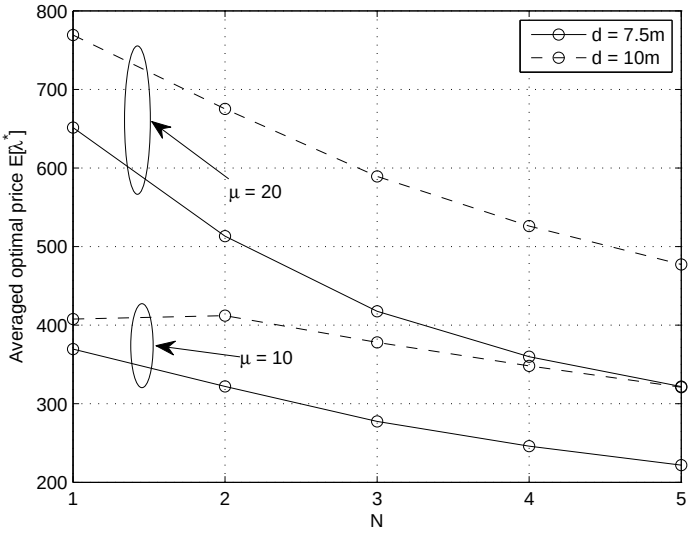

Figure 4.9: Averaged optimal energy price for the AP in the game-theoretical scheme versus the number of PBs with different values of d and μ.

for the social welfare optimization scheme. As shown in Fig. 4.8, the three averaged values of the social welfare optimization scheme are all larger than those of the game-theoretical scheme, which means that the PBs can transmit with relatively higher powers in the former scheme. Moreover, the averaged maximum of the PBs' optimal transmit powers of both schemes increases as the value of N grows, while the averaged minimum of the PBs' optimal transmit powers of both schemes shows an opposite trend. On the whole, the optimal transmit powers of the PBs in both schemes become smaller as the number of PBs increases, since the averaged mean of the optimal transmit powers of all PBs is shown to be a decreasing function of N in Fig. 4.8 (c). In Fig. 4.9, we plot the curves of the averaged optimal energy price, denoted by $\mathbb{E}[\lambda^*]$, for the AP in the game-theoretical scheme with variable values of parameters d and μ. We can see from Fig. 4.9 that the value of $\mathbb{E}[\lambda^*]$ decreases as the number of PBs increase. Besides, the larger the parameter μ, the higher the averaged optimal energy

price, which is consistent with our observation in Fig. 4.3. It can also be observed from Fig. 4.9 that the reduction of the distance between the source and PBs can also diminish the optimal energy price. This is because the shorter the distance between the source and PBs, the more energy the source can harvest on average for the same transmit powers of the PBs, which leads to a lower energy price.

Chapter 5

Distributed Power Splitting for a Large-Scale WPCCN with SWIPT using Game Theory

In this chapter, we consider SWIPT in a large-scale WPCCN, where multiple source-destination pairs communicate through their dedicated wireless-powered relays. Each relay needs to split its received signal from sources into two streams: one for information forwarding and the other for energy harvesting. We develop a distributed power splitting framework using the non-cooperative game theory to derive a profile of power splitting ratios for all relays that can achieve a good network-wide performance. Specifically, non-cooperative games are respectively formulated for pure AF and DF networks, in which each link is modeled as a strategic player who aims to maximize its own achievable rate. The existence and uniqueness for the NEs of the formulated games are analyzed and a distributed algorithm with provable convergence to achieve the NEs is also developed. Subsequently, the developed framework is extended to the more general network setting with mixed AF and DF relays. All the theoretical analyses are validated by extensive numerical results.

5.1 Introduction

Besides the cooperation scenarios investigated in the previous chapters, the paradigm SWIPT also opens up a new cooperation pattern for WPCCNs, where a wireless-powered relay node harvests energy from the source signal to enable forwarding the received signal from the source to its destination [48]. Two practical relaying protocols were proposed for a three-node cooperative network in [48]. Analytical expressions for the outage probability and the ergodic capacity of the proposed protocols were derived for delay-limited and delay-tolerant modes, respectively. This work was further extended in [86], by considering an adaptive time-switching protocol for a SWIPT relaying network and analytical expressions of the achievable throughput were derived for both AF and DF relaying networks. A similar idea for SWIPT in two-way relaying networks was proposed and analyzed in [87]. Very recently, [52] considered SWIPT in a relatively large relay network, where multiple source-destination pairs communicate with each other via a common energy harvesting relay. Specifically, several power allocation schemes were proposed to efficiently distribute the power harvested at the relay among multiple pairs.

In practice, many source-relay-destination links could coexist and interfere with each other. This general network setup can be modeled by the relay interference channels, which have many practical applications such as cellular networks, wireless sensor networks, WLANs etc. [88–93]. In this model, multiple source-destination pairs communicate with the help of dedicated relays using the same spectral resources[1]. However, to the best of our knowledge, no work in the open literature has considered

[1]Such a model is also called two-hop interference channels since the multiple source-relay-destination links, which constitute a cascade of two interference channels, transmit and interfere in each hop.

SWIPT in relay interference channels except [94]. Note that although [48, 52, 86, 87] also designed SWIPT for relay networks, none of them considered relay interference channels. By using the advanced stochastic geometry theory, [94] analyzed the outage performance of SWIPT in large-scale networks with/without relaying, where the transmitters and the relays (if they exist) are assumed to be connected to a power supply, while the receivers harvest the energy from the signals received from the source and relay based on a power splitting technique [21].

In this chapter, we also focus on the design of SWIPT in a large-scale WPCCN that constitutes relay interference channels. Different from [94] in the model, objective, and approach, we consider that multiple source-destination pairs communicate simultaneously with the help of their dedicated wireless-powered relays, which do not have their own power supply and need to harvest energy from the source signal before forwarding. Each relay node splits the signal received from all source nodes into two parts according to a power splitting ratio: one part is sent to the information processing unit, and the rest is used to harvest energy for forwarding the received information in the second time slot. We consider that each link's performance is characterized by its achievable rate and thus regard the sum-rate of all links as a network-wide performance metric. The first natural question that arises from this system is "*how should the relays split their received signals for information receiving and energy harvesting in order to achieve a good network-wide performance?*". This is actually a very complex question to answer. The reason is that the power splitting ratio of each link not only affects the performance of this link, but also affects the performance of other links due to mutual interference between different links. This means that the optimization of each ratio depends on all other ratios and they are

tangled together. Moreover, the maximization of the sum-rate of all links is shown to be a non-convex optimization problem. The global optimal power splitting ratios cannot be efficiently achieved even in a centralized fashion, and there is a heavy signaling overhead required by the centralized method.

To tackle the aforementioned problem, we apply the non-cooperative game theory to develop a distributed power splitting framework for SWIPT in relay interference channels. We investigate both pure and hybrid networks in this chapter. In a pure network, all relays adopt the same relaying protocol. Considering that AF relaying and DF relaying protocols are most-frequently used in practice [71], we further classify a pure network into a pure AF network and a pure DF network. On the other hand, in a hybrid network, a mixture of AF and DF relaying protocols are implemented at the relays. To the best of our knowledge, this is the first game-theoretical framework for the design of SWIPT in relay interference channels.

In this chapter, we develop a distributed power splitting framework for the SWIPT in relay interference channels. In particular, each source-relay-destination link in the relay interference channels is modeled as a strategic player who chooses its dedicated relay's power splitting ratio to maximize its individual rate. We then analyze the existence and uniqueness of the NE for the formulated game in the pure network, where all relays employ either AF or DF relaying protocol. In addition, a distributed algorithm is proposed with provable convergence to achieve the NEs. The theoretical analysis for the pure networks is then extended to a more general hybrid network with mixed AF and DF relays coexisting. All analytical results are validated by extensive numerical simulations, which show that the proposed game-theoretical approach can achieve a near-optimal network-wide performance on average.

The remainder of this chapter is organized as follows. Section 5.2 describes the system model. In Section 5.3, we present the proposed game-theoretical power splitting framework for the pure networks, where the non-cooperative games are formulated for the pure AF and pure DF networks, followed by the existence and uniqueness analysis of the NEs as well as the development of the distributed algorithm. The extension of the proposed framework to the hybrid network is discussed in Section 5.4. Numerical results are provided in Section 5.5.

5.2 System Model

We consider SWIPT in a large-scale WPCCN that constitutes relay interference channels, as depicted in Fig. 5.1. The system consists of N source-relay-destination (S-R-D) links and the set of these links is denoted as $\mathcal{N} = \{1, \ldots, N\}$. More specifically, in the link $S_i \rightarrow R_i \rightarrow D_i$, $i \in \mathcal{N}$, the source S_i communicates with its corresponding destination D_i, assisted by a dedicated relay R_i. The relay nodes can employ either AF or DF relaying schemes [34]. The direct source-destination channels are neglected due to a high path loss and shadowing attenuation. Since these two-hop links share the same spectrum, they interfere with each other over the dual hops.

We assume that all the nodes (i.e., sources, relays and destinations) are equipped with only one antenna[2] and operate in a half-duplex mode. The relay nodes do not have their own power supply and need to harvest energy from the received signal in order to forward the received signal to the destinations. It is assumed that the

[2]The considered single-antenna model could correspond to cost/size constrained networks in practice. A good example is the wireless sensor network, where the sources, relays and destinations are all sensor nodes that cannot be equipped with multiple antennas due to the size and/or cost constraints.

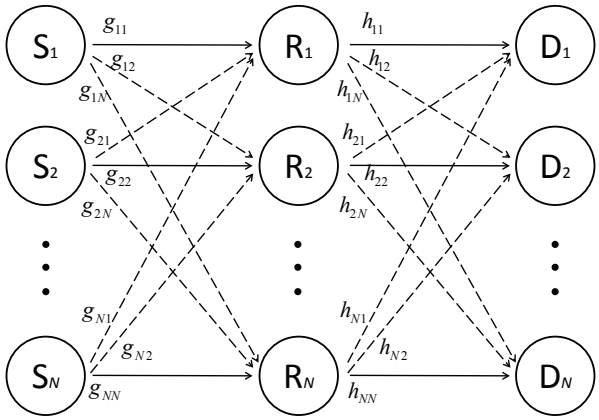

Figure 5.1: System model for SWIPT in a large-scale WPCCN that comprises interference relay channels.

energy harvesting and information transmission are implemented for every received message block. For the purpose of exposition, *the processing power consumed by the transmit/receive circuitry at the relay nodes is assumed to be negligible as compared to the power used for signal forwarding* [48]. Moreover, we consider that all links experience slow and frequency-flat fading.

Let g_{ij} and h_{ij} denote the channel gain from S_i to R_j in the first hop and from R_i to D_j in the second hop, respectively. In the first time slot, all sources transmit simultaneously and the signal received by the relay R_i can be written as

$$y_{R_i} = \sqrt{P_i} g_{ii} x_i + \sum\nolimits_{j=1, j\neq i}^{N} \sqrt{P_j} g_{ji} x_j + n_i^a, \tag{5.2.1}$$

where P_i is the fixed transmit power, x_i is the transmitted information of the source S_i with $\mathbb{E}\left\{|x_i|^2\right\} = 1$, and $n_i^a \sim \mathcal{CN}\left(0, \sigma_{i,a}^2\right)$ is the additive noise introduced by the receiver antenna at the relay R_i.

Subsequently, the received signal at the relay R_i is split into two streams, with the power splitting ratio ρ_i, as shown in Fig. 5.2. The fraction $\sqrt{\rho_i}$ of the received

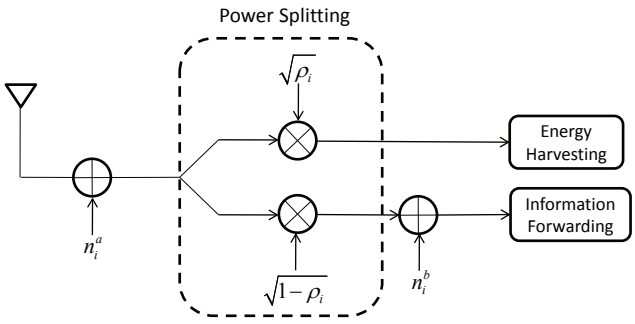

Figure 5.2: Diagram of the power splitting technique at the relay nodes.

signal is used for energy harvesting, while the remaining one is sent to the information processing unit. In practice, the antenna noise n_i^a has a negligible impact on both the information receiving and energy harvesting, since $\sigma_{i,a}^2$ is generally much smaller than the noise power introduced by the baseband processing circuit, and thus even lower than the average power of the received signal [95]. For simplicity, we ignore the noise term n_i^a in the following analysis, i.e., setting $\sigma_{i,a}^2 = 0$ [95]. For the sake of simplicity, we assume a normalized transmission time for each hop (i.e., the transmission duration of each hop is equal to one). Then, the terms "energy" and "power" can be used interchangeably. In this case, the energy harvested at relay R_i can thus be expressed as

$$Q_i = \eta\rho_i \sum\nolimits_{n=1}^{N} P_n |g_{ni}|^2. \tag{5.2.2}$$

Meanwhile, the information signal received by the information processing unit at relay R_i is given by

$$\begin{aligned} y_{R_i}^I =& \sqrt{1-\rho_i} y_{R_i} + n_i^b \\ =& \sqrt{1-\rho_i}\sqrt{P_i} g_{ii} x_i + \sqrt{1-\rho_i} \sum\nolimits_{j=1, j\neq i}^{N} \sqrt{P_j} g_{ji} x_j + n_i^b, \end{aligned} \tag{5.2.3}$$

where $n_i^b \sim \mathcal{CN}\left(0, \sigma_{R_i}^2\right)$ is the AWGN introduced by the signal processing circuit from passband to baseband. Then, in the second time slot, the relay nodes will exhaust[3]

[3]Generally, the relay nodes may be interested in keeping part of the energy harvested from the

the harvested energy to forward the information signal $y_{R_i}^I$ by employing either AF or DF relaying protocol. In the following subsections, we derive the expressions for the achievable rates of the ith link for the AF and DF relaying protocols, respectively.

5.2.1 AF Relaying

When the AF relaying scheme is adopted, the relay node R_i will exhaust the harvested energy to amplify and forward the signal received by the information processing unit in the first time slot. Thus, the transmit power of the relay R_i is Q_i and the received signal at the destination D_i can be expressed as [71]

$$\begin{aligned} y_{D_i}^{AF} =& \sqrt{Q_i} h_{ii} \beta_i y_{R_i}^I + \sum\nolimits_{j=1, j\neq i}^{N} \sqrt{Q_j} h_{ji} \beta_j y_{R_j}^I + n_{D_i} \\ =& \sqrt{Q_i} h_{ii} \beta_i \sqrt{1-\rho_i} \sqrt{P_i} g_{ii} x_i + \\ & \sqrt{Q_i} h_{ii} \beta_i \sqrt{1-\rho_i} \sum\nolimits_{j=1, j\neq i}^{N} \sqrt{P_j} g_{ji} x_j + \\ & \sqrt{Q_i} h_{ii} \beta_i n_i^b + \sum\nolimits_{j=1, j\neq i}^{N} \sqrt{Q_j} h_{ji} \beta_j y_{R_j}^I + n_{D_i}, \end{aligned} \tag{5.2.4}$$

where

$$\beta_i = 1 / \sqrt{(1-\rho_i) P_i |g_{ii}|^2 + (1-\rho_i) \sum_{j=1, j\neq i}^{N} P_j |g_{ji}|^2 + \sigma_{R_i}^2}$$

is the power constraint factor at the relay R_i, and $n_{D_i} \sim \mathcal{CN}\left(0, \sigma_{D_i}^2\right)$ is the additive white noise at the destination D_i. Without loss of generality, we hereafter assume that $\sigma_{R_i}^2 = \sigma_{D_i}^2 = \sigma^2$, for any $i \in \mathcal{N}$. The second equality of (5.2.4) is obtained by inserting the expression of $y_{R_i}^I$ given by (5.2.3) into the first equality of (5.2.4). Note that only the first term on the right-hand side of the second equality in (5.2.4) is the useful signal to the destination D_i, while the remaining terms should be regarded as interference plus noise. Based on this observation and after some algebraic manipulations, we can

RF signals. In this chapter, we consider the relay protocol to maximize the achievable rate of each link. In this regard, the relay should exhaust the harvested energy to forward the source information and thus has no incentive to keep any part of the energy.

write the end-to-end SINR of the ith link as

$$\gamma_i^{AF} = \frac{\rho_i \left(1-\rho_i\right) X_i Z_i}{\rho_i \left(1-\rho_i\right) Y_i Z_i + \left(1-\rho_i\right)\left(X_i + Y_i\right)\left(W_i + 1\right) + \rho_i Z_i + W_i + 1}, \tag{5.2.5}$$

where

$$X_i = P_i |g_{ii}|^2 / \sigma^2, \tag{5.2.6a}$$

$$Y_i = \sum\nolimits_{j=1, j\neq i}^{N} P_j |g_{ji}|^2 / \sigma^2, \tag{5.2.6b}$$

$$Z_i = \eta \left(\sum\nolimits_{n=1}^{N} P_n |g_{ni}|^2 \right) |h_{ii}|^2 / \sigma^2, \tag{5.2.6c}$$

$$W_i = \sum\nolimits_{j=1, j\neq i}^{N} \rho_j \eta \left(\sum\nolimits_{n=1}^{N} P_n |g_{nj}|^2 \right) |h_{ji}|^2 / \sigma^2, \tag{5.2.6d}$$

are defined for the simplicity of notations. It is worth noticing that the above equations (5.2.6a)-(5.2.6d) have physical meanings. More specifically, (5.2.6a) and (5.2.6b) respectively denote the SNR and the interference-to-noise ratio (INR) at the relay R_i when the received signal is fully forwarded to D_i without harvesting any energy at the relay (i.e., $\rho_i = 0$). On the other hand, (5.2.6c) represents the SNR at the destination D_i when the received signal of the relay R_i is fully used for energy harvesting (i.e., $\rho_i = 1$). Finally, (5.2.6d) is the INR at the destination D_i.

Then, the achievable rate of the link i when the AF relaying technique is employed at its dedicated relay can be expressed as

$$u_i^{AF}\left(\boldsymbol{\rho}\right) = \frac{1}{2} \log\left(1 + \gamma_i^{AF}\right), \tag{5.2.7}$$

where $\boldsymbol{\rho} = \left[\rho_1, \ldots, \rho_N\right]^T$ denotes the vector of all links' power splitting ratios.

5.2.2 DF Relaying

For the case when the DF relaying protocol is employed, the relay node will first decode the information based on the received information signal $y_{R_i}^I$ given in (5.2.3).

Thus, the received SINR at relay R_i can be written as

$$\gamma_{i,1}^{DF} = \frac{(1-\rho_i) X_i}{(1-\rho_i) Y_i + 1}, \tag{5.2.8}$$

where X_i and Y_i are defined in (5.2.6a) and (5.2.6b), respectively.

In the second time slot, the relay nodes forward the decoded information to their corresponding destinations using the energy harvested in the first time slot. The received signal at D_i is given by

$$y_{D_i} = \sqrt{Q_i} h_{ii} x_i + \sum\nolimits_{j=1, j\neq i}^{N} \sqrt{Q_j} h_{ji} x_j + n_{D_i}. \tag{5.2.9}$$

The received SINR at the destination D_i can thus be written as

$$\gamma_{i,2}^{DF} = \frac{\rho_i Z_i}{W_i + 1}, \tag{5.2.10}$$

where Z_i and W_i are defined in (5.2.6c) and (5.2.6d), respectively. The achievable rate of the ith link in this case is thus given by

$$\begin{aligned} u_i^{DF}(\boldsymbol{\rho}) &= \frac{1}{2} \min\left(\log\left(1+\gamma_{i,1}^{DF}\right), \log\left(1+\gamma_{i,2}^{DF}\right)\right) \\ &= \frac{1}{2} \log\left(1+\gamma_i^{DF}\right), \end{aligned} \tag{5.2.11}$$

where

$$\gamma_i^{DF} = \min\left(\gamma_{i,1}^{DF}, \gamma_{i,2}^{DF}\right) \tag{5.2.12}$$

can be regarded as the end-to-end SINR of the ith link with a DF relay.

We consider that each link's performance is characterized by its achievable rate and thus regard the sum-rate of all links as a network-wide performance metric. In the following sections, we will develop a distributed power splitting scheme to achieve a good network-wide performance.

5.3 Distributed Power Splitting of Pure Networks

In this section, we focus on the the design of distributed power splitting for pure AF and DF networks, where all the relay nodes employ the same relaying protocol, i.e., either AF or DF relaying. To choose an efficient profile of the power splitting ratios (i.e., $\boldsymbol{\rho}$) that can achieve a globally optimal network-wide performance, one needs to solve the following network utility maximization problem:

$$\begin{array}{c} \max\limits_{\boldsymbol{\rho}} \sum_{i=1}^{N} u_i^X(\boldsymbol{\rho}) \\ \text{s.t. } \rho \in \mathcal{A} \end{array}, \tag{5.3.1}$$

where X refers to AF (DF) for the pure AF (DF) network, $u_i^{AF}(\boldsymbol{\rho})$ and $u_i^{DF}(\boldsymbol{\rho})$ are respectively defined in (5.2.7) and (5.2.11), and $\mathcal{A} = \{\boldsymbol{\rho} | \, 0 \leq \rho_i \leq 1, \, \forall i \in \mathcal{N}\}$ is the feasible set of $\boldsymbol{\rho}$.

However, it can be easily verified that the optimization problem in (5.3.1) is not convex for an AF network. Moreover, for a DF network, the optimization problem in (5.3.1) is not only non-convex but also non-differentiable due to the min operator. This means that the globally optimal power splitting profile for the pure network (i.e., the solution of (5.3.1)) cannot be efficiently calculated even in a centralized fashion and there will be a heavy signaling overhead required by the centralized method. Motivated by this, we will develop a distributed framework by considering that all links are strategic and they aim to maximize their individual achievable rates by choosing their own power splitting ratios. For example, in an AF network, this will involve the ith link solving the following optimization problem

$$\begin{array}{cc} \max\limits_{\rho_i} & u_i^{AF}(\rho_i, \boldsymbol{\rho}_{-i}) \\ \text{s.t.} & \rho_i \in \mathcal{A}_i \end{array}, \tag{5.3.2}$$

where $\boldsymbol{\rho}_{-i} = [\rho_1, \ldots, \rho_{i-1}, \rho_{i+1}, \ldots \rho_N]^T$ denotes the vector of all links' power splitting

ratios, except the ith one, and $\mathcal{A}_i = \{\rho_i | \, 0 \leq \rho_i \leq 1\}$ is the feasible set of the ith link's power splitting ratio.

We can observe from (5.3.2) that the optimization problem to be solved by each link is coupled together due to the mutual interference over two hops. To solve this problem, we model the considered power splitting problem to be a non-cooperative game in game theory [96]. Particularly, the considered power splitting problem for an AF network can be modeled by the following non-cooperative game:

- *Players*: The N *S-R-D* links.
- *Actions*: Each link determines its power splitting ratio $\rho_i \in \mathcal{A}_i$ to maximize the achievable rate for its own link.
- *Utilities*: The achievable rate $u_i^{AF}\left(\rho_i, \boldsymbol{\rho}_{-i}\right)$ defined in (5.2.7).

For convenience, we denote the formulated non-cooperative game as

$$\mathcal{G}_{AF} = \left\langle \mathcal{N}, \{\mathcal{A}_i\}, \left\{u_i^{AF}\left(\rho_i, \boldsymbol{\rho}_{-i}\right)\right\}\right\rangle. \tag{5.3.3}$$

Note that we regard each link consisting of three nodes as a "virtual" single player for the sake of presentation. In practice, each player is supposed to be one node of each link (e.g., relay) that acts as the coordinator of each link.

Similarly, we can formulate the following non-cooperative game for the DF network:

$$\mathcal{G}_{DF} = \left\langle \mathcal{N}, \{\mathcal{A}_i\}, \left\{u_i^{DF}\left(\rho_i, \boldsymbol{\rho}_{-i}\right)\right\}\right\rangle. \tag{5.3.4}$$

It is worth mentioning that although the structure of the games formulated for the AF and DF networks is similar, their solution analyses are actually quite different. So we discuss them separately in the following subsections.

5.3.1 Existence of the Nash Equilibrium

The most well-known solution to the non-cooperative games is the (pure strategy) NE [96]. A NE of a given non-cooperative game $\langle \mathcal{N}, \{\mathcal{Q}_n\}, \{\mathcal{U}_n(\mathbf{x}_n, \mathbf{x}_{-n})\}\rangle$ is a feasible point $\mathbf{x}^*$ such that

$$\mathcal{U}\left(\mathbf{x}_n^*, \mathbf{x}_{-n}^*\right) \geq \mathcal{U}\left(\mathbf{x}_n, \mathbf{x}_{-n}^*\right), \ \forall \mathbf{x}_n \in \mathcal{Q}_n. \tag{5.3.5}$$

In other words, a NE is a feasible strategy profile with the property that no single player can increase the utility by deviating from the strategy corresponding to the equilibrium, given the strategies of the other players. The following theorem proposed in [97] is usually adopted to verify the existence of the NE:

Theorem 5.3.1. *A NE* exists *in the game* $\langle \mathcal{N}, \{\mathcal{Q}_n\}, \{\mathcal{U}_n(\mathbf{x}_n, \mathbf{x}_{-n})\}\rangle$ *if* $\forall n \in \mathcal{N}$, $\mathcal{Q}_n$ *is a* compact and convex *set;* $\mathcal{U}_n(\mathbf{q})$ *is continuous in* $\mathbf{q}$ *and* quasi-concave *in* $\mathbf{q}_n$, *where* $\mathbf{q} = (\mathbf{q}_n, \mathbf{q}_{-n})$.

After investigating the properties of the action sets and the utility functions for the formulated games $\mathcal{G}_{AF}$ and $\mathcal{G}_{DF}$, we have the following proposition regarding the existence of the NE:

Proposition 5.3.1. *The utility function* $u_i^{AF}(\rho_i, \boldsymbol{\rho}_{-i})$ *is quasi-concave in* ρ_i *for any* $i \in \mathcal{N}$. *Moreover, the formulated power splitting game* $\mathcal{G}_{AF}$ *for the AF network possesses at least one NE. Moreover, the formulated power splitting game* $\mathcal{G}_{DF}$ *for the DF network also admits at least one NE.*

Proof. See Appendix C.1. □

5.3.2 Uniqueness for the NE of the game $\mathcal{G}_{AF}$

Once the NE is shown to exist, a natural question that arises is whether it is unique. This is important not only for predicting the state of the network but also crucial for convergence issues. In principle, the uniqueness of the NE can be analyzed by several methods, which have been summarized in [98]. However, since the formulated game $\mathcal{G}_{AF}$ is not a convex one, most of the methodologies cannot be applied except the standard function approach [99] because, as shown below, it only requires that the best response function satisfies certain properties. To proceed, we first figure out the best response functions of the links (players), for which we have the following lemma:

Lemma 5.3.1. *Given a power splitting strategy profile $\boldsymbol{\rho}$, the best response function of the link $S_i \to R_i \to D_i$ in the game $\mathcal{G}_{AF}$ can be expressed as*

$$\mathcal{B}_i^{AF}(\boldsymbol{\rho}) = \begin{cases} \frac{1}{2}, & \text{if } (X_i + Y_i)(W_i + 1) = Z_i \\ \frac{\sqrt{(X_i+Y_i+1)(W_i+1)}}{\sqrt{(X_i+Y_i+1)(W_i+1)}+\sqrt{Z_i+W_i+1}}, & \text{if } (X_i + Y_i)(W_i + 1) \neq Z_i \end{cases}. \tag{5.3.6}$$

Proof. See Appendix C.2. □

Now let us verify the correctness of the best response function (5.3.6) by utilizing the special case that $(X_i + Y_i)(W_i + 1) = Z_i$. If we insert this condition into the expression of SINR (5.2.5), we can readily obtain that the SINR is maximized when the term $\rho_i(1 - \rho_i)$ is maximized. This implies that the best response $\rho_i^* = 1/2$, which is consistent with our previous analysis of the best response function. To gain more insights, let us rewrite $(X_i + Y_i)(W_i + 1) = Z_i$ as $X_i + Y_i = Z_i/(W_i + 1)$. Then we can note that the left-hand side of the previous equation represents the SINR ratio of the first hop when the relay only perform information forwarding (i.e., $\rho_i = 0$), while

the right-hand side denotes the SINR of the second hop with only energy harvesting at the relay (i.e., $\rho_i = 1$). This special case reveals that the relay R_i should equally split its received signal, when the SINR ratio of the first hop for $\rho_i = 0$ equals the SINR of the second hop for $\rho_i = 1$.

We now define the vector function $\boldsymbol{\mathcal{B}}^{AF}(\boldsymbol{\rho}) = \left[\mathcal{B}_1^{AF}(\boldsymbol{\rho}), \ldots, \mathcal{B}_N^{AF}(\boldsymbol{\rho})\right]^T$. Then, according to the well-known fixed point theorem [98], the strategy profile $\boldsymbol{\rho}^*$ is a NE of the formulated game $\mathcal{G}_{AF}$ if and only if it is the fixed point of the function $\boldsymbol{\mathcal{B}}^{AF}(\boldsymbol{\rho})$ (i.e, $\boldsymbol{\mathcal{B}}^{AF}(\boldsymbol{\rho}^*) = \boldsymbol{\rho}^*$). Hence, the uniqueness for the NE of the formulated game is equivalent to that for the fixed point of the function $\boldsymbol{\mathcal{B}}^{AF}(\boldsymbol{\rho})$. Furthermore, it is shown in [99] that the fixed point of the function $\boldsymbol{\mathcal{B}}^{AF}(\boldsymbol{\rho})$ is unique if $\boldsymbol{\mathcal{B}}^{AF}(\boldsymbol{\rho})$ is a *standard* function. The standard function is defined as follows:

Definition 5.3.1. A function $\mathbf{f}(\mathbf{x})$ is said to be standard if it satisfies the following properties for all $\mathbf{x} \geq 0$:

- *Positivity*: $\mathbf{f}(\mathbf{x}) > \mathbf{0}$.
- *Monotonicity*: If $\mathbf{x} \geq \mathbf{x}'$, then $\mathbf{f}(\mathbf{x}) \geq \mathbf{f}(\mathbf{x}')$.
- *Scalability*: For all $\alpha > 1$, $\alpha\mathbf{f}(\mathbf{x}) > \mathbf{f}(\alpha\mathbf{x})$.

Here, all the inequalities are componentwise.

After investigating the properties of the best response functions given in Lemma 5.3.1, we have the following proposition regarding the uniqueness of the NE:

Proposition 5.3.2. *The formulated game $\mathcal{G}_{AF}$ for the AF network always admits a unique NE.*

Proof. See Appendix C.3. □

5.3.3 Uniqueness for the NE of the game $\mathcal{G}_{DF}$

To validate the uniqueness for the NE of the game $\mathcal{G}_{DF}$, most of the methodologies also fail to apply except the approach of standard function [99] due to the non-differentiability of the utility functions (the min operator). Similarly, we first derive the best response functions of the links (players) in the game $\mathcal{G}_{DF}$ and have the following lemma:

Lemma 5.3.2. *Given a power splitting strategy profile $\boldsymbol{\rho}$, the best response function of the link $S_i \to R_i \to D_i$ in the game $\mathcal{G}_{DF}$ can be expressed as*

$$\mathcal{B}_i^{DF}(\boldsymbol{\rho}) = \left[(X_i W_i + X_i + Y_i Z_i + Z_i) - \sqrt{(X_i W_i + X_i - Y_i Z_i + Z_i)^2 + 4 Y_i Z_i^2}\right] / (2 Y_i Z_i). \tag{5.3.7}$$

Proof. See Appendix C.4. □

We now define the vector function $\boldsymbol{\mathcal{B}}^{DF}(\boldsymbol{\rho}) = \left[\mathcal{B}_1^{DF}(\boldsymbol{\rho}), \ldots, \mathcal{B}_N^{DF}(\boldsymbol{\rho})\right]^T$. After investigating the properties of the function $\boldsymbol{\mathcal{B}}^{DF}(\boldsymbol{\rho})$, we have the following proposition regarding the uniqueness of the NE:

Proposition 5.3.3. *The game $\mathcal{G}_{DF}$ also always possesses a unique NE.*

Proof. See Appendix C.5. □

5.3.4 Distributed Algorithm

So far, we have proved that the formulated games $\mathcal{G}_{AF}$ and $\mathcal{G}_{DF}$ for pure networks always have a unique NE for any channel conditions and network topologies. However, this equilibrium is meaningful in practice only if one can develop an algorithm that is able to achieve such an equilibrium from non-equilibrium states. In this subsection, we

propose a distributed and iterative algorithm with provable convergence to achieve the NE, in which the links update their power splitting ratios simultaneously. In addition, we discuss the practical implementation of the proposed algorithm.

Algorithm Description

Various kinds of distributed algorithms have been proposed to find the NEs (see [100] for more information). Here, we are interested in best response-based algorithms since we have obtained the best response functions of the formulated games. Relying on the derived best response functions in (5.3.6) and (5.3.7), we develop a distributed power splitting algorithm for the pure networks, which is formally described in **Algorithm 1**. In terms of the convergence of Algorithm 1, we have the following result:

Proposition 5.3.4. *From any initial point, Algorithm 1 always converges to the unique NE of the formulated games $\mathcal{G}_{AF}$ and $\mathcal{G}_{DF}$.*

Proof. Since the best response vector functions $\boldsymbol{\mathcal{B}}^{AF}(\boldsymbol{\rho})$ and $\boldsymbol{\mathcal{B}}^{DF}(\boldsymbol{\rho})$ are both standard (proved in Appendix C.3 and C.5), the proof of this proposition follows with reference to [99, Thm. 2]. □

Implementation Discussion

Note that the distributed nature of the above algorithm is based on modeling each link as a single player. However, each link consists of three nodes (i.e., source, relay, and destination), which are geographically separated in practical networks. Thus, an efficient implementation of the proposed algorithm with the minimum information sharing should be designed.

Algorithm 1 : Distributed Power Splitting Algorithm for the Pure Networks

1: Set $t = 0$ and each player (link) $i \in \mathcal{N}$ chooses a random power splitting ratio $\rho_i(0)$ from the feasible set $\mathcal{A}_i$.
2: If a suitable termination criterion is satisfied: STOP.
3: Each link $i \in \mathcal{N}$ updates the power splitting ratio via executing

$$\rho_i(t+1) = \begin{cases} \mathcal{B}_i^{AF}(\boldsymbol{\rho}(t)) & \text{for AF network} \\ \mathcal{B}_i^{DF}(\boldsymbol{\rho}(t)) & \text{for DF network} \end{cases}. \tag{5.3.8}$$

4: $t \leftarrow t+1$; go to STEP 2.

In our design, the relay node is expected to be the link coordinator that undertakes the information collection and the best-response computation. Here, we assume that the energy consumed for the algorithm computations at the relay nodes are negligible compared with the harvested energy used for information forwarding since these computations are quite simple. This assumption can be further supported by the rapid development of the low-power chips. Next, we aim to identify the information that is needed to collect or exchange for the implementation of the proposed algorithm. According to the best response functions given in (5.3.6), the relay R_i needs to know the values of the parameters X_i, Y_i, Z_i, and W_i defined in (5.2.6). To this end, the relay R_i should perform the following tasks:

- *Task 1*: Measure the channel gains g_{ii} and h_{ii}, acquire the transmission power P_i from its source, and then calculate the value of X_i based on this information.

- *Task 2*: Measure[4] the power of its received signal, acquire the power of the received signal at the destination D_i, and then calculate the values of Y_i, Z_i, W_i.

[4]The measurement of the signal power can be performed by the radio scene analyzer [91].

- *Task 3*: Calculate the optimal power splitting ratio ρ_i based on (5.3.6).

From the above description, we can observe that the overheads are required in transmitting the following three kinds of information for each link in the proposed algorithm: (1) pilots for estimating the CSI from the source to its dedicated relay and CSI from relay to destination, (2) the value of the transmit power from the source to relay, and (3) the power of the received signal at the destination, which needs to be sent from the destination to its dedicated relay. The first two kinds of overheads are only needed once for each channel realization, while the third one is required in each iteration of the proposed algorithm. From the above discussion, we can see that in the proposed algorithm, only some local information needs to be exchanged within each link and no information needs to be exchanged among different links.

Finally, note that a possible termination criterion for the proposed Algorithm 1 can be

$$\left[\rho_i\left(t+1\right)-\rho_i\left(t\right)\right]/\rho_i\left(t+1\right)\leq\zeta,$$

where ζ is a sufficiently small constant.

5.4 Extension to Hybrid Network

In this section, we generalize the proposed game-theoretical power splitting scheme to a hybrid network containing both AF and DF relays. The hybrid network considered in this section could correspond to the practical case that the relays are deployed by different users and may be made by different manufacturer with different protocols. The set of the links with AF relays and DF relays are denoted by $\mathcal{N}_{AF}$ and $\mathcal{N}_{DF}$, respectively. Before formally describing the non-cooperative game for this case,

it is important to notice that for a given power splitting ratio profile $\boldsymbol{\rho}_{-i}$, the amount of interference received by the destination D_i is fixed. This is because for a given realization of channels, the interference at each destination is only determined by the transmit powers of relays in other links and is independent of the relaying protocols (i.e., AF or DF) adopted by these relays. Thus, the achievable rate of the ith link in the hybrid network can still be expressed by (5.2.7), when the AF relaying protocol is adopted at the relay R_i, and by (5.2.11), when the DF relaying protocol is adopted at the relay R_i.

Now, we can formulate the following non-cooperative game for the considered hybrid network:

- *Players*: The N *S-R-D* links.
- *Actions*: Each link determines its power splitting ratio $\rho_i \in \mathcal{A}_i$ to maximize the achievable rate for its own link.
- *Utilities*: The achievable rate

$$u_i^{HD}\left(\rho_i, \boldsymbol{\rho}_{-i}\right) = \begin{cases} u_i^{AF}\left(\rho_i, \boldsymbol{\rho}_{-i}\right) \text{ in (5.2.7)}, & \text{if } i \in \mathcal{N}_{AF} \\ u_i^{DF}\left(\rho_i, \boldsymbol{\rho}_{-i}\right) \text{ in (5.2.11)}, & \text{if } i \in \mathcal{N}_{DF} \end{cases}. \tag{5.4.1}$$

For convenience, we denote the above non-cooperative game as

$$\mathcal{G}_{HD} = \left\langle \mathcal{N}, \{\mathcal{A}_i\}, \left\{u_i^{HD}\left(\rho_i, \boldsymbol{\rho}_{-i}\right)\right\}\right\rangle. \tag{5.4.2}$$

Subsequently, according to Proposition 5.3.1, Lemma 5.3.1, Proposition 5.3.2, Lemma 5.3.2, and Proposition 5.3.3, we have the following corollary regarding the best response function and the existence and uniqueness of the NE for the game $\mathcal{G}_{HD}$:

Corollary 5.4.1. *The best response function of the ith link in the game $\mathcal{G}_{HD}$ can be*

expressed as

$$\mathcal{B}_i^{HD}(\boldsymbol{\rho}) = \begin{cases} \mathcal{B}_i^{AF}(\boldsymbol{\rho}) \text{ in (5.3.6)}, & \text{if } i \in \mathcal{N}_{AF} \\ \mathcal{B}_i^{DF}(\boldsymbol{\rho}) \text{ in (5.3.7)}, & \text{if } i \in \mathcal{N}_{DF} \end{cases}. \tag{5.4.3}$$

Furthermore, the game $\mathcal{G}_{HD}$ always possesses one and only one NE.

Then, replacing the best response update (5.3.8) in Algorithm 1 by the one in (5.4.3), we can have a best response-based distributed algorithm for the links to achieve the NE of the game $\mathcal{G}_{HD}$. This algorithm is referred as to **Algorithm 2**, which is omitted here due to its similarity with Algorithm 1.

5.5 Numerical Results

In this section, we will present some numerical results to illustrate and validate the above theoretical analyses. To obtain meaningful results, we restrict our attention to a linear topology for each link. Specifically, S_i-R_i-D_i forms a straight line with unit length, i.e., $d_{S_iD_i} = d_{S_iR_i} + d_{R_iD_i} = 1, \forall i \in \mathcal{N}$, with d_{XY} denoting the distance between nodes X and Y. Note that in order to obtain meaningful insights into the system performance, we treat the node distances as constants in this chapter. In practical systems, the spatial node distributions [79, 80] should be considered, but it will require a new analytical framework, which is out of the scope of this chapter. The channels between all transceiver pairs are assumed to be subject to mutually independent Rayleigh fading. To take into account the impact of path loss, we adopt the channel model that $\mathbb{E}\left\{|g_{ij}|^2\right\} = \left(d_{S_iR_j}\right)^{-\tau}$ and $\mathbb{E}\left\{|h_{ij}|^2\right\} = \left(d_{R_iD_j}\right)^{-\tau}$, where $\tau \in [2, 5]$ is the path loss factor [81]. In all the simulations, without loss of generality, we set $\sigma^2 = 1$ and $\eta = 0.5$.

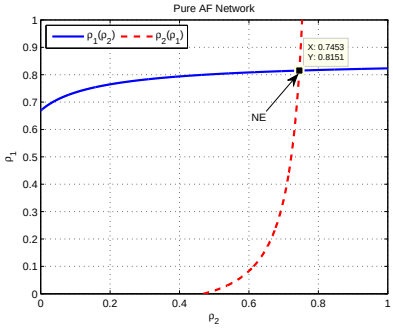

(a) Best responses of the game $\mathcal{G}_{AF}$

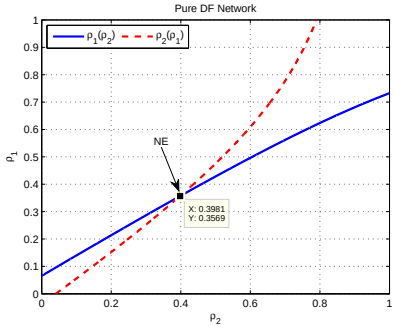

(b) Best responses of the game $\mathcal{G}_{DF}$

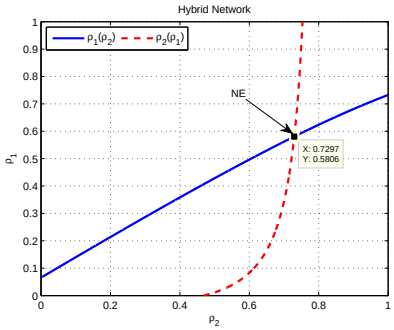

(c) Best responses of the game $\mathcal{G}_{HD}$

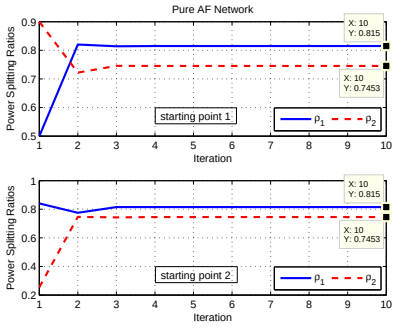

(d) Convergence of Algorithm 1

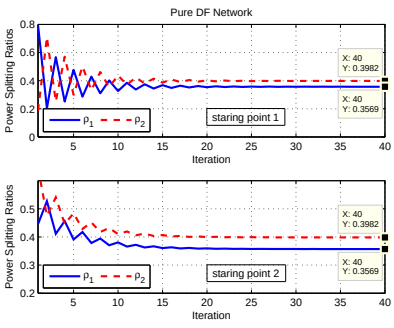

(e) Convergence of Algorithm 1

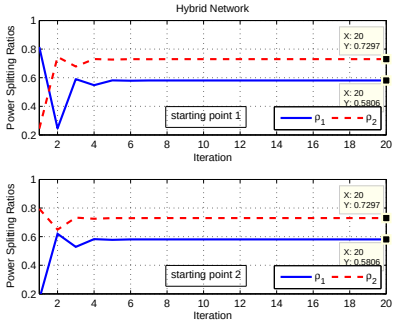

(f) Convergence of Algorithm 2

Figure 5.3: The best response functions of the three formulated games and the convergence of Algorithm 1-2 from different starting points in the considered two-link network with parameters given in (5.5.1)-(5.5.3).

We first consider a simple network consisting of two links with the following randomly generated parameters:

$$[P_1, P_2] = [5.3080, 7.1917], \tag{5.5.1}$$

$$\begin{bmatrix} |g_{11}|^2 & |g_{12}|^2 \\ |g_{21}|^2 & |g_{22}|^2 \end{bmatrix} = \begin{bmatrix} 2.1713 & 1.4836 \\ 3.0937 & 0.9773 \end{bmatrix}, \tag{5.5.2}$$

$$\begin{bmatrix} |h_{11}|^2 & |h_{12}|^2 \\ |h_{21}|^2 & |h_{22}|^2 \end{bmatrix} = \begin{bmatrix} 0.4475 & 1.5760 \\ 1.5406 & 2.6081 \end{bmatrix}. \tag{5.5.3}$$

Both links in the game $\mathcal{G}_{AF}$ ($\mathcal{G}_{DF}$) adopt the AF (DF) relaying protocol, while link 1 implements the DF relaying scheme and link 2 implements the AF relaying scheme in the game $\mathcal{G}_{HD}$. In Fig. 5.3 (a)-(c), we first plot the best response functions (i.e., $\rho_1(\rho_2)$ and $\rho_2(\rho_1)$) of the three games, respectively. With reference to [98], the intersection points of the best response functions are actually the NEs of the corresponding games. From Fig. 5.3 (a)-(c), we can see that the two curves only admit one intersection point in all cases, which indicates that all the formulated games in the considered two-link network possess a unique NE. In Fig. 5.3 (d)-(f), the proposed algorithms are executed to achieve the corresponding NEs from randomly generated initial points. It can be seen from Fig. 5.3 (d)-(f) that the proposed algorithms can converge to the corresponding NEs obtained in Fig. 5.3 (a)-(c) from different starting points. Hence, the observations from Fig. 5.3 (a)-(f) verify the correctness of our theoretical analyses.

To show that the proposed algorithm can also converge to the NE in multi-link scenarios, we illustrate its convergence performance for an example of a randomly generated four-link hybrid network in Fig. 5.4. As can be observed from Fig. 5.4, the proposed algorithm can converge to the same values (i.e., the NE) from two different initial points, which further validates the theoretical analyses. Note that due to

space limitation, we only show results in Figs. 5.3-5.4 for one random realization of transmit powers and channel gains, although similar results can also be shown for other realizations.

Next, we investigate the average sum-rate of the relay interference networks that implement the proposed power splitting scheme. We consider both a two-link scenario and a multi-link scenario. For simplification and illustrative purpose, we consider that all links in the considered networks are mutually parallel. Thus, the two-link setting is characterized by the interlink distance, denoted by d_L. In the multi-link setting, we assume that the distances between adjacent links are equal. Hence, this scenario is characterized by the number of links N and the distance between the farthest two links, denoted by $d_{\max}$. In the following figures, each curve is plotted by averaging over the results from 10000 independent channel realizations. In addition, it is straightforward to imagine that the performance curves of the hybrid network should be located between that of the AF and DF network. Thus, we will omit the curves of hybrid networks in the following to avoid crowded figures.

Fig. 5.5 illustrates the average sum-rate of a two-link network, where the performances are compared across the optimal sum-rate obtained by the centralized optimization problem in (5.3.1) solved via an exhaustive search, the proposed game-theoretical approach, the random scheme in which the power splitting ratios are randomly generated over $[0, 1]$. Both AF and DF networks with symmetric and asymmetric topologies are simulated. We can observe from Fig. 5.5 that the proposed game-theoretical method outperforms the random scheme in the AF network when d_L exceeds a certain value, and is always superior to the random scheme in the DF network for all cases. In addition, the performance gap between these two

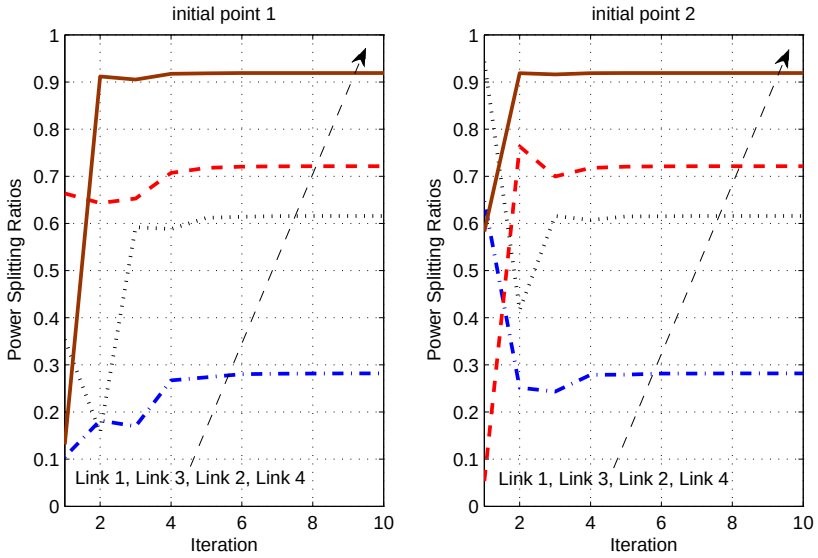

Figure 5.4: Convergence of the proposed algorithm for a randomly generated four-link hybrid network with two different initial points, $\mathcal{N}_{DF} = [1\ 3]$ and $\mathcal{N}_{AF} = [2\ 4]$.

schemes becomes larger when the inter-link distance d_L increases. Moreover, it can be seen from Fig. 5.5 that the proposed game-theoretical approach suffers performance loss compared to the optimal scheme when the inter-link distance is very small, i.e., in high interference scenarios. However, as the inter-link distance increases, it approaches the centralized optimal scheme in the AF network and quickly coincides with the centralized optimal scheme in the DF network. Therefore, we can claim that the proposed game-theoretical approach can achieve a near-optimal performance on average, especially for the scenarios with medium and large interlink distance (i.e., relatively low and moderate interference).

Figs. 5.6 and 5.7 respectively demonstrate the impacts of the number of links and the transmit powers on the average sum-rates and average power splitting ratios of AF and DF networks in the multi-link scenario, where all relays are assumed in middle positions (i.e., $d_{S_iR_i} = d_{R_iD_i} = 0.5,\ \forall i$). In Fig. 5.6 (a), we plot the

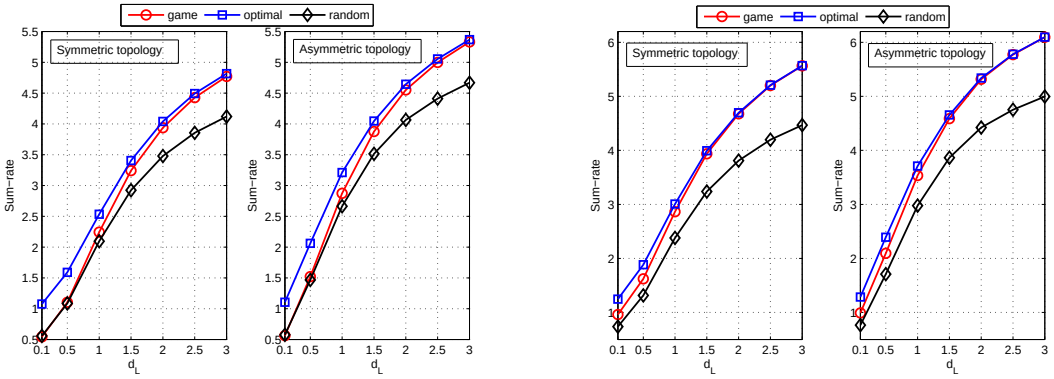

(a) AF network

(b) DF network

Figure 5.5: The average sum-rates of two-link AF and DF networks for (a) symmetric network with $d_{S_iR_i} = d_{R_iD_i} = 0.5$ and $P_i = 15$ dB, $\forall i = 1, 2$, (b) asymmetric network with $d_{S_1R_1} = d_{R_2D_2} = 0.25$ and $P_i = 15$ dB, $\forall i = 1, 2$.

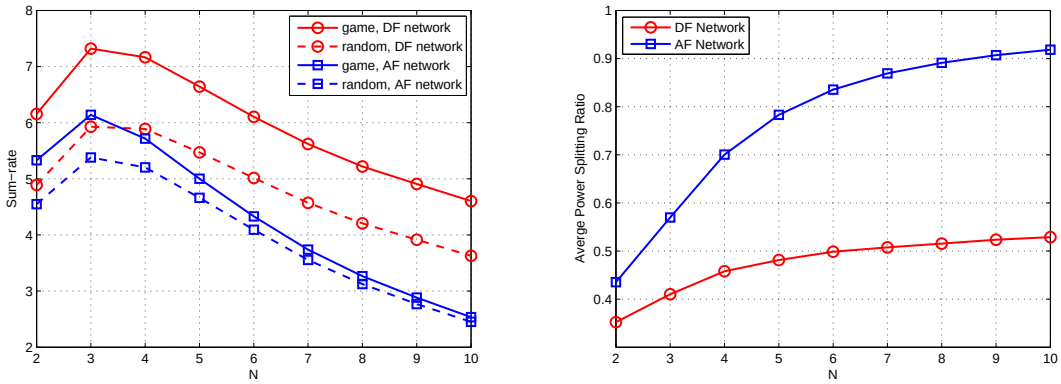

(a) Average sum-rate

(b) Average power splitting ratio

Figure 5.6: The impact of link numbers on (a) average sum-rate and (b) average power splitting ratio in AF and DF networks with $d_{\max} = 5$ and $P_i = 15$ (dB), $\forall i$.

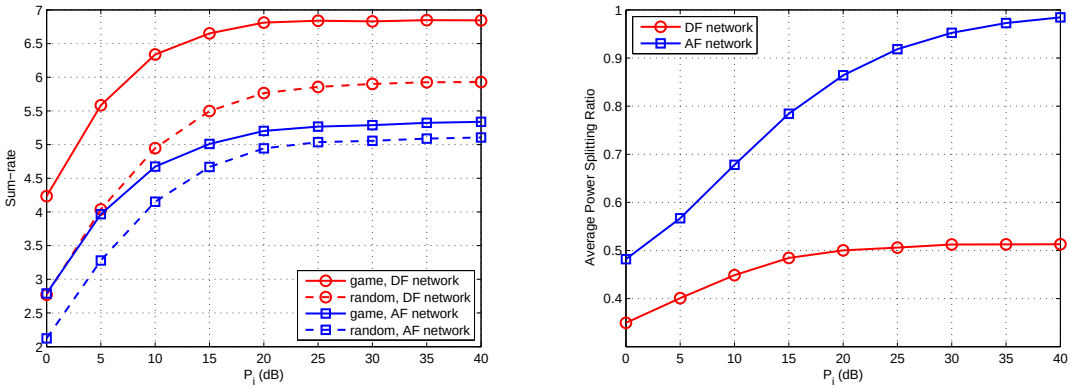

(a) Average sum-rate

(b) Average power splitting ratio

Figure 5.7: The impact of the transmit powers on (a) average sum-rate and (b) average power splitting ratio in AF and DF networks with $d_{\max} = 5$ and $N = 5$.

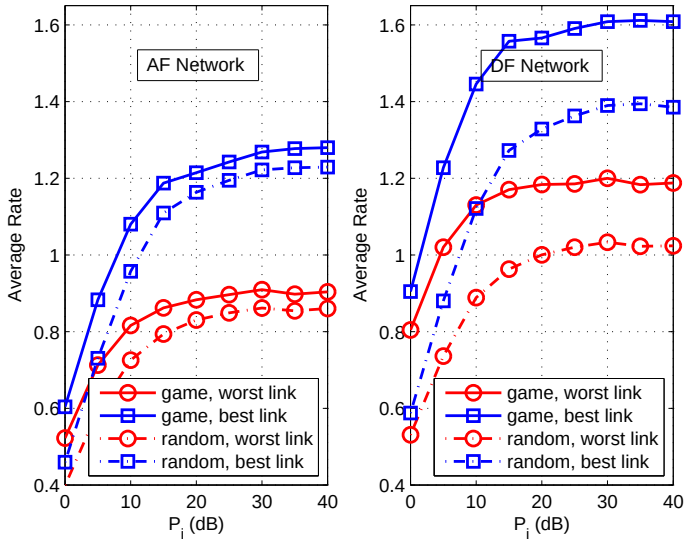

Figure 5.8: The average rate of the best and worst links in AF and DF networks with $d_{\max} = 5$ and $N = 5$.

average sum-rate curves of the AF and DF networks achieved by the proposed game-theoretical scheme and the random scheme versus the number of links with $d_{\max} = 5$ and $P_i = 15$ dB, $\forall i$. Note that the performance of the centralized optimal scheme is omitted here because the corresponding optimization problem is non-convex and thus cannot be efficiently solved in a multi-link scenario. From Fig. 5.6 (a), we observe that the average sum-rates of both AF and DF networks first increase and then keep decreasing with the growth of the number of links. This observation is understandable. Specifically, the initial sum-rate increase is actually a multiplexing gain as more links share the same spectrum with relatively low mutual interference. Nevertheless, with a further increase in the number of links, the interlink interference becomes stronger, which leads to a monotonically decreasing sum-rate. We can also see from Fig. 5.6 (a) that the proposed game-theoretical approach always outweighs the random method in both AF and DF networks for all cases. The performance gap between these two schemes in the DF network is significantly larger than that in the AF networks. This indicates that the proposed game-theoretical approach can achieve a higher performance improvement in a DF network than the one in a AF network. In addition, it can be observed from Fig. 5.6 (a) that the performance gap decreases gradually as the number of links increases, which is due to a more severe interference. Fig. 5.6 (b) depicts the average power splitting ratios[5] of both AF and DF networks, when the proposed game-theoretical scheme is implemented. We can observe from this figure that the average power splitting ratio of the AF networks is always larger than that of the DF networks. Furthermore, the average power splitting

[5]Since plotting the curve for each link's power splitting ratio will create too many curves, which is difficult to illustrate, we choose the average power splitting ratio of all links as the performance metric for the purpose of facilitating the illustration. This metric can effectively reflect the changes of the ratios in the majority of links.

ratios of both AF and DF networks experience a steady increase when the number of links grows. A similar phenomenon can be observed from Fig. 5.7 (b), in which the curves for the average power splitting ratios of both AF and DF networks are plotted versus the sources' transmit powers. This is because increasing the number of links and raising the transmit powers of all links achieves the same effect as increased mutual interference. The impact of the transmit powers of all links on the average sum-rates of both AF and DF networks is shown in Fig. 5.7 (a). As can be observed from this figure, the average sum-rate achieved by the proposed game-theoretical approach steadily increases from a low to a moderate SNR region and tends to get saturated at high SNR, above 20 (dB). This indicates that at high SNR, the power control at the sources should be jointly considered with the power splitting at the relays to further improve the sum-rate, which will be considered in our future work. Finally, we can see from Figs. 5.6 (a) and 5.7 (a) that a DF network can achieve a higher average sum-rate than an AF network with the same settings.

In Fig. 5.8, we plot the average rate curves for the best and worst links in both AF and DF networks with the same network setting as in Fig. 5.7. Similar phenomena shown in Fig. 5.7 (a) can also be observed in this figure. Besides, we can see from Fig. 5.8 that compared with the random scheme, the proposed game-theoretical scheme can effectively improve the average rates of the best and worst links in both AF and DF networks. Furthermore, this performance improvement in the DF network is shown to be more significant than that in the AF network.

Chapter 6

Conclusions and Future Work

In this thesis, we proposed new cooperative protocols, analyzed network performance, and designed resource allocation for the emerging WPCCNs. The key results and findings, which provide useful insights for the practical design of WPCCNs, are first summarized in this chapter. Then, we suggest a number of future topics based on the contents presented in this thesis.

6.1 Summary of Results and Insights

In Chapter 2, we first proposed a HTC protocol for a WPCCN with wireless-powered source and relay(s). The proposed HTC protocol was first described based on the three-node reference model. We then derived the approximate closed-form expression of the average throughput for the proposed protocol over Rayleigh fading channels. This analysis was subsequently extended to the multi-relay scenario, where the throughput of the proposed protocol with opportunistic relaying and partial relay selection schemes was analyzed. Numerical results showed that the proposed HTC protocol outperforms the harvest-then-transmit one in all simulated scenarios. The performance gain of the proposed HTC protocol can be further improved when the

number of relays increases. With the optimal values of the time allocation parameter and relay position, the opportunistic relaying scheme achieves the best throughput performance. Moreover, the partial relay selection scheme based on the second hop can perform better than that based on the first hop.

Then, in Chapter 3 we developed two cooperative protocols, namely energy cooperation (E-C) and dual cooperation (D-C), for an alternative network setup of WPCCNs consisting of a hybrid AP, a hybrid relay and a wireless-powered source. The throughput maximization problems in terms of joint power and time allocation were formulated and resolved for the proposed protocols. Numerical results showed that in a linear topology, the E-C protocol achieves better throughput at high SNRs, especially when the distance between the source and relay is large. In contrast, when the SNR is not high and the relay is relatively close to the source, the D-C protocol is superior to the E-C protocol.

Next, in Chapter 4 we designed an energy trading framework for a PB-assisted WPCCN. Considering the strategic behaviors of the hybrid AP and PBs, we formulated a Stackelberg game for the considered network, in which the AP is the leader and the PBs are the followers. The Stackelberg equilibrium of the formulated game was subsequently derived. As a comparison, the social welfare optimization problem was also formulated and solved. Numerical results showed that the social welfare optimization scheme always outperforms the game-theoretical scheme. Moreover, both schemes can achieve better performance as either the numbers of the PBs or the value of the gain per unit throughput increase, and as the distance between the source and PBs decreases. At the same time, these changes also lead to a shorter downlink energy transfer time, more involved PBs, smaller transmit powers of the PBs and a

lower energy price for the AP.

Finally, in Chapter 5 we developed a game-theoretical framework to address the distributed power splitting problem for SWIPT in a large-scale WPCCN that constitutes relay interference channels. We formulated non-cooperative games for three different network scenarios, in which each link is modeled as a strategic player who aims to maximize its individual achievable rate by choosing the dedicated relay's power splitting ratio. We showed that the formulated games always achieve a unique NE. Best response-based distributed algorithms with provable convergence were also developed to achieve the NEs. The numerical results showed that the proposed algorithms can converge to the corresponding NEs from different starting points, and the developed game-theoretical approach can achieve a near-optimal network-wide performance on average, especially for the scenarios with relatively low and moderate interference.

6.2 Future Work

We propose the following extensions to the work presented in this thesis.

The performance analysis of the proposed protocol in Chapter 2 is valid for the Rayleigh fading scenario. As a more general model, Rician fading is another practical channel model for WPCCNs, especially when the distance between nodes is limited and the light of sight exists. Thus, the first effective extension to the work in Chapter 2 could be the performance analysis of WPCCN under Rician fading. Moreover, the results in Chapter 2 are based on the assumption that the selected relay only uses the harvested energy in the current transmission block to forward the signals received from the source. To be more practical, the energy accumulation process at the relay

nodes should be taken into consideration. More specifically, if a relay node is not selected in a particular transmission block, then the amount of harvested energy in this block should be accumulated in its battery. In this case, the relay selection procedure needs to jointly consider both the channel gains and the *residual* energy of the relay nodes. Discrete Markov chains [101] would be a suitable mathematical tool to model the charging and discharging behaviors of the relay nodes' batteries.

It will be interesting to extend the work in Chapter 3 to the multi-relay scenario. In this context, the hybrid relays could perform collaborative beamforming [102] for not only DL energy transfer but also the UL information forwarding. Due to the individual energy constraint of each relay, the energy beamforming vector and the information beamforming vector tangle together and thus should be jointly designed. The work in Chapter 4 could be extended to a more general network setup with multiple PBs and multiple AP-source pairs. Such a scenario would lead to two levels of strategic interactions and could be modeled by a multi-leader-follower game [103]. In addition, the relay selection schemes in Chapter 2 and the resource allocation in Chapter 3 need the process of CSI acquisition, which may consume extra time and energy resources in practice. Thus, the characterization of system performance with this practical consideration could be another interesting future work.

The results in Chapter 5 are achieved based on the assumption that the transmit power of all source nodes are constant. However, in practice, the transmit power of the source nodes may also be controllable such that it should be jointly optimized with the power splitting ratios at the relay nodes. But, this may make the formulated game non-convex, which is more challenging than the convex one when analyzing its equilibria. A new concept of equilibrium, named the quasi-Nash equilibrium [104],

could be applied to resolve this non-convex game. To effectively manage interlink interference and achieve more efficient resource allocation, we can also introduce cooperation between the strategic links, which are enabled to form a group and compete with others if their utilities can be improved. In this case, the coalitional game theory [105] would be a good mathematical tool to model the cooperative but strategic behaviors of the links (players).

Appendix A

Proofs for Chapter 2. A Harvest-Then-Cooperate Protocol for Wireless-Powered Cooperative Communications

A.1 Proof of Proposition 2.3.1

To proceed, the mutual information between the source and hybrid AP is given by

$$I_{SA} = \frac{1}{2}\log_2\left(1+\gamma_A\right). \tag{A.1.1}$$

Then, we can write the outage probability as

$$\begin{aligned} P_{\text{out}}^{\text{HTC}} &= \Pr\left(I_{SA} < R\right) = \Pr\left(\gamma_A < \nu\right) \\ &= \Pr\left(\gamma_{SA} < \nu, \gamma_{SRA} < \nu\right). \end{aligned} \tag{A.1.2}$$

Here, it is worth emphasizing that γ_{SA} and γ_{SRA} are correlated since both of them contain the random variable h_{AS}. Thus, we have

$$\Pr\left(\gamma_{SA} < \nu, \gamma_{SRA} < \nu\right) \neq \Pr\left(\gamma_{SA} < \nu\right)\Pr\left(\gamma_{SRA} < \nu\right).$$

This is in contrast to the conventional constant-powered cooperative networks, where the SNRs of different paths are normally independent. Due to this correlation and the complex structure of γ_{SRA}, it is hard to obtain a closed-form expression of (A.1.2). To tackle this, we make the following approximation to the expression of γ_{SRA} given in (2.2.6) [76, 106]:

$$\gamma_{SRA} \approx \frac{\mu h_{AS} h_{SR} \mu h_{AR} h_{RA}}{\mu h_{AS} h_{SR} + \mu h_{AR} h_{RA}} \leq \mu \min\left(h_{AS} h_{SR}, h_{AR} h_{RA}\right). \tag{A.1.3}$$

The approximate SNR value in (A.1.3) is analytically more tractable than the exact value in (2.2.6) and thus facilitates the derivation of the closed-form expression of the outage probability.

Based on the approximation in (A.1.3), we can obtain the outage probability of the HTC protocol approximately given by

$$\begin{aligned} P_{\text{out}}^{\text{HTC}} \approx & \Pr\left(h_{AS} h_{SA} < \nu/\mu, \min\left(h_{AS} h_{SR}, h_{AR} h_{RA}\right) < \nu/\mu\right) \\ = & \Pr\left(h_{AS} h_{SA} < \nu/\mu\right) - \Pr\left(h_{AS} h_{SA} < \nu/\mu, \min\left(h_{AS} h_{SR}, h_{AR} h_{RA}\right) > \nu/\mu\right) \\ = & \Pr\left(h_{AS} h_{SA} < \nu/\mu\right) - \Pr\left(h_{AR} h_{RA} > \nu/\mu\right) \Pr\left(h_{AS} h_{SA} < \nu/\mu, h_{AS} h_{SR} > \nu/\mu\right), \end{aligned} \tag{A.1.4}$$

where the second equality follows by the fact $\Pr(A, B) = \Pr(A) - \Pr\left(A, \bar{B}\right)$ [107, pp. 21] and the last equality holds since h_{AR} and h_{RA} are independent of h_{AS}. Next, we calculate the three probabilities in the last step of (A.1.4), respectively. Firstly, we have

$$\begin{aligned} \Pr\left(h_{AS} h_{SA} < \frac{\nu}{\mu}\right) = & \int_0^\infty \Pr\left(h_{AS} < \frac{\nu}{\mu y}\right) f_{h_{SA}}(y)\, dy \\ = & 1 - \frac{1}{\sigma_{SA}^2} \int_0^\infty \exp\left(-\frac{\nu}{\sigma_{AS}^2 \mu y} - \frac{y}{\sigma_{SA}^2}\right) dy \\ = & 1 - \mathcal{S}\left(\frac{4\nu}{\mu \sigma_{AS}^2 \sigma_{SA}^2}\right), \end{aligned} \tag{A.1.5}$$

where [77, Eq. (3.324.1)] is used to solve the second integral. Similarly, we have

$$\Pr\left(h_{AR}h_{RA} > \nu/\mu\right) = \mathcal{S}\left(\frac{4\nu}{\mu\sigma_{AR}^2\sigma_{RA}^2}\right). \tag{A.1.6}$$

For the last term, we have

$$\begin{aligned}
&\Pr\left(h_{AS}h_{SA} < \nu/\mu, h_{AS}h_{SR} > \nu/\mu\right)\\
=&\int_0^\infty \Pr\left(h_{SA} < \frac{\nu}{\mu y}, h_{SR} > \frac{\nu}{\mu y}\right) f_{h_{AS}}(y)\, dy\\
=&\int_0^\infty \Pr\left(h_{SA} < \frac{\nu}{\mu y}\right) \Pr\left(h_{SR} > \frac{\nu}{\mu y}\right) f_{h_{AS}}(y)\, dy\\
=&\int_0^\infty \left(1 - \exp\left(-\frac{\mu\gamma}{\sigma_{SA}^2 y}\right)\right) \exp\left(-\frac{\mu\gamma}{\sigma_{SR}^2 y}\right) f_{h_{AS}}(y)\, dy\\
=&\frac{1}{\sigma_{AS}^2}\int_0^\infty \exp\left(-\frac{\nu}{\sigma_{SR}^2\mu y} - \frac{y}{\sigma_{AS}^2}\right) dy - \frac{1}{\sigma_{AS}^2}\int_0^\infty \exp\left(-\frac{1}{y}\left(\frac{\nu}{\sigma_{SA}^2\mu} + \frac{\nu}{\sigma_{SR}^2\mu}\right) - \frac{y}{\sigma_{AS}^2}\right) dy\\
=&\mathcal{S}\left(\frac{4\nu}{\mu\sigma_{AS}^2\sigma_{SR}^2}\right) - \mathcal{S}\left(\frac{4\nu}{\mu\sigma_{AS}^2\sigma_{SR}^2} + \frac{4\nu}{\mu\sigma_{AS}^2\sigma_{SA}^2}\right).
\end{aligned} \tag{A.1.7}$$

By substituting (A.1.5)-(A.1.7) into (A.1.4), we obtain the desired result in (2.3.1). This completes the proof.

A.2 Proof of Proposition 2.4.1

According to the selection criterion of the OR protocol given in (2.4.2) and the SNR approximation in (A.1.3), the outage probability of the OR protocol can be approximately given by

$$\begin{aligned}
P_{\text{out}}^{\text{HTC,OR}} &\approx \Pr\left(h_{AS}h_{SA} < \frac{\nu}{\mu}, \min\left(h_{AS}h_{SR_b}, h_{AR_b}h_{R_bA}\right) < \frac{\nu}{\mu}\right)\\
&= \Pr\left(h_{AS}h_{SA} < \frac{\nu}{\mu}, \max_{i\in\mathcal{N}}\left\{\min\left(h_{AS}h_{SR_i}, h_{AR_i}h_{R_iA}\right)\right\} < \frac{\nu}{\mu}\right)\\
&= \int_0^\infty \underbrace{\Pr\left(yh_{SA} < \frac{\nu}{\mu}\right)}_{\mathcal{T}_1} \underbrace{\Pr\left(\max_{i\in\mathcal{N}}\left\{\min\left(yh_{SR_i}, h_{AR_i}h_{R_iA}\right)\right\} < \frac{\nu}{\mu}\right)}_{\mathcal{T}_2} f_{h_{AS}}(y)\, dy.
\end{aligned} \tag{A.2.1}$$

To proceed, it is straightforward to obtain

$$\mathcal{T}_1 = \Pr\left(h_{SA} < \frac{\nu}{\mu}\frac{1}{y}\right) = 1 - \exp\left(-\frac{\nu}{\mu\sigma_{SA}^2}\frac{1}{y}\right). \tag{A.2.2}$$

For the term $\mathcal{T}_2$ in (A.2.1), we have

$$\begin{aligned}\mathcal{T}_2 &= \Pr\left(\min\left(yh_{SR_1}, h_{AR_1}h_{R_1A}\right) < \frac{\nu}{\mu}\right) \times \ldots \times \Pr\left(\min\left(yh_{SR_N}, h_{AR_N}h_{R_NA}\right) < \frac{\nu}{\mu}\right) \\ &= \left[\Pr\left(\min\left(yh_{SR_1}, h_{AR_1}h_{R_1A}\right) < \frac{\nu}{\mu}\right)\right]^N \\ &= \left[1 - \Pr\left(\min\left(yh_{SR_1}, h_{AR_1}h_{R_1A}\right) > \frac{\nu}{\mu}\right)\right]^N \\ &= \left[1 - \exp\left(-\frac{\nu}{\mu\sigma_{SR}^2}\frac{1}{y}\right)\underbrace{\Pr\left(h_{AR_1}h_{R_1A} > \frac{\nu}{\mu}\right)}_{\mathcal{T}_3}\right]^N,\end{aligned} \tag{A.2.3}$$

where the second equation follows since the random variables $\{h_{SR_i}\}$, $\{h_{AR_i}\}$, and $\{h_{R_iA}\}$ are respectively independent and identically distributed (i.i.d). Note that the term $\mathcal{T}_3$ can be written as

$$\mathcal{T}_3 = \mathcal{S}\left(\sqrt{\frac{4\nu}{\mu\sigma_{AR}^2\sigma_{RA}^2}}\right). \tag{A.2.4}$$

Substituting (A.2.4) into (A.2.3) and expanding the term $\mathcal{T}_2$ based on the binomial theorem [59, Eq. (3.1.1)], we can further write (A.2.3) as

$$\begin{aligned}\mathcal{T}_2 =& \left[1 - \exp\left(-\frac{\nu}{\mu\sigma_{SR}^2}\frac{1}{y}\right)\mathcal{S}\left(\frac{4\nu}{\mu\sigma_{AR}^2\sigma_{RA}^2}\right)\right]^N \\ =& 1 + \sum_{n=1}^{N}\binom{N}{n}(-1)^n\left[\mathcal{S}\left(\frac{4\nu}{\mu\sigma_{AR}^2\sigma_{RA}^2}\right)\right]^n \exp\left(-\frac{n\nu}{\mu\sigma_{SR}^2}\frac{1}{y}\right).\end{aligned} \tag{A.2.5}$$

Substituting (A.2.2) and (A.2.5) into (A.2.1), we have

$$P_{\text{out}}^{\text{HTC,OR}} \approx \int_0^\infty \frac{1}{\sigma_{AS}^2} \exp\left(-\frac{y}{\sigma_{AS}^2}\right) dy - \frac{1}{\sigma_{AS}^2} \int_0^\infty \exp\left(-\frac{y}{\sigma_{AS}^2} - \frac{\nu}{\mu\sigma_{SA}^2}\frac{1}{y}\right) dy + \sum_{n=1}^{N} \binom{N}{n} (-1)^n \left[\mathcal{S}\left(\frac{4\nu}{\mu\sigma_{AR}^2\sigma_{RA}^2}\right)\right]^n \frac{1}{\sigma_{AS}^2} \left\{ \int_0^\infty \exp\left(-\frac{y}{\sigma_{AS}^2} - \frac{n\nu}{\mu\sigma_{SR}^2}\frac{1}{y}\right) dy - \int_0^\infty \exp\left(-\frac{y}{\sigma_{AS}^2} - \frac{n\nu}{\mu\sigma_{SR}^2}\frac{1}{y} - \frac{\nu}{\mu\sigma_{SA}^2}\frac{1}{y}\right) dy \right\}. \tag{A.2.6}$$

Solving the integrals in (A.2.6) by following the routine in the proof of Proposition 2.3.1, we obtain the desired result in (2.4.5).

A.3 Proof of Proposition 2.4.2

To obtain the asymptotic analysis of the throughput, we need to perform the asymptotic analysis for the function $\mathcal{S}(x)$ defined in (2.3.2). Moreover, it is straightforward to observe that all terms inside the function $\mathcal{S}(\cdot)$ in (2.4.5) approach zero when $P_A/N_0 \to \infty$. Thus, to obtain the asymptotic performance of the throughput, we should find the approximation of $\mathcal{S}(x)$ for $x \to 0$.

By applying the series representation of the modified Bessel function of the second kind [77, Eq. (8.446)], we can re-write the function $\mathcal{S}(x)$ as follows:

$$\begin{aligned}
\mathcal{S}(x) =& 1 + \sqrt{x} I_1\left(\sqrt{x}\right)\left(\ln\frac{\sqrt{x}}{2} + \boldsymbol{C}\right) - \frac{1}{2}\sum_{l=0}^{\infty} \frac{\left(\frac{\sqrt{x}}{2}\right)^{2l+1}\sqrt{x}}{l!\,(l+1)!}\left(\sum_{k=1}^{l}\frac{1}{k} + \sum_{k=1}^{l+1}\frac{1}{k}\right) \\
\approx& 1 + \frac{x}{2}\left(\ln\frac{\sqrt{x}}{2} + \boldsymbol{C} - \frac{1}{2}\right) - \frac{1}{2}\sum_{l=1}^{\infty} \frac{\left(\frac{\sqrt{x}}{2}\right)^{2l+1}\sqrt{x}}{l!\,(l+1)!}\left(\sum_{k=1}^{l}\frac{1}{k} + \sum_{k=1}^{l+1}\frac{1}{k}\right) \\
\approx& 1 + \frac{x}{2}\ln\frac{\sqrt{x}}{2},
\end{aligned} \tag{A.3.1}$$

where $I_1(\cdot)$ is the modified Bessel function of the first kind with first order and $\boldsymbol{C}$ is the

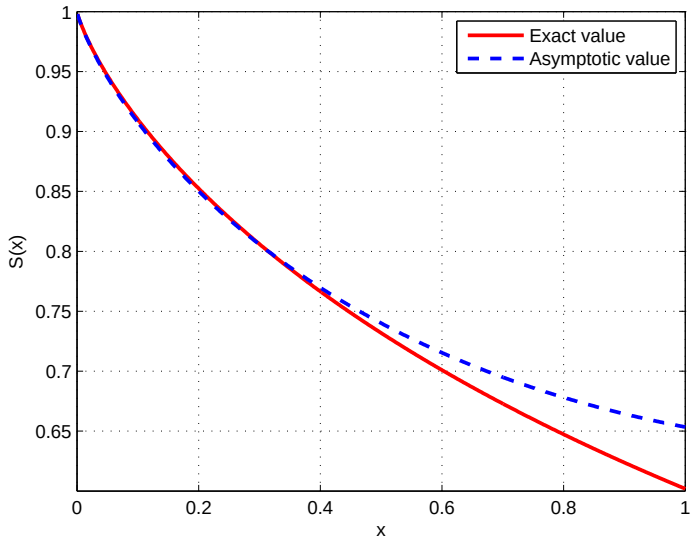

Figure A.1: Verification of the approximation for the function $\mathcal{S}(x)$.

Euler's constant [77, Eq. (8.367)]. The fact that $I_1(x) \to \frac{x}{2}$ if $x \to 0$ [77, Eq. (8.447)] is used to obtain the first approximation. Moreover, the second approximation follows since the term $\boldsymbol{C} - \frac{1}{2}$ is negligible compared with the term $\ln \frac{\sqrt{x}}{2}$ for $x \to 0$ and the terms in the summation are with higher orders.

In Fig. A.1, we plot the exact and asymptotic values of the function $\mathcal{S}(x)$ based on the formulas in (2.3.2) and (A.3.1). As can be observed in Fig. A.1, the exact and asymptotic values coincide with each other very well when x approaches zero, which validates the approximation in (A.3.1).

By using (A.3.1) and performing some simplifications, we can write the asymptotic throughput of the OR scheme at high SNR as (2.4.7).

A.4 Proof of Proposition 2.4.3

Analogous to the proof of Proposition 2.3.1, we can obtain an approximate expression for the outage probability of the PRS protocols given by

$$\begin{aligned} P_{\text{out}}^{\text{HTC,PRS}} \approx &\Pr\left(h_{AS}h_{SA} < \frac{\nu}{\mu}\right) - \Pr\left(h_{AR_b}h_{R_bA} > \frac{\nu}{\mu}\right) \times \\ &\Pr\left(h_{AS}h_{SA} < \frac{\nu}{\mu}, h_{AS}h_{SR_b} > \frac{\nu}{\mu}\right). \end{aligned} \tag{A.4.1}$$

For the case that the relay is selected only based on the hop $\{S \to R_i\}$ with the selection criterion given in (2.4.3), we can claim that the selected relay R_b should meet the following condition

$$h_{SR_b} = \max_{i\in\mathcal{N}} \{h_{SR_i}\}. \tag{A.4.2}$$

Since the variables $\{h_{SR_i}\}$'s are i.i.d, we can obtain the PDF of h_{SR_b} given by

$$f_{h_{SR_b}}(z) = \frac{N}{\sigma_{SR}^2} \sum_{n=0}^{N-1} \binom{N-1}{n} (-1)^n \exp\left(-\frac{n+1}{\sigma_{SR}^2} z\right). \tag{A.4.3}$$

Moreover, the random variables h_{AR_b} and h_{R_bA} follow the exponential distribution with average values σ_{AR}^2 and σ_{RA}^2, since the links A-R_i and R_i-A are not taken into account for relay selection. Substituting the PDFs into (A.4.1) and solving the integrals, we can obtain the desired result in (2.4.9).

When it comes to the PRS protocol with the criterion in (2.4.4), the selected relay R_b should satisfy

$$h_{AR_b}h_{R_bA} = \max_{i\in\mathcal{N}} \{h_{AR_i}h_{R_iA}\}. \tag{A.4.4}$$

Thus, we have

$$\begin{aligned}\Pr\left(h_{AR_b}h_{R_bA} > \frac{\nu}{\mu}\right) &= 1 - \Pr\left(h_{AR_b}h_{R_bA} < \frac{\nu}{\mu}\right) \\ &= 1 - \left[1 - \mathcal{S}\left(\frac{4\nu}{\mu\sigma_{AR}^2\sigma_{RA}^2}\right)\right]^N \\ &= \sum_{n=1}^{N}\binom{N}{n}(-1)^{n+1}\left[\mathcal{S}\left(\frac{4\nu}{\mu\sigma_{AR}^2\sigma_{RA}^2}\right)\right]^n.\end{aligned} \tag{A.4.5}$$

In contrast, the random variable h_{SR_b} only follows an exponential distribution with average values σ_{SR}^2. This is because the links S-R_i's are not taken into consideration during the relay selection process. Then, the expression (2.4.10) can be obtained by repeating the integral calculation in (A.4.1). This completes the proof.

Appendix B

Proofs for Chapter 4. Energy Trading in Power Beacon-Assisted WPCCNs using Stackelberg Game

B.1 Proof of Proposition 4.3.1

To solve Problem (P4.3.2), we calculate the first-order derivative of $\mathcal{U}_a''(\tau,\lambda)$ with respect to λ and set it equal to zero to find the stationary points. That is, $\frac{\partial \mathcal{U}_a''(\tau,\lambda)}{\partial \lambda}=0$. After some simple algebraic manipulations, we can obtain the following equation:

$$\ell(\lambda) = (\lambda X_N - Y_N)^2 + \left(\frac{C}{D} - Y_N\right)(\lambda X_N - Y_N) - \frac{W' X_N}{2\tau} = 0. \tag{B.1.1}$$

The above quadratic equation $\ell(\lambda)=0$ possesses the following two solutions:

$$\lambda_1 = \frac{-\left(\frac{C}{D} - 3Y_N\right) + \sqrt{\left(\frac{C}{D} - Y_N\right)^2 + \frac{2X_N W'}{\tau}}}{2X_N}, \tag{B.1.2}$$

$$\lambda_2 = \frac{-\left(\frac{C}{D} - 3Y_N\right) - \sqrt{\left(\frac{C}{D} - Y_N\right)^2 + \frac{2X_N W'}{\tau}}}{2X_N}. \tag{B.1.3}$$

Let us next verify the validity of these two solutions. Recall that the objective function of Problem (P4.3.2) given in (4.3.6) includes a logarithm function term. Then, according to the definition of logarithm functions, the term inside the logarithm

function, i.e., $1+\frac{D}{C}\left(\lambda X_N-2Y_N\right)$, should be no less than zero. We check the sign of this term for solution λ_1 and get

$$\begin{aligned}
&1+\frac{D}{C}\left(\lambda_1 X_N-2Y_N\right)\\
=&\frac{1}{2}+\frac{D}{2C}\left(-Y_N+\sqrt{\left(\frac{C}{D}-Y_N\right)^2+\frac{2X_N W'}{\tau}}\right)\\
>&\frac{1}{2}+\frac{D}{2C}\left(-Y_N+\left|\frac{C}{D}-Y_N\right|\right)\\
=&\frac{1}{2}-\frac{D}{2C}Y_N+\left|\frac{1}{2}-\frac{D}{2C}Y_N\right|\geq 0.
\end{aligned} \tag{B.1.4}$$

Similarly, we obtain the following formula for solution λ_2

$$1+\frac{D}{C}\left(\lambda_2 X_N-2Y_N\right)<0. \tag{B.1.5}$$

Thus, only stationary point λ_1 is valid. We then calculate the second-order derivative of $\mathcal{U}_a''\left(\tau,\lambda\right)$ with respective to λ and obtain

$$\frac{\partial^2 U_a''\left(\tau,\lambda\right)}{\partial\lambda^2}=-2\tau X_N-\frac{W'X_N^2}{\left[\frac{C}{D}+\left(\lambda X_N-2Y_N\right)\right]^2}<0, \tag{B.1.6}$$

which indicates that the function $\mathcal{U}_a''\left(\tau,\lambda\right)$ with a given τ achieves its maximum value at the valid stationary point λ_1. Furthermore, we can easily check that $\lambda_1>0$, which meets the constraint of the Problem (P4.3.2). Therefore, we can conclude that the optimal solution to Problem (P4.3.2), denoted by $\lambda^\star$, is the stationary point λ_1. That is, $\lambda^\star=\lambda_1$, which completes the proof.

B.2 Proof of Proposition 4.3.2

We first prove the "if" statement of this proposition. Recall that we reduce Problem (P4.3.1) to Problem (P4.3.2) by assuming that $\lambda>\frac{b_m}{G_{m,s}}$, $\forall m$ holds. Hence, if $\lambda^\star$ given in (4.3.7) is also the solution to Problem (P4.3.1), the following inequality

should hold

$$\lambda^\star > \max_{m\in\mathcal{N}} Z_m, \tag{B.2.1}$$

where $Z_m = \frac{b_m}{G_{m,s}}$. Substituting the expression of $\lambda^\star$ into the above inequality and rearranging it, we get

$$\sqrt{\left(\frac{C}{D} - Y_N\right)^2 + \frac{2X_N W'}{\tau}} > 2X_N \max_{m\in\mathcal{N}} Z_m - 3Y_N + \frac{C}{D}. \tag{B.2.2}$$

To further simplify the above inequality, we check the sign of the term $2X_N \max_{m\in\mathcal{N}} Z_m - 3Y_N$ on its right-hand side and obtain

$$\begin{aligned} &2X_N \max_{m\in\mathcal{N}} Z_m - 3Y_N \\ =&\sum\nolimits_{n=1}^{N} \left(\frac{G_{n,s}^2}{a_n} \max_{m\in\mathcal{N}} \frac{b_m}{G_{m,s}} - \frac{3b_n G_{n,s}}{4a_n}\right) \\ \geq&\sum\nolimits_{n=1}^{N} \left(\frac{G_{n,s}^2}{a_n} \frac{b_n}{G_{n,s}} - \frac{3b_n G_{n,s}}{4a_n}\right) \\ =&\sum\nolimits_{n=1}^{N} \frac{b_n G_{n,s}}{4a_n} > 0. \end{aligned} \tag{B.2.3}$$

Based on the above result, we can square double sides of the inequality (B.2.2) without affecting the direction of the inequality symbol. Substituting the expression of W' and making some rearrangements, we can rewrite (B.2.2) as the desired result given in (4.3.8), which completes the proof of the "if" statement.

Subsequently, we prove the "only if" statement by contradiction. For the ease of exposition, we assume that the PBs are sorted by the following order:

$$Z_1 < \ldots < Z_{N-1} < Z_N.$$

In this case, the condition given in (4.3.8) can be simplified as

$$\mu > Q_N, \tag{B.2.4}$$

where

$$Q_N = \frac{2\tau (\ln 2) \left(X_N Z_N - 2Y_N + \frac{C}{D}\right) (X_N Z_N - Y_N)}{X_N (1-\tau) W}. \tag{B.2.5}$$

Then, the "only if" statement means that the energy price $\lambda^\star$ is the optimal solution to Problem (P4.3.1) *only if* $\mu > Q_N$. To prove this by contradiction, we assume that $\lambda^\star$ given in (4.3.7) is still the optimal solution to Problem (P4.3.1) even if $\mu \leq Q_N$. Then, the proof follows if we can show that this hypothesis is false.

Without loss of generality, we assume that $Q_{N-1} < \mu \leq Q_N$, where Q_{N-1} is defined later. When $\mu \leq Q_N$, we can obtain from the proof of the "if" statement that $\lambda^\star \leq Z_N$, which indicates $\kappa_N = 0$, according to its definition in (4.3.3). In this case, the following optimization problem reduced from Problem (P4.3.1) should be solved to find the optimal energy price:

$$\text{(P.A.1)}: \begin{array}{c} \max\limits_{\boldsymbol{\kappa}',\lambda} \ \mathcal{U}_a'''(\tau, \boldsymbol{\kappa}', \lambda) \\ \text{s.t. } \kappa_m' \in \{0,1\}, \forall m \in \mathcal{N}\backslash N, \\ \lambda \geq 0, \end{array} \tag{B.2.6}$$

where $\boldsymbol{\kappa}' = \left[\kappa_1', \ldots, \kappa_{N-1}'\right]^T$ is a new indicator vector with $\kappa_m' = \kappa_m,\ \forall m \in \mathcal{N}\backslash N$, $A\backslash B$ denotes the relative complement of the set B in the set A, and

$$\begin{aligned} \mathcal{U}_a'''(\tau, \boldsymbol{\kappa}', \lambda) =& W' \ln C - \sum_{m=1}^{N-1} \kappa_m' \lambda \tau \frac{\lambda G_{m,s} - b_m}{2a_m} G_{m,s} + \\ & W' \ln \left(1 + \frac{D}{C} \sum_{m=1}^{N-1} \kappa_m' \frac{\lambda G_{m,s} - b_m}{2a_m} G_{m,s}\right). \end{aligned} \tag{B.2.7}$$

It is straightforward to observe that Problem (P.A.1) has exactly the same structure as Problem (P4.3.1). Following the analysis in Appendix B.1 and the proof of the "if" statement, we can express the optimal solution of Problem (P.A.1) as

$$\tilde{\lambda}^\star = \frac{-\left(\frac{C}{D} - 3Y_{N-1}\right) + \sqrt{\left(\frac{C}{D} - Y_{N-1}\right)^2 + \frac{2X_{N-1}W'}{\tau}}}{2X_{N-1}}, \tag{B.2.8}$$

if $\mu > Q_{N-1}$, where $X_{N-1} = \sum_{n=1}^{N-1} \frac{G_{n,s}^2}{2a_n}$, $Y_{N-1} = \sum_{n=1}^{N-1} \frac{b_n G_{n,s}}{4a_n}$, and

$$Q_{N-1} = \frac{2\tau (\ln 2) \left(X_{N-1}Z_{N-1} - 2Y_{N-1} + \frac{C}{D}\right)\left(X_{N-1}Z_{N-1} - Y_{N-1}\right)}{X_{N-1}(1-\tau)W}. \tag{B.2.9}$$

The optimal energy price given in (B.2.8) for the case $Q_{N-1} < \mu \leq Q_N$ is obviously

different from the one given in (4.3.7) for the case $\mu > Q_N$. This is not consistent with our previous hypothesis that the energy price $\lambda^\star$ given in (4.3.7) is still the optimal solution to the Problem (P4.3.1) even if $\mu \leq Q_N$. Thus, the contradiction appears and the proof of the "only if" part follows.

By combining the proofs for the "if" and "only if" statements, we have completed the proof of Proposition 4.3.2.

B.3 Proof of Proposition 4.3.4

Following a similar procedure to solve Problem (P4.3.1), we first consider the situation that the parameter μ is sufficiently large such that all PBs are involved during the DL energy transfer phase (i.e., the transmit powers of all PBs are larger than 0). In this case, the constraint of the Problem (P4.3.5), i.e., $\boldsymbol{p} \geq \mathbf{0}$, can be ignored. Since the objective function $\mathcal{U}'_{sw}(\boldsymbol{p})$ is concave in terms of p_m for any $m \in \mathcal{N}$, we can obtain the optimal value of p_m for the unconstrained problem by taking the first-order derivative of $\mathcal{U}'_{sw}(\boldsymbol{p})$ with respect to p_m and setting it equal to zero. Specifically, the optimal value of p_m, denoted by $p_m^\dagger$, should be a solution of the equation $\frac{\partial \mathcal{U}'_{sw}(\boldsymbol{p})}{\partial p_m} = 0$. After some algebraic manipulations, we have N equations with the mth one given by

$$\frac{W'/\tau}{\frac{C}{D} + \sum\limits_{m=1}^{N} p_m G_{m,s}} = \frac{2a_m p_m + b_m}{G_{m,s}}. \tag{B.3.1}$$

It can be easily verified that the left-hand side of (B.3.1) is the same for any m on the right-hand side. Then, by equaling the right-hand sides of (B.3.1) for two different

indexes m and n, we get

$$p_n = \frac{(2a_m p_m + b_m)\, G_{n,s}}{2a_n G_{m,s}} - \frac{b_n}{2a_n}, \forall n. \tag{B.3.2}$$

Substituting the above p_n into (B.3.1) and making some simplifications, we get

$$\frac{W'/\tau}{\frac{C}{D} + \frac{2a_m p_m + b_m}{G_{m,s}} \sum_{n=1}^{N} \frac{G_{n,s}^2}{2a_n} - \sum_{n=1}^{N} \frac{b_n G_{n,s}}{2a_n}} = \frac{2a_m p_m + b_m}{G_{m,s}}. \tag{B.3.3}$$

Setting $\tilde{p}_m = \frac{2a_m p_m + b_m}{G_{m,s}}$ and recalling the definition of X_N and Y_N, we can re-write (B.3.3) as

$$X_N (\tilde{p}_m)^2 + \left(\frac{C}{D} - 2Y_N\right) \tilde{p}_m - W'/\tau = 0. \tag{B.3.4}$$

It is straightforward to observe that the above quadratic equation possesses one positive solution and one negative solution since $X_N > 0$ and $-W'/\tau < 0$. Note that $\tilde{p}_m \geq 0$, which means only the larger solution is valid. Thus, we have the following equation regarding the optimal value of p_m, denoted by $p_m^\dagger$,

$$\frac{2a_m p_m^\dagger + b_m}{G_{m,s}} = \Lambda_N, \tag{B.3.5}$$

where

$$\Lambda_N = \frac{-\left(\frac{C}{D} - 2Y_N\right) + \sqrt{\left(\frac{C}{D} - 2Y_N\right)^2 + \frac{4X_N W'}{\tau}}}{2X_N} \tag{B.3.6}$$

is the larger root of the quadratic equation (B.3.4). Thus, if the value of μ is large enough such that all PBs are involved, their optimal transmit power $p_m^\dagger$ can be expressed as

$$p_m^\dagger = \frac{\Lambda_N G_{m,s} - b_m}{2a_m}, \ \forall\, m \in \mathcal{N}. \tag{B.3.7}$$

The subsequent question is how large should the value of μ be such that $p_m^\dagger > 0, \ \forall\, m$ holds. Based on the structure of (B.3.7), we can deduce that $p_m^\dagger > 0, \ \forall\, m$ if $\Lambda_N > \max_{m \in \mathcal{N}} Z_m$. Recall that $Z_m = \frac{b_m}{G_{m,s}}$. We can observe from (B.3.6) that the value of Λ_N is proportional to that of parameter μ. By assuming that the PBs

are sorted in the order $Z_1 < \ldots < Z_{N-1} < Z_N$ and repeating the procedures from Appendix B.2, we can reduce the condition $\Lambda_N > \max_{m\in\mathcal{N}} Z_m$ to

$$\mu > \widetilde{Q}_N, \tag{B.3.8}$$

where

$$\widetilde{Q}_N = \frac{(\ln 2)\,\tau\left(X_N Z_N - 2Y_N + \frac{C}{D}\right) Z_N}{(1-\tau)\,W}. \tag{B.3.9}$$

Next, let us consider the case $\widetilde{Q}_{N-1} < \mu \leq \widetilde{Q}_N$ with $\widetilde{Q}_{N-1}$ denoting the minimum threshold of μ such that the PBs ranked from 1 to $N-1$ will all get involved during the DL phase. In this situation, the Nth PB will not be included during the energy transfer since $\mu \leq \widetilde{Q}_N$. We can find the optimal transmit powers of the involved PBs by repeating the steps as in (B.3.1)-(B.3.7). Similarly, we can obtain the desired results of other cases given in (4.3.19). This completes the proof of this proposition.

Appendix C

Proofs for Chapter 5. Distributed Power Splitting for a Large-Scale WPCCN with SWIPT using Game Theory

C.1 Proof of Proposition 5.3.1

Firstly, it is straightforward to observe that the utility function $u_i^{AF}(\rho_i, \boldsymbol{\rho}_{-i})$ is continuous in ρ_i. Then, a feasible method to prove the quasi-concavity of the utility function $u_i^{AF}(\rho_i, \boldsymbol{\rho}_{-i})$ is to use the following theorem [108, pp. 99]:

Theorem C.1.1. *A continuous function $f : \mathbb{R} \to \mathbb{R}$ is quasi-concave if and only if at least one of the following conditions holds:*

- *f is non-decreasing*
- *f is non-increasing*
- *there is a point $c \in$ **dom** f such that for $t \leq c$ (and $t \in$ **dom** f), f is non-decreasing, and for $t \geq c$ (and $t \in$ **dom** f), f is non-increasing.*

Next, let us prove the quasi-concavity of the utility function by showing that it is first non-decreasing and then non-increasing in the feasible domain. This will be achieved by demonstrating that the first-order derivative of the utility is no less than zero when the variable is smaller than a certain value and is no larger than zero in the remaining domain.

To proceed, we derive the first-order derivative of the function $u_i^{AF}\left(\rho_i, \boldsymbol{\rho}_{-i}\right)$ with respect to (w.r.t) ρ_i, which, after some algebra manipulations, can be expressed as

$$\frac{\partial u_i^{AF}\left(\rho_i, \boldsymbol{\rho}_{-i}\right)}{\partial \rho_i} = \frac{1}{\ln 2} \frac{C_i(\rho_i)^2 - 2D_i\rho_i + D_i}{\left[\rho_i\left(1-\rho_i\right)Y_iZ_i - C_i\rho_i + D_i\right]^2 / X_iZ_i + \rho_i\left(1-\rho_i\right)}, \tag{C.1.1}$$

where

$$C_i = \left(X_i + Y_i\right)\left(W_i + 1\right) - Z_i, \tag{C.1.2a}$$

$$D_i = \left(X_i + Y_i + 1\right)\left(W_i + 1\right), \tag{C.1.2b}$$

are defined for the simplicity of notations.

After a careful observation on the right-hand side of (C.1.1), we can deduce that the sign of $\frac{\partial u_i^{AF}\left(\rho_i, \boldsymbol{\rho}_{-i}\right)}{\partial \rho_i}$ is only determined by the numerator

$$\kappa_i\left(\rho_i\right) = C_i(\rho_i)^2 - 2D_i\rho_i + D_i, \tag{C.1.3}$$

since the denominator is always large than zero. To further determine the monotonicity of the function $u_i^{AF}\left(\rho_i, \boldsymbol{\rho}_{-i}\right)$, we need to investigate the properties of the quadratic function $\kappa_i\left(\rho_i\right)$ on the feasible set of ρ_i (i.e., $[0, 1]$). Firstly, we note that

$$\kappa_i\left(0\right) = D_i > 0, \tag{C.1.4a}$$

$$\kappa_i\left(1\right) = C_i - D_i = -(Z_i + W_i + 1) < 0. \tag{C.1.4b}$$

Then, we can draw all possible shapes of the function $\kappa_i\left(\rho_i\right)$ versus ρ_i for different cases, as depicted in Fig. C.1. From Fig. C.1, we can see that in spite of the sign of the term C_i, there always exists a point $\epsilon_i \in [0, 1]$ such that $\kappa_i\left(\epsilon_i\right) = 0$, $\kappa_i\left(\rho_i\right) > 0$

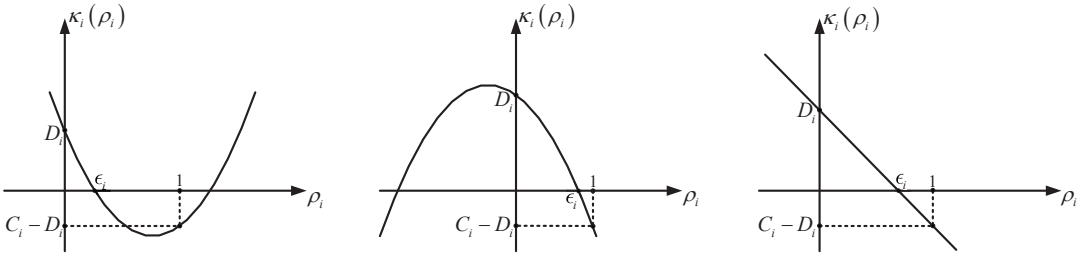

(a) When $C_i > 0$ (b) When $C_i < 0$ (c) When $C_i = 0$

Figure C.1: All possible shapes for the function $\kappa_i(\rho_i)$ versus ρ_i for different cases.

for $\rho_i < \epsilon_i$, and $\kappa_i(\rho_i) < 0$ for $\rho_i > \epsilon_i$. This means that on its feasible domain, the function $u_i^{AF}(\rho_i, \boldsymbol{\rho}_{-i})$ is increasing in ρ_i before the point ϵ_i and is decreasing in ρ_i after the point ϵ_i. Then, according to Theorem C.1.1, we can claim that the utility function $u_i^{AF}(\rho_i, \boldsymbol{\rho}_{-i})$ is quasi-concave in ρ_i.

In addition, it is easy to check that the feasible set $\mathcal{A}_i$ is compact and convex and the utility function $u_i^{AF}(\rho_i, \boldsymbol{\rho}_{-i})$ is continuous in $\boldsymbol{\rho}$ for any $i \in \mathcal{N}$. Then, with reference to Theorem 5.3.1, we can further claim that the formulated game $\mathcal{G}_{AF}$ for the pure AF network (i.e., all relays implement AF protocol) possesses at least one NE.

For the formulated game $\mathcal{G}_{DF}$, it is straightforward to check that both $\gamma_{i,1}^{DF}$ and $\gamma_{i,2}^{DF}$ are concave functions of ρ_i. Moreover, the minimum of two concave functions is also concave, which means that the SINR γ_i^{DF} is a concave function of the strategy ρ_i. Since the function $f(x) = \log(1+x)$ is concave and non-decreasing, we can claim[1] that the utility function $u_i^{DF}(\rho_i, \boldsymbol{\rho}_{-i})$ is concave (quasi-concave) in ρ_i. Thus, according to Theorem 5.3.1, we can conclude that the formulated game $\mathcal{G}_{DF}$ also

[1]The composite function $h(x) = f(g(x))$ is concave in x if $f(x)$ is concave and non-decreasing, and $g(x)$ is concave [108].

admits at least one NE. This completes the proof.

C.2 Proof of Lemma 5.3.1

According to the analysis in Appendix C.1, for a given power splitting profile $\boldsymbol{\rho}$, the expression of the parameter ϵ_i is actually the best response function of the ith link. Moreover, ϵ_i is one solution of the following quadratic equation:

$$\kappa_i(\epsilon_i) = C_i(\epsilon_i)^2 - 2D_i\epsilon_i + D_i = 0. \tag{C.2.1}$$

According to the value of C_i, we divide the derivation for the expression of ϵ_i into three cases:

(a) When $C_i = 0$: The equation in (C.2.1) is simplified as

$$-2D_i\epsilon_i + D_i = 0. \tag{C.2.2}$$

Thus, $\epsilon_i = 1/2$ when $C_i = 0$.

(b) When $C_i > 0$: In this case, the quadratic equation in (C.2.1) possesses the following two roots:

$$\epsilon_{i,1} = \frac{D_i + \sqrt{(D_i)^2 - C_iD_i}}{C_i} = \frac{\sqrt{D_i}\left(\sqrt{D_i} + \sqrt{D_i - C_i}\right)}{D_i - (D_i - C_i)} = \frac{\sqrt{D_i}}{\sqrt{D_i} - \sqrt{D_i - C_i}}, \tag{C.2.3}$$

$$\epsilon_{i,2} = \frac{D_i - \sqrt{(D_i)^2 - C_iD_i}}{C_i} = \frac{\sqrt{D_i}}{\sqrt{D_i} + \sqrt{D_i - C_i}}. \tag{C.2.4}$$

Since $C_i > 0$ and $D_i > D_i - C_i > 0$, we have $\epsilon_{i,1} > 1$ and $\frac{1}{2} < \epsilon_{i,2} < 1$. Thus, the valid expression of ϵ_i when $C_i > 0$ is given by

$$\epsilon_i = \epsilon_{i,2} = \frac{\sqrt{D_i}}{\sqrt{D_i} + \sqrt{D_i - C_i}}, \tag{C.2.5}$$

because the feasible set of ϵ_i is $[0, 1]$.

(c) When $C_i < 0$: In this case, we have $D_i - C_i > D_i > 0$. Thus, the roots $\epsilon_{i,1} < 0$

and $0 < \epsilon_{i,2} < \frac{1}{2}$. Hence, the valid expression of ϵ_i when $C_i < 0$ is the same with the case when $C_i > 0$, i.e.,

$$\epsilon_i = \epsilon_{i,2} = \frac{\sqrt{D_i}}{\sqrt{D_i} + \sqrt{D_i - C_i}}. \tag{C.2.6}$$

Therefore, substituting the expressions of C_i and D_i defined in (C.1.2) and setting $\mathcal{B}_i^{AF}(\boldsymbol{\rho}) = \epsilon_i$, we can obtain the desired result in (5.3.6) for the best response function of the ith link in a pure AF network. This completes the proof.

C.3 Proof of Proposition 5.3.2

To prove this proposition, we need to show that the function $\mathcal{B}^{AF}(\boldsymbol{\rho})$ for the formulated game is standard. Firstly, based on the analysis in Appendix C.2, it is easy to verify that the best response function satisfies the conditions in Definition 5.3.1 when $(X_i + Y_i)(W_i + 1) = Z_i$ (i.e., $C_i = 0$). Thus, we only need to show the function

$$\mathcal{B}_i^{AF}(\boldsymbol{\rho}) = \frac{\sqrt{(X_i + Y_i + 1)(W_i + 1)}}{\sqrt{(X_i + Y_i + 1)(W_i + 1)} + \sqrt{Z_i + W_i + 1}} \tag{C.3.1}$$

also satisfies the three properties of the standard function for any i, which are proved in the following:

(1) Positivity: According to the analysis in Appendix C.2, for any player i and any strategy profile $\boldsymbol{\rho}$, the best response function $\mathcal{B}_i^{AF}(\boldsymbol{\rho})$ is always larger than 0, which guarantees the positivity of the function $\mathcal{B}^{AF}(\boldsymbol{\rho})$.

(2) Monotonicity: Recall the definition of the terms X_i, Y_i, Z_i and W_i in (5.2.6). We can see that only the term W_i is related to the strategy profile $\boldsymbol{\rho}$. Suppose $\boldsymbol{\rho}$ and $\boldsymbol{\rho}'$ are two different strategy profiles and $\boldsymbol{\rho} \geq \boldsymbol{\rho}'$. Then, the corresponding best

response functions of any player i can be written as

$$\mathcal{B}_i^{AF}(\boldsymbol{\rho}) = \frac{\sqrt{(X_i + Y_i + 1)(W_i + 1)}}{\sqrt{(X_i + Y_i + 1)(W_i + 1)} + \sqrt{Z_i + W_i + 1}}, \tag{C.3.2}$$

and

$$\mathcal{B}_i^{AF}(\boldsymbol{\rho}') = \frac{\sqrt{(X_i + Y_i + 1)(W_i' + 1)}}{\sqrt{(X_i + Y_i + 1)(W_i' + 1)} + \sqrt{Z_i + W_i' + 1}}, \tag{C.3.3}$$

where $W_i' = \sum_{j=1, j\neq i}^{N} \rho_j' \eta \left(\sum_{n=1}^{N} P_n |g_{nj}|^2 \right) |h_{ji}|^2 / \sigma^2$.

After a careful comparison of (C.3.2) and (C.3.3), we can see that all the terms in $\mathcal{B}_i^{AF}(\boldsymbol{\rho})$ and $\mathcal{B}_i^{AF}(\boldsymbol{\rho}')$ are the same except W_i and W_i'. Hence, the inequity $\mathcal{B}_i^{AF}(\boldsymbol{\rho}) \geq \mathcal{B}_i^{AF}(\boldsymbol{\rho}')$ holds if we can prove $\mathcal{B}_i^{AF}(W_i) \geq \mathcal{B}_i^{AF}(W_i')$. Moreover, we have $W_i \geq W_i'$ since $\boldsymbol{\rho} \geq \boldsymbol{\rho}'$. Thus, the proof of $\mathcal{B}_i^{AF}(\boldsymbol{\rho}) \geq \mathcal{B}_i^{AF}(\boldsymbol{\rho}')$ is equivalent to proving that the $\mathcal{B}_i^{AF}(W_i)$ is non-decreasing in W_i. To proceed, we re-write the best response function $\mathcal{B}_i^{AF}(\boldsymbol{\rho})$ as

$$\mathcal{B}_i^{AF}(\boldsymbol{\rho}) = \frac{1}{1 + \sqrt{\frac{Z_i}{(X_i+Y_i+1)(W_i+1)} + \frac{1}{X_i+Y_i+1}}}. \tag{C.3.4}$$

From (C.3.4), we can easily observe that $\mathcal{B}_i^{AF}(\boldsymbol{\rho})$ is increasing in W_i, which completes the proof of monotonicity.

(3) Scalability: For any given $\alpha > 1$, we have

$$\begin{aligned} \alpha \mathcal{B}_i^{AF}(\boldsymbol{\rho}) &= \frac{\alpha}{1 + \sqrt{\frac{Z_i}{(X_i+Y_i+1)(W_i+1)} + \frac{1}{X_i+Y_i+1}}} \\ &= \frac{1}{\frac{1}{\alpha} + \sqrt{\frac{Z_i}{\alpha^2(X_i+Y_i+1)(W_i+1)} + \frac{1}{\alpha^2(X_i+Y_i+1)}}} \\ &> \frac{1}{1 + \sqrt{\frac{Z_i}{(X_i+Y_i+1)(\alpha W_i+1)} + \frac{1}{(X_i+Y_i+1)}}} \\ &= \mathcal{B}_i^{AF}(\alpha\boldsymbol{\rho}), \end{aligned} \tag{C.3.5}$$

which proves that the best response function $\mathcal{B}_i^{AF}(\boldsymbol{\rho})$ meets the scalability property. This completes the proof.

C.4 Proof of Lemma 5.3.2

Let ρ_i^* denote the best response of the ith link corresponding to a given power splitting strategy profile $\boldsymbol{\rho}$. That is, ρ_i^* is the maximizer of $u_i^{DF}(\boldsymbol{\rho})$. It can be easily observed that $\gamma_{i,1}^{DF}$ in (5.2.8) is monotonically decreasing in ρ_i, while $\gamma_{i,2}^{DF}$ in (5.2.10) is monotonically increasing in ρ_i. Thus, ρ_i^* must satisfy the following condition:

$$\gamma_{i,1}^{DF}(\rho_i^*) = \gamma_{i,2}^{DF}(\rho_i^*). \tag{C.4.1}$$

Substituting the expression of $\gamma_{i,1}^{DF}$ and $\gamma_{i,2}^{DF}$, we have

$$\frac{(1-\rho_i^*)X_i}{(1-\rho_i^*)Y_i+1} = \frac{\rho_i^* Z_i}{W_i+1}. \tag{C.4.2}$$

After rearranging (C.4.2), we obtain

$$Y_i Z_i (\rho_i^*)^2 - [X_i(W_i+1) + Y_i Z_i + Z_i]\rho_i^* + X_i(W_i+1) = \ell_i(\rho_i^*) = 0. \tag{C.4.3}$$

Note that (C.4.3) is a quadratic equality of ρ_i^*, denoted by $\ell_i(\rho_i^*) = 0$. Thus, the value of ρ_i^* can be obtained by solving the quadratic equality in (C.4.3).

We note that

$$Y_i Z_i > 0, \tag{C.4.4a}$$

$$\ell_i(0) = X_i(W_i+1) > 0, \tag{C.4.4b}$$

$$\ell_i(1) = -Z_i < 0. \tag{C.4.4c}$$

Based on (C.4.4), we can deduce that the quadratic equality $\ell_i(\rho_i^*) = 0$ admits two roots lying in $(0,1)$ and $(1,+\infty)$. Since the feasible set of the power splitting ratio is $[0,1]$, the valid value of ρ_i^* can only be the smaller root of the equality $\ell_i(\rho_i^*) = 0$.

Mathematically, we have,

$$\begin{aligned}\rho_i^* &= \left[(X_iW_i + X_i + Y_iZ_i + Z_i) - \right. \\ &\quad \left. \sqrt{(X_iW_i + X_i - Y_iZ_i + Z_i)^2 + 4Y_iZ_i^2}\right] / (2Y_iZ_i) \\ &= \mathcal{B}_i^{DF}(\boldsymbol{\rho}),\end{aligned} \tag{C.4.5}$$

which completes the proof.

C.5 Proof of Proposition 5.3.3

Similar to the proof of Proposition 5.3.2 in Appendix C.3, the proof of this proposition follows by showing that the function $\boldsymbol{\mathcal{B}}^{DF}(\boldsymbol{\rho})$ of the formulated game is standard. In the following, we show that the function $\boldsymbol{\mathcal{B}}^{DF}(\boldsymbol{\rho})$ satisfies the three properties of the standard function.

(1) Positivity: As shown in Appendix C.4, for any player i and any strategy profile $\boldsymbol{\rho}$, the best response function $\mathcal{B}_i^{DF}(\boldsymbol{\rho})$ is always larger than 0, which guarantees the positivity of the function $\boldsymbol{\mathcal{B}}^{DF}(\boldsymbol{\rho})$.

(2) Monotonicity: Suppose $\boldsymbol{\rho}$ and $\boldsymbol{\rho}'$ are two different strategy profiles and $\boldsymbol{\rho} \geq \boldsymbol{\rho}'$. Then, the corresponding best response functions of any player i can be written as

$$\begin{aligned}\mathcal{B}_i^{DF}(\boldsymbol{\rho}) = \left[(X_iW_i + X_i + Y_iZ_i + Z_i) - \right. \\ \left. \sqrt{(X_iW_i + X_i - Y_iZ_i + Z_i)^2 + 4Y_iZ_i^2}\right] / (2Y_iZ_i),\end{aligned} \tag{C.5.1}$$

and

$$\begin{aligned}\mathcal{B}_i^{DF}(\boldsymbol{\rho}') = \left[(X_iW_i' + X_i + Y_iZ_i + Z_i) - \right. \\ \left. \sqrt{(X_iW_i' + X_i - Y_iZ_i + Z_i)^2 + 4Y_iZ_i^2}\right] / (2Y_iZ_i),\end{aligned} \tag{C.5.2}$$

where X_i, Y_i, Z_i, W_i are defined in (5.2.6), and
$W_i' = \sum_{j=1, j\neq i}^{N} \rho_j' \eta \left(\sum_{n=1}^{N} P_n |g_{nj}|^2\right) |h_{ji}|^2/\sigma^2$.

Analogous to the analyses in Appendix C.3, the proof of $\mathcal{B}_i^{DF}(\boldsymbol{\rho}) \geq \mathcal{B}_i^{DF}(\boldsymbol{\rho}')$ is

equivalent to proving that $\frac{\partial \mathcal{B}_i^{DF}(W_i)}{W_i} \geq 0$. Expanding $\frac{\partial \mathcal{B}_i^{DF}(W_i)}{W_i} \geq 0$, we have

$$\frac{\partial \mathcal{B}_i^{DF}(W_i)}{W_i} = \frac{X_i}{2Y_iZ_i}\left[1 - \frac{X_iW_i + X_i - Y_iZ_i + Z_i}{\sqrt{(X_iW_i + X_i - Y_iZ_i + Z_i)^2 + 4Y_iZ_i^2}}\right]. \tag{C.5.3}$$

Since the term $X_i/(2Y_iZ_i) > 0$ and the term in the square bracket of (C.5.3) is always large than zero, we can claim that $\frac{\partial \mathcal{B}_i^{DF}(W_i)}{W_i} > 0$, which completes the proof of monotonicity.

(3) Scalability: For any $\alpha > 1$, we define the function $\mathcal{F}_i(\alpha, \boldsymbol{\rho}) = \alpha \mathcal{B}_i^{DF}(\boldsymbol{\rho}) - \mathcal{B}_i^{DF}(\alpha\boldsymbol{\rho})$. Then, the proof of the scalability is equivalent to proving that $\mathcal{F}_i(\alpha, \boldsymbol{\rho}) > 0$ for any $\alpha > 1$. Firstly, it is obvious that $\mathcal{F}_i(1, \boldsymbol{\rho}) = 0$. Thus, a sufficient condition for $\mathcal{F}_i(\alpha, \boldsymbol{\rho}) > 0$ is that $\mathcal{F}_i(\alpha, \boldsymbol{\rho})$ is an increasing function of α, i.e., $\frac{\partial \mathcal{F}_i(\alpha, \boldsymbol{\rho})}{\partial \alpha} > 0$. To proceed, we first derive the first-order and second-order partial derivatives of $\mathcal{F}_i(\alpha, \boldsymbol{\rho})$ w.r.t α and obtain

$$\begin{aligned}\frac{\partial \mathcal{F}_i(\alpha, \boldsymbol{\rho})}{\partial \alpha} = \frac{1}{2Y_iZ_i}\{&X_i + Y_iZ_i + Z_i \\ &+ \frac{(\alpha X_iW_i + X_i - Y_iZ_i + Z_i)X_iW_i}{\sqrt{(\alpha X_iW_i + X_i - Y_iZ_i + Z_i)^2 + 4Y_iZ_i{}^2}} \\ &- \sqrt{(X_iW_i + X_i - Y_iZ_i + Z_i)^2 + 4Y_iZ_i^2}\Big\},\end{aligned} \tag{C.5.4}$$

$$\frac{\partial^2 \mathcal{F}_i(\alpha, \boldsymbol{\rho})}{\partial \alpha^2} = \frac{2Z_i(X_iW_i)^2}{\left[(\alpha X_iW_i + X_i - Y_iZ_i + Z_i)^2 + 4Y_iZ_i^2\right]^{3/2}}. \tag{C.5.5}$$

From (C.5.5), we can see that $\frac{\partial^2 \mathcal{F}_i(\alpha, \boldsymbol{\rho})}{\partial \alpha^2}$ is always larger than 0, which indicates that $\frac{\partial \mathcal{F}_i(\alpha, \boldsymbol{\rho})}{\partial \alpha}$ is increasing in α. Thus, a sufficient condition for $\mathcal{F}_i(\alpha, \boldsymbol{\rho}) > 0$ can now be

simplified as $\frac{\partial \mathcal{F}_i(\alpha,\boldsymbol{\rho})}{\partial \alpha}\Big|_{\alpha=1} > 0$. Substituting $\alpha = 1$ into (C.5.4), we get

$$\begin{aligned}\frac{\partial \mathcal{F}_i(\alpha,\boldsymbol{\rho})}{\partial \alpha}\Big|_{\alpha=1} = \frac{1}{2Y_iZ_i}\{&X_i + Y_iZ_i + Z_i \\ &+ \frac{(X_iW_i + X_i - Y_iZ_i + Z_i)X_iW_i}{\sqrt{(X_iW_i + X_i - Y_iZ_i + Z_i)^2 + 4Y_iZ_i^2}} \\ &- \sqrt{(X_iW_i + X_i - Y_iZ_i + Z_i)^2 + 4Y_iZ_i^2}\Big\}.\end{aligned} \tag{C.5.6}$$

To proceed, we derive the first-order derivative for the right-hand side of (C.5.6) with respect to W_i. After some algebraic manipulations, we obtain

$$\partial\left(\frac{\partial \mathcal{F}_i(\alpha,\boldsymbol{\rho})}{\partial \alpha}\Big|_{\alpha=1}\right)/\partial W_i = \frac{2Z_iW_iX_i^2}{\left[(X_iW_i + X_i - Y_iZ_i + Z_i)^2 + 4Y_iZ_i^2\right]^{3/2}},$$

which is shown to be always positive. Thus, $\frac{\partial \mathcal{F}_i(\alpha,\boldsymbol{\rho})}{\partial \alpha}\Big|_{\alpha=1}$ is an increasing function in W_i. Since $W_i > 0$, we further have

$$\begin{aligned}\frac{\partial F_i(\alpha,\boldsymbol{\rho})}{\partial \alpha}\Big|_{\alpha=1} &> \frac{\partial F_i(\alpha,\boldsymbol{\rho})}{\partial \alpha}\Big|_{\alpha=1,W_i=0} \\ &= \frac{1}{2Y_iZ_i}\{X_i + Y_iZ_i + Z_i - \sqrt{(X_i + Y_iZ_i + Z_i)^2 - 4X_iY_iZ_i}\Big\} > 0.\end{aligned} \tag{C.5.7}$$

Therefore, we can claim that $\alpha\mathcal{B}_i^{DF}(\boldsymbol{\rho}) > \mathcal{B}_i^{DF}(\alpha\boldsymbol{\rho})$, which completes the proof.

Bibliography

[1] B. Medepally and N. Mehta, "Voluntary energy harvesting relays and selection in cooperative wireless networks," *IEEE Trans. Wireless Commun.*, vol. 9, no. 11, pp. 3543–3553, November 2010.

[2] O. Ozel, K. Tutuncuoglu, J. Yang, S. Ulukus, and A. Yener, "Transmission with energy harvesting nodes in fading wireless channels: Optimal policies," *IEEE J. Sel. Areas Commun.,*, vol. 29, no. 8, pp. 1732–1743, September 2011.

[3] J. Yang and S. Ulukus, "Optimal packet scheduling in an energy harvesting communication system," *IEEE Trans. Commun.*, vol. 60, no. 1, pp. 220–230, January 2012.

[4] C. K. Ho and R. Zhang, "Optimal energy allocation for wireless communications with energy harvesting constraints," *IEEE Trans. Signal Process.*, vol. 60, no. 9, pp. 4808–4818, Sept 2012.

[5] J. Xu and R. Zhang, "Throughput optimal policies for energy harvesting wireless transmitters with non-ideal circuit power," *IEEE J. Sel. Areas Commun.*, vol. 32, no. 2, pp. 322–332, February 2014.

[6] H. Visser and R. Vullers, "RF energy harvesting and transport for wireless sensor network applications: Principles and requirements," *Proceedings of the IEEE*, vol. 101, no. 6, pp. 1410–1423, June 2013.

[7] X. Lu, P. Wang, D. Niyato, and Z. Han, "Resource allocation in wireless networks with rf energy harvesting and transfer," *IEEE Network*, 2014.

[8] Z. Popovic, "Cut the cord: Low-power far-field wireless powering," *IEEE Microw. Mag.*, vol. 14, no. 2, pp. 55–62, March 2013.

[9] C. A. Balanis, *Antenna theory: analysis and design*. John Wiley & Sons, 2012.

[10] N. Tesla, "The transmission of electrical energy without wires," *Electrical World and Engineer*, vol. 1, 1904.

[11] ——, *Experiments with alternate currents of high potential and high frequency*. New York: McGraw-Hill, 1904.

[12] N. Shinohara, "Power without wires," *IEEE Microwave Mag.*, vol. 12, no. 7, pp. S64–S73, Dec 2011.

[13] L. Xie, Y. Shi, Y. Hou, and A. Lou, "Wireless power transfer and applications to sensor networks," *IEEE Wireless Commun.*, vol. 20, no. 4, pp. 140–145, August 2013.

[14] H. Liu, "Maximizing efficiency of wireless power transfer with resonant inductive coupling," *available online: http://hxhl95.github.io/media/ib_ee.pdf*, 2011.

[15] S. Bi, C. K. Ho, and R. Zhang, "Wireless powered communication: Opportunities and challenges," *available online: http://arxiv.org/abs/1408.2335*, 2014.

[16] A. Kurs, A. Karalis, R. Moffatt, J. D. Joannopoulos, P. Fisher, and M. Soljačić, "Wireless power transfer via strongly coupled magnetic resonances," *science*, vol. 317, no. 5834, pp. 83–86, 2007.

[17] X. Lu, P. Wang, D. Niyato, D. I. Kim, and Z. Han, "Wireless networks with RF energy harvesting: A contemporary survey," *available online: http://arxiv.org/abs/1406.6470*, 2014.

[18] I. Krikidis, S. Timotheou, S. Nikolaou, G. Zheng, D. W. K. Ng, and R. Schober, "Simultaneous wireless information and power transfer in modern communication systems," *IEEE Commun. Mag., avaliable online: http://arxiv.org/abs/1409.0261*, 2014.

[19] K. Huang and X. Zhou, "Cutting last wires for mobile communication by microwave power transfer," *available online: http://arxiv.org/abs/1408.3198*, 2014.

[20] L. Varshney, "Transporting information and energy simultaneously," in *IEEE International Symposium on Information Theory (ISIT)*, 2008, pp. 1612–1616.

[21] R. Zhang and C. K. Ho, "MIMO broadcasting for simultaneous wireless information and power transfer," *IEEE Trans. Wireless Commun.*, vol. 12, no. 5, pp. 1989–2001, 2013.

[22] I. Krikidis, S. Sasaki, S. Timotheou, and Z. Ding, "A low complexity antenna switching for joint wireless information and energy transfer in mimo relay channels," *IEEE Trans. Commun.*, vol. 62, no. 5, pp. 1577–1587, May 2014.

[23] X. Zhou, R. Zhang, and C. K. Ho, "Wireless information and power transfer: Architecture design and rate-energy tradeoff," *IEEE Trans. Commun.*, vol. 61, no. 11, pp. 4754–4767, 2013.

[24] S. Timotheou, I. Krikidis, G. Zheng, and B. Ottersten, "Beamforming for MISO interference channels with QoS and RF energy transfer," *IEEE Trans. Wireless Commun.*, vol. 13, no. 5, pp. 2646–2658, May 2014.

[25] K. Huang and E. Larsson, "Simultaneous information and power transfer for broadband wireless systems," *IEEE Trans. Signal Process.*, vol. 61, no. 23, pp. 5972–5986, 2013.

[26] D. W. K. Ng, E. S. Lo, and R. Schober, "Wireless information and power transfer: Energy efficiency optimization in OFDMA systems," *IEEE Trans. Wireless Commun.*, vol. 12, no. 12, pp. 6352–6370, Nov 2013.

[27] J. R. Smith, *Wirelessly Powered Sensor Networks and Computational RFID*. Springer, 2013.

[28] *Powercast Corporation*, P2110-EVAL-01 Overview and User's Manual, http://www.powercastco.com.

[29] Y. Zuo, "Survivable rfid systems: Issues, challenges, and techniques," *IEEE Trans. Systems, Man, and Cybernetics, Part C: Applications and Reviews.*, vol. 40, no. 4, pp. 406–418, July 2010.

[30] N. Barroca, H. M. Saraiva, P. T. Gouveia, J. Tavares, L. M. Borges, F. J. Velez, C. Loss, R. Salvado, P. Pinho, R. Goncalves, N. BorgesCarvalho, R. Chavez-Santiago, and I. Balasingham, "Antennas and circuits for ambient rf energy harvesting in wireless body area networks," in *IEEE 24th International Symposium on Personal Indoor and Mobile Radio Communications (PIMRC)*, Sept 2013, pp. 532–537.

[31] J. Hoydis, M. Kobayashi, and M. Debbah, "Green small-cell networks," *IEEE Veh. Tech. Mag.*, vol. 6, no. 1, pp. 37–43, March 2011.

[32] Z. Pi and F. Khan, "An introduction to millimeter-wave mobile broadband systems," *IEEE Commun. Mag.*, vol. 49, no. 6, pp. 101–107, June 2011.

[33] J. Hoydis, S. ten Brink, and M. Debbah, "Massive mimo in the ul/dl of cellular networks: How many antennas do we need?" *IEEE J. Sel. Areas Commun.*, vol. 31, no. 2, pp. 160–171, February 2013.

[34] A. Nosratinia, T. E. Hunter, and A. Hedayat, "Cooperative communication in wireless networks," *IEEE Commun. Magazine*, vol. 42, no. 10, pp. 74–80, 2004.

[35] A. Scaglione, D. Goeckel, and J. Laneman, "Cooperative communications in mobile ad hoc networks," *IEEE Signal Process. Mag.*, vol. 23, no. 5, pp. 18–29, Sept 2006.

[36] A. Chakrabarti, E. Erkip, A. Sabharwal, and B. Aazhang, "Code designs for cooperative communication," *IEEE Signal Process. Mag.*, vol. 24, no. 5, pp. 16–26, Sept 2007.

[37] Y. Li, "Distributed coding for cooperative wireless networks: An overview and recent advances," *IEEE Commun. Mag.*, vol. 47, no. 8, pp. 71–77, August 2009.

[38] Q. Zhang, J. Jia, and J. Zhang, "Cooperative relay to improve diversity in cognitive radio networks," *IEEE Commun. Mag.*, vol. 47, no. 2, pp. 111–117, February 2009.

[39] H. Shan, W. Zhuang, and Z. Wang, "Distributed cooperative mac for multihop wireless networks," *IEEE Commun. Mag.*, vol. 47, no. 2, pp. 126–133, February 2009.

[40] Z. Sheng, K. Leung, and Z. Ding, "Cooperative wireless networks: from radio to network protocol designs," *IEEE Commun. Mag.*, vol. 49, no. 5, pp. 64–69, May 2011.

[41] X. Tao, X. Xu, and Q. Cui, "An overview of cooperative communications," *IEEE Commun. Mag.*, vol. 50, no. 6, pp. 65–71, June 2012.

[42] T. Cover and A. Gamal, "Capacity theorems for the relay channel," *IEEE Trans. Info. Theory*, vol. 25, no. 5, pp. 572–584, Sep 1979.

[43] S. Abdulhadi, M. Jaseemuddin, and A. Anpalagan, "A survey of distributed relay selection schemes in cooperative wireless ad hoc networks," *Wireless Personal Communications*, vol. 63, no. 4, pp. 917–935, 2012.

[44] A. Bletsas, A. Khisti, D. Reed, and A. Lippman, "A simple cooperative diversity method based on network path selection," *IEEE J. Sel. Areas Commun.*, vol. 24, no. 3, pp. 659–672, March 2006.

[45] I. Krikidis, J. Thompson, S. McLaughlin, and N. Goertz, "Amplify-and-forward with partial relay selection," *IEEE Commun. Lett.*, vol. 12, no. 4, pp. 235–237, April 2008.

[46] E. Beres and R. Adve, "Selection cooperation in multi-source cooperative networks," *IEEE Trans. Wireless Commun.*, vol. 7, no. 1, pp. 118–127, Jan 2008.

[47] K. Huang and V. Lau, "Enabling wireless power transfer in cellular networks: Architecture, modeling and deployment," *IEEE Trans. Wireless Commun.*, vol. 13, no. 2, pp. 902–912, February 2014.

[48] A. A. Nasir, X. Zhou, S. Durrani, and R. A. Kennedy, "Relaying protocols for wireless energy harvesting and information processing," *IEEE Trans. Wireless Commun.*, vol. 12, no. 7, pp. 3622–3636, 2013.

[49] B. K. Chalise, W.-K. Ma, Y. D. Zhang, H. A. Suraweera, and M. G. Amin, "Optimum performance boundaries of ostbc based af-mimo relay system with energy harvesting receiver," *IEEE Trans Signal Process.*, vol. 61, no. 17, pp. 4199–4213, 2013.

[50] G. Zhu, C. Zhong, H. A. Suraweera, G. K. Karagiannidis, Z. Zhang, and T. A. Tsiftsis, "Wireless information and power transfer in relay systems with multiple antennas and interference," *Accepted to appear in IEEE Trans. Commun., available online: http://arxiv.org/abs/1501.05376*, 2015.

[51] C. Zhong, H. Suraweera, G. Zheng, I. Krikidis, and Z. Zhang, "Wireless information and power transfer with full duplex relaying," *IEEE Trans Commun.*, vol. 62, no. 10, pp. 3447–3461, Oct 2014.

[52] Z. Ding, S. M. Perlaza, I. Esnaola, and H. V. Poor, "Power allocation strategies in energy harvesting wireless cooperative networks," *IEEE Trans. Wireless Commun.*, vol. 13, no. 2, pp. 846–860, 2014.

[53] D. S. Michalopoulos, H. A. Suraweera, and R. Schober, "Relay selection for simultaneous information transmission and wireless energy transfer: A tradeoff perspective," *Accepted to appear in IEEE J. on Sel. Areas Commun., available online: http://arxiv.org/abs/1303.1647*, 2015.

[54] Z. Ding, C. Zhong, D. W. K. Ng, M. Peng, H. A. Suraweera, R. Schober, and H. V. Poor, "Application of smart antenna technologies in simultaneous wireless information and power transfer," *Accepted to appear in IEEE Commun. Mag., available online: http://arxiv.org/abs/1412.1712*, 2015.

[55] J. N. Laneman, D. N. C. Tse, and G. W. Wornell, "Cooperative diversity in wireless networks: Efficient protocols and outage behavior," *IEEE Trans. Inf. Theory*, vol. 50, no. 12, pp. 3062–3080, 2004.

[56] M. K. Simon and M.-S. Alouini, *Digital communication over fading channels*. New York: John Wiley and Sons, 2000.

[57] H. Ju and R. Zhang, "Throughput maximization in wireless powered communication networks," *IEEE Trans. Wireless Commun.*, vol. 13, no. 1, pp. 418–428, 2014.

[58] Z. Han, D. Niyato, W. Saad, T. Basar, and A. Hjorungnes, *Game theory in wireless and communication networks: theory, models, and applications*. Cambridge University Press, 2012.

[59] M. Abramowitz and I. A. Stegun, *Handbook of Mathematical Functions with Formulas, Graphs, and Mathematical Tables*. National Bureau of Standards Applied Mathematics Series 55, Tenth Printing, 1972.

[60] B. Wang, Z. Han, and K. Liu, "Distributed relay selection and power control for multiuser cooperative communication networks using stackelberg game," *IEEE Trans. Mobile Computing*, vol. 8, no. 7, pp. 975–990, July 2009.

[61] X. Kang, R. Zhang, and M. Motani, "Price-based resource allocation for spectrum-sharing femtocell networks: A stackelberg game approach," *IEEE J. Sel. Areas Commun.*, vol. 30, no. 3, pp. 538–549, April 2012.

[62] V. Liu, A. Parks, V. Talla, S. Gollakota, D. Wetherall, and J. R. Smith, "Ambient backscatter: Wireless communication out of thin air," in *Pro. ACM SIGCOMM'13*, 2013.

[63] P. Nintanavongsa, M. Naderi, and K. Chowdhury, "Medium access control protocol design for sensors powered by wireless energy transfer," in *Proc. IEEE INFOCOM 2013*, 2013.

[64] S. Lee, R. Zhang, and K. Huang, "Opportunistic wireless energy harvesting in cognitive radio networks," *IEEE Trans. Wireless Commun.*, vol. 12, no. 9, pp. 4788–4799, September 2013.

[65] X. Chen, X. Wang, and X. Chen, "Energy-efficient optimization for wireless information and power transfer in large-scale mimo systems employing energy beamforming," *IEEE Wireless Commun. Lett.,*, vol. 2, no. 6, pp. 667–670, December 2013.

[66] X. Chen, C. Yuen, and Z. Zhang, "Wireless energy and information transfer tradeoff for limited-feedback multiantenna systems with energy beamforming," *IEEE Trans. Vehicular Tech.*, vol. 63, no. 1, pp. 407–412, Jan 2014.

[67] L. Liu, R. Zhang, and K.-C. Chua, "Multi-antenna wireless powered communication with energy beamforming," *available online: http://arxiv.org/abs/1312.1450*, 2013.

[68] H. Ju and R. Zhang, "Optimal resource allocation in full-duplex wireless-powered communication network," *IEEE Trans. Commun., available online: http://arxiv.org/abs/1403.2580*, 2014.

[69] X. Kang, C. K. Ho, and S. Sun, "Full-duplex wireless-powered communication network with energy causality," *available online: http://arxiv.org/abs/1404.0471*, 2014.

[70] G. Yang, C. K. Ho, R. Zhang, and Y. L. Guan, "Throughput optimization for massive mimo systems powered by wireless energy transfer," *available online: http://arxiv.org/abs/1403.3991*, 2014.

[71] M. Dohler and Y. Li, *Cooperative communications: hardware, channel and PHY*. John Wiley & Sons, 2010.

[72] G. L. Moritz, J. L. Rebelatto, R. D. Souza, B. F. Uchôa-Filho, and Y. Li, "Time-switching uplink network-coded cooperative communication with downlink energy transfer," *IEEE Trans. Signal Process.*, vol. 62, no. 19, pp. 5009–5019, Oct 2014.

[73] K. Ishibashi, H. Ochiai, and V. Tarokh, "Energy harvesting cooperative communications," in *Proc. of the IEEE 23rd International Symposium on Personal, Indoor and Mobile Radio Communications (PIMRC'12)*, 2012.

[74] H. Suraweera, D. Michalopoulos, and G. Karagiannidis, "Performance of distributed diversity systems with a single amplify-and-forward relay," *IEEE Trans Veh. Tech.*, vol. 58, no. 5, pp. 2603–2608, Jun 2009.

[75] N. Shinohara, *Wireless Power Transfer Via Radiowaves*. John Wiley & Sons, 2014.

[76] S. Ikki and M. Ahmed, "Performance analysis of cooperative diversity wireless networks over nakagami-m fading channel," *IEEE Commun. Lett.*, vol. 11, no. 4, pp. 334–336, 2007.

[77] I. S. Gradshteyn and I. M. Ryzhik, *Table of integrals, series, and products*. Elsevier, 2007.

[78] D. da Costa and S. Aissa, "Performance analysis of relay selection techniques with clustered fixed-gain relays," *IEEE Signal Process. Lett.*, vol. 17, no. 2, pp. 201–204, Feb 2010.

[79] Z. Ding and H. Poor, "Cooperative energy harvesting networks with spatially random users," *IEEE Signal Process. Lett.*, vol. 20, no. 12, pp. 1211–1214, Dec 2013.

[80] Z. Ding, I. Krikidis, B. Sharif, and H. Poor, "Wireless information and power transfer in cooperative networks with spatially random relays," *accepted by IEEE Trans. Wireless Commun.*, vol. 13, no. 8, pp. 4440–4453, Aug 2014.

[81] H. Chen, J. Liu, L. Zheng, C. Zhai, and Y. Zhou, "Approximate SEP analysis for DF cooperative networks with opportunistic relaying," *IEEE Signal Process. Letters*, vol. 17, no. 9, pp. 779–782, 2010.

[82] I. Krikidis, S. Timotheou, and S. Sasaki, "RF energy transfer for cooperative networks: Data relaying or energy harvesting?" *IEEE Commun. Letters*, vol. 16, no. 11, pp. 1772–1775, 2012.

[83] B. Gurakan, O. Ozel, J. Yang, and S. Ulukus, "Energy cooperation in energy harvesting communications," *IEEE Trans. Commun.*, vol. 61, no. 12, pp. 4884–4898, 2013.

[84] D. Niyato and P. Wang, "Competitive wireless energy transfer bidding: A game theoretic approach," in *2014 IEEE International Conference on Communications (ICC)*, June 2014.

[85] A. Mohsenian-Rad, V. W. S. Wong, J. Jatskevich, R. Schober, and A. Leon-Garcia, "Autonomous demand-side management based on game-theoretic energy consumption scheduling for the future smart grid," *IEEE Transactions on Smart Grid*, vol. 1, no. 3, pp. 320–331, 2010.

[86] A. A. Nasir, X. Zhou, S. Durrani, and R. A. Kennedy, "Wireless-powered relays in cooperative communications: Time-switching relaying protocols and throughput analysis," *avaliable online: http://arxiv.org/abs/1310.7648*, 2013.

[87] Z. Chen, B. Wang, B. Xia, and H. Liu, "Wireless information and power transfer in two-way amplify-and-forward relaying channels," *avaliable online: http://arxiv.org/abs/1307.7447*, 2013.

[88] O. Simeone, O. Somekh, Y. Bar-Ness, H. V. Poor, and S. Shamai, "Capacity of linear two-hop mesh networks with rate splitting, decode-and-forward relaying and cooperation," in *Proc. of the 45th Annual Allerton Conference on Communication, Control and Computing*, 2007.

[89] P. Thejaswi, A. Bennatan, J. Zhang, R. Calderbank, and D. Cochran, "Rate-achievability strategies for two-hop interference flows," in *Proc. of 46th Annual Allerton Conference on Communication, Control, and Computing*, 2008, pp. 1432–1439.

[90] Y. Cao and B. Chen, "Capacity bounds for two-hop interference networks," in *Proc. of 47th Annual Allerton Conference on Communication, Control, and Computing*, 2009, pp. 272–279.

[91] Y. Shi, J. Wang, K. Letaief, and R. Mallik, "A game-theoretic approach for distributed power control in interference relay channels," *IEEE Trans. on Wireless Commun.*, vol. 8, no. 6, pp. 3151–3161, 2009.

[92] Y. Shi, K. Letaief, R. Mallik, and X. Dong, "Distributed power allocation in two-hop interference channels: An implicit-based approach," *IEEE Trans. Wireless Commun.*, vol. 11, no. 5, pp. 1911–1921, 2012.

[93] K. T. Truong and W. Robert Jr, "A distributed algorithm using interference pricing for relay interference channels," *EURASIP J. Advances in Signal Process.*, vol. 2013, no. 1, pp. 1–16, 2013.

[94] I. Krikidis, "Simultaneous information and energy transfer in large-scale networks with/without relaying," *IEEE Trans. Commun.*, vol. 62, no. 3, pp. 900–912, March 2014.

[95] L. Liu, R. Zhang, and K.-C. Chua, "Wireless information and power transfer: A dynamic power splitting approach," *IEEE Trans. Commun.*, vol. 61, no. 9, pp. 3990–4001, 2013.

[96] D. Fudenberg and J. Tirole, *Game Theory*. The MIT Press Cambrigge, Massachusetts London, England, 1992.

[97] I. L. Glicksberg, "A further generalization of the kakutani fixed point theorem with application to nash equilibrium points," *Proc. American Mathematical Society*, vol. 3, no. 1, pp. 170–174, 1952.

[98] S. Lasaulce, M. Debbah, and E. Altman, "Methodologies for analyzing equilibria in wireless games," *IEEE Signal Process. Magazine*, vol. 26, no. 5, pp. 41–52, 2009.

[99] R. Yates, "A framework for uplink power control in cellular radio systems," *IEEE J. on Selected Areas in Commun.*, vol. 13, no. 7, pp. 1341–1347, 1995.

[100] S. Lasaulce and H. Tembine, *Game theory and learning for wireless networks: fundamentals and applications*. Elsevier, 2011.

[101] R. Billinton and R. N. Allan, "Discrete markov chains," in *Reliability Evaluation of Engineering Systems*. Springer, 1992, pp. 260–279.

[102] G. Zheng, K.-K. Wong, A. Paulraj, and B. Ottersten, "Collaborative-relay beamforming with perfect csi: optimum and distributed implementation," *IEEE Signal Process. Lett.*, vol. 16, no. 4, pp. 257–260, 2009.

[103] J.-S. Pang and M. Fukushima, "Quasi-variational inequalities, generalized nash equilibria, and multi-leader-follower games," *Computational Management Science*, vol. 2, no. 1, pp. 21–56, 2005.

[104] J.-S. Pang and G. Scutari, "Nonconvex games with side constraints," *SIAM Journal on Optimization*, vol. 21, no. 4, pp. 1491–1522, 2011.

[105] W. Saad, Z. Han, M. Debbah, A. Hjorungnes, and T. Basar, "Coalitional game theory for communication networks," *IEEE Signal Process. Mag.*, vol. 26, no. 5, pp. 77–97, 2009.

[106] P. Anghel and M. Kaveh, "Exact symbol error probability of a cooperative network in a rayleigh-fading environment," *IEEE Trans. Wireless Commun.*, vol. 3, no. 5, pp. 1416–1421, 2004.

[107] A. Papoulis and S. U. Pillai, *Probability, random variables, and stochastic processes*. New York: McGraw-Hill, 2002.

[108] S. Boyd and L. Vandenberghe, *Convex Optimization*. Cambridge University Press, 2004.